PONTIFICIA UNIVERSIDAD CATOLICA DE CHILE

SCHOOL OF ENGINEERING

MODELING AND OPTIMAL OPERATION OF TRADITIONAL ALEMBICS TO DISTILL FRUIT WINES

RICARDO ALONSO LUNA HERNÁNDEZ

Thesis submitted to the Office of Graduate Studies in partial fulfillment of the requirements of the Degree of Doctor in Engineering Sciences

Advisor:

JOSÉ RICARDO PÉREZ.

Santiago de Chile, January, 2019

MODELING AND OPTIMAL OPERATION OF TRADITIONAL ALEMBICS TO DISTILL FRUIT WINES

RICARDO ALONSO LUNA HERNÁNDEZ

Members of the Committee:

J. RICARDO PÉREZ
CLAUDIO GELMI
MARIO FERNÁNDEZ
FRANCISCO CUBILLOS
FRANCISCO LÓPEZ
JORGE VÁSQUEZ

Thesis submitted to the Office of Research and Graduate Studies in partial fulfillment of the requirements for the Degree of Doctor in Engineering Sciences

Santiago de Chile, January, 2019

"Up to the top of my dreams you will able to see it,

my dreams are lies that one day will stop being it"

- Ignacio José Fornés Olmo (Nach), <u>Manifiesto</u>

To my family, my great love and Friends.

ACKNOWLEDGEMENTS

I want to express my appreciation to my supervisor, Prof. José Ricardo Pérez Correa for his guidance, technical, professional and personal support throughout my PhD. Moreover, I would like to give thank Prof. Francisco Lopez for his good reception and complete support when I worked with him during my internship.

I would like to give thanks to laboratory coworkers I met throughout my PhD: Franco, José Vergara, Francisco Palma, Simón Diaz, Gustavo Puga, Felipe Huerta, Pamela Rivera, Nils Huaman, Daniela Silva and Fernanda Erpel. Thanks to all for making a good and pleasant work environment. In particular, I want to thank Ivan Urbina whom I appreciate very much and became a great friend throughout my PhD. Moreover, I would like to thank Rodolfo Nicoletti who was my first student and I had the opportunity to guide and support his thesis project; my thesis would not have been possible without his help. I would like to give thanks to the people I met in my internship in Tarragona; Eduardo Garza, Pau Matias, Wael Kaade, Francisco Paco Medina, Lucas Bonfim and Felix Blakk. Thanks a lot for making my stay so special and enjoyable; it was nice to meet you and I hope to see you again someday.

I would like to give special thanks to my family, my siblings, especially my parents Patricia Hernández and Heraldo Luna. Thanks a lot for your unconditional love and support. I would like to give special thanks to my favorite person, my great love, Victoria; thanks a lot for your unconditional love and support, for illuminating my life; you are the most beautiful thing that happened to me during these last years, and I will be eternally grateful. As great Violeta Parra said, "thank you to life, which has given me so much."

LIST OF PAPERS

This thesis is based on the following journal manuscripts, referred in the text by respective chapters:

Chapter II: Luna, R., Duarte-Mermoud, M. A., Pérez-Correa, J.R. **Fractional order control in Charentais alembic distillation**. (sent for publication).

Chapter III: Luna, R., López, F., Pérez-Correa, J.R. **Minimizing methanol content in experimental Charentais alembic distillations**. Journal of Industrial and Engineering Chemistry, 57, 160-170.

Chapter IV: Luna, R., Matias-Guiu, P., López, F., Pérez-Correa, J.R. **Modeling and multi-objective Dynamic optimization of Muscat wine batch distillations**. (to be submitted).

PROCEEDINGS

Partial advances of this work have also been presented at national and international congresses as the following references:

Luna, R., Pérez-Correa, J.R. (2017). Estrategias de operación para minimizar la concentración de metanol en destilados obtenidos en alambiques Charentais. *XX Congreso Chileno de Ingeniería Química (CChIQ 2017).* **(Oral presentation)**

Pérez-Correa, J.R, **Luna, R**. (2016). New developments for the automatic control of spirits distillation. *Proceedings of the IEEE International Conference on Automatica (ICA ACCA 2016), Institute of Electrical and Electronics Engineers (IEEE), 19-21 October 2016, Curicó, Chile,* 756(1). **(Oral presentation).**

Fernández-Fernández, M., Lefranc, G., **Luna, R.**, Pérez-Correa, J.R. (2016). Comparison of PID-IMC and Hill Control applied to heating power of a fruit-derived alcohol production alembic. *Proceedings of CHILECON 2015 - 2015 IEEE Chilean Conference on Electrical, Electronics Engineering, Information and Communication Technologies, Proceedings of IEEE Chilecon 2015,* 89-94. **(Oral presentation).**

Luna, R., Pérez-Correa, J.R., López, F., Fernández-Fernández, M. (2015). Operating strategies to minimise the methanol content in distillates obtained in alembics. *Proceedings of the International Food Operations and Processing Simulation Workshop, FoodOPS 2015,* 65-72. **(Oral presentation).**

Luna, R., Corneloup, T., Pérez-Correa, J.R, Fernández, M., López, F. (2015). Operating strategies to reduce the methanol content in distillates obtained in alembics. In *Distilled Spirits, Future Challenges, New Solutions*, eds., I. Goodall, R. Fotheringham, D. Murray, R.A, Speers, G.M, Walker. *The Institute of Brewing and Distilling*, 111-113. **(Poster).**

FIGURE INDEX

TABLE INDEX

LIST OF CONTENT

PONTIFICIA UNIVERSIDAD CATÓLICA DE CHILE

ESCUELA DE INGENIERÍA

MODELING AND OPTIMAL OPERATION OF TRADITIONAL ALEMBICS TO DISTILL FRUIT WINES

Thesis submitted to the Office of Graduate Studies in partial fulfillment of the requirements for the Degree of Doctor in Engineering Sciences by

RICARDO ALONSO LUNA HERNÁNDEZ

ABSTRACT

Fruit spirits are alcoholic beverages that are produced and consumed all over the world. Their variety depends mainly on raw material available in a given region, and they are characterized by a distinctive aroma. The aroma of spirits is defined by hundreds of low compounds called congeners. The concentration of these congeners depends on many variables such as growing conditions, fermentation variables, yeast strain, distillation equipment, distillation variables, as well as maturation and aging conditions. Distillation plays a key role in preserving the distinctive aroma of young spirits. In spirits distillation, Charentais stills operating in batch mode are most often used in small-scale production. During distillation, three cuts are recovered (head, heart and tail) to obtain highly aromatic spirits with low levels of toxic components and off-flavors. Since the operation of this process is apparently simple, it is usually carried out manually. However, spirits distillation is subjected to many disturbances that generate variability in the composition of the final product. In addition, it is hard and time consuming to adapt the distillation recipe to the market demand for new products. The challenge of this productive sector is to keep up with and to follow developing initiatives and strategies that allow improvements in the production quality, to diversify their products in an increasingly competitive market. Therefore, the application of modern engineering tools such as mathematical modeling, optimization and automatic control would be a fundamental

support to produce consistently spirits which are rich in specific aromas, and free from off-flavors and toxic compounds. The hypothesis that guides this work is that the aromatic characteristic of fruit spirits obtained in Charentais stills can be shaped by proper handling of the boiler´s heat as well as the volumes of the head and heart cuts. The methodology of this thesis involves the following steps. First, the development of a dynamic process model derived from mass and energy balances. Second, the application of various model-based optimization techniques to establish a heat addition policy and volume cuts. Third, the development of automatic control systems able to follow closely a given heat addition policy, despite unmeasured disturbances. Finally, experimental validation with artificial fruit wines. The results of this thesis will allow the design of distillation recipes for Charentais stills to produce any spirit with enhanced specific aromatic characteristic and with minimum levels of toxic compounds and aromatic defects.

Members of the Doctoral Thesis Committee:

José Ricardo Pérez Correa

Claudio Gelmi

Mario Fernández

Francisco Cubillos

Francisco López

Jorge Vásquez

Santiago, January, 2019

PONTIFICIA UNIVERSIDAD CATÓLICA DE CHILE

ESCUELA DE INGENIERÍA

MODELAMIENTO Y OPERACIÓN ÓPTIMA DE ALAMBIQUES TRADICIONALES PARA DESTILAR VINOS DE FRUTAS

Tesis enviada a la Dirección de Investigación y Postgrado en cumplimiento parcial de los requisitos para el grado de Doctor en Ciencias de la Ingeniería

RICARDO ALONSO LUNA HERNÁNDEZ

RESUMEN

Los destilados de frutas son bebidas alcohólicas producidas y consumidas en todo el mundo. La variedad de éstas depende principalmente de la materia prima disponible en una región en particular, que caracteriza un aroma distintivo. El aroma de las bebidas destiladas se define por cientos de compuestos en bajas concentraciones llamados congéneres. La concentración de estos congéneres depende de muchas variables como las condiciones de crecimiento de la fruta, las variables de fermentación, la cepa de levadura, el equipo de destilación, las variables de destilación, así como las condiciones de maduración y envejecimiento del destilado. La destilación juega un papel clave en la preservación del aroma distintivo de los destilados jóvenes. En la destilación de licores, los alambiques Charentais operados por lote son utilizados con mayor frecuencia en la producción a pequeña escala. Durante la destilación se recuperan tres cortes (cabeza, corazón y cola) para obtener destilados altamente aromáticos con bajos niveles de componentes tóxicos y sabores desagradables. Dado que la operación de este proceso es aparentemente simple, generalmente se lleva a cabo manualmente. Sin embargo, la destilación está sujeta a muchas perturbaciones que generan variabilidad en la composición del producto final. Además, es difícil y lento adaptar recetas de destilación a la demanda de nuevos productos por el mercado. El reto en este sector productivo es mantener y seguir desarrollando iniciativas y estrategias que permitan mejorar la calidad del producto,

además de diversificar y ofrecer productos a un mercado cada vez más competitivo. Por lo tanto, la aplicación de herramientas de ingeniería modernas como el modelamiento matemático, la optimización y el control automático sería un soporte fundamental para producir consistentemente destilados ricos en aromas específicos y libres de sabores desagradables y compuestos tóxicos. La hipótesis que guía este trabajo es que la característica aromática de los destilados de fruta obtenidos en alambiques Charentais se puede adaptar manejando adecuadamente la adición de calor en la caldera y los cortes de volumen de la cabeza y el cuerpo. La metodología de esta tesis implica los siguientes pasos; primero, el desarrollo de un modelo dinámico del proceso derivado de los balances de masa y energía. Segundo, la aplicación de técnicas de optimización dinámica basadas en modelos para establecer una estrategia óptima de adición de calor y volúmenes de corte en la destilación. Tercero, el desarrollo de un sistema de control automático capaz de seguir de cerca una determinada política de adición de calor, a pesar de las perturbaciones no medidas. Finalmente, la validación experimental de las estrategias óptimas de destilación con vinos de frutas artificiales y reales. Los resultados de esta tesis permitirán diseñar recetas de destilación para alambiques Charentais para producir cualquier tipo de destilado de fruta con características aromáticas específicas mejoradas y con niveles mínimos de compuestos tóxicos y defectos aromáticos.

Miembros de la Comisión de Tesis Doctoral:

José Ricardo Pérez Correa

Claudio Gelmi

Mario Fernández

Francisco Cubillos

Francisco López

Jorge Vásquez

Santiago, Enero, 2019

CHAPTER 1: INTRODUCTION

1.1 Motivation

Pisco is a young fruit spirit traditional of Chile and Peru, made from Muscat wine distillation. In Chile, pisco is protected by origin denomination in the law N° 18445. This origin denomination recognizes the special characteristics of pisco, reflecting the factors of climate, people and traditions of the Chilean valleys of Regions III and IV.

The pisco market has had changes and dynamism, in the decade of the '90s and the beginning of the new millennium; the demand for pisco has decreased in the internal market, being replaced by other distillates like rum, vodka and gin, and by beer. Nevertheless, in recent years, this situation began to revert and the demand of pisco has begun to improve, indicating that the national consumption would reach 2.1 liters per capita in 2016 (Odepa, 2017). The Chilean pisco production is mainly consumed by national market (98.9%) obtaining US$ 250 million of annual sales. In turn, the international market has had an increase both in price and volume in the last years. This is mainly due to a better quality, variety and presentation of the product. However, the international sales are still much smaller than national sales, representing only 1.1% of the total production. Therefore, the challenge of this productive sector is to keep up with and to follow developing initiatives and strategies that allow the industry to improve the production quality, diversify their products and consolidate their presence in the international markets. In this context, the application of modern engineering tools such as mathematical modeling, optimization and automatic control would be a fundamental support to attain these goals.

1.2 Pisco

Pisco is an aromatic spirit produced from Muscat grapes. According to origin denomination, pisco corresponds to a brandy produced in the regions of Atacama (III) and Coquimbo (IV). These regions have an ideal ecosystem (warm and dry weather) for Muscat grapes production and they are formed by Copiapó, Huasco, Elqui, Limarí and Choapa valleys. In 2015, the surface planted with pisco vines was more than 8,500 hectares mainly in the Coquimbo region (95 %). The grapes also are regulated to include only some Vitis Vinifera varieties: Moscatel de Alejandría o Italia, Moscatel Rosada o Pastilla, Torontel, Moscatel de Austria,

Pedro Jiménez, Moscatel Blanca o Temprana, Chaselas Musque Vrai, Moscatel Amarilla, Moscato de Canelli, Moscatel de Frontignan, Moscatel de Hamburgo, Moscatel Negra and Muscat Orange (the first five are the main varieties). The grapes provide the typical aromatic quality of pisco, mainly from terpenes (Muscat aroma). Moscatel Amarilla contains the highest terpenes concentration followed by Moscatel de Alejandría and Moscatel Rosada (Agosin et al., 2000). Pedro Jimenez is a non-aromatic grape and is preferred by the farmers since it has a higher productivity and it improves the cost effectiveness of their fields (Odepa, 2017). Therefore, the grape variety used results in obtaining wines and distillates with different aromatic qualities. Four types of pisco are commercialized in Chile: Pisco corriente (30°), Pisco especial (35°), Pisco reservado (40°) and gran Pisco (43°). In addition, sometimes pisco is aged in oak barrels for more than six months and up to ten years, using a mixture of non-aromatic grape varieties, to increase flavors and aromas coming from oak, yielding a distillate color between light and dark amber. White pisco is a young distillate with less than six months of aging, most of the times using Muscat varieties with high terpenes concentration.

1.3 Pisco production

Pisco elaboration consists of many stages (Figure 1-1). The first stage is a vintage of grapes in sunny valleys. Then, the grapes are ground to extract the Muscat must. The second stage is the alcoholic fermentation. Here, yeasts transform the glucose and fructose from Muscat must into ethanol, and the fruity aromas of grapes are complemented with fermentation aromas to produce a wine with a complex Muscat aroma. The third stage is a distillation of Muscat wine, to produce a spirit where the volatile components are concentrated. In Chile, the pisco is usually distilled around 70° alcoholic strength. Later, the distillate is diluted with demineralized water to adjust the ethanol concentration to commercial alcoholic grades (30°, 35°, 40° and 45°). Finally, in some cases, the distilled alcohol is stored in oak barrels for a short aging process.

Young distillates like white pisco are characterized by a delicate aroma that resembles the original fruit. Thus, in young spirits' production process, distillation plays a key role to ensure the quality standards of the distillate, i.e., rich in ethanol, fruity and floral aromas (esters and

terpenes) and low in off-flavors (fatty acids) and toxic compounds (methanol, acetaldehyde and furfural).
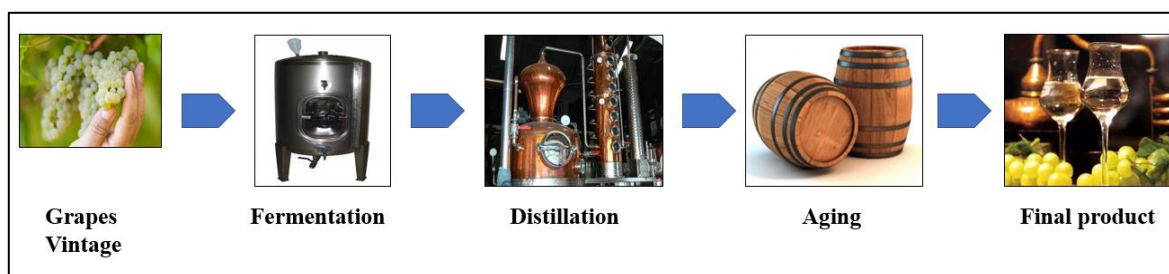
Figure 1-1. Stages of pisco manufacture.

1.4 Alcoholic Beverages distillation

Distillation is a technique used to carry out the separation of a liquid mixture by evaporation and condensation, based on the differences in boiling temperature (relative volatile) by the application of heat. Distillation was already used by ancient cultures (2000 BC) in China, Egypt, and Mesopotamia for medicinal purposes as well as to create balms, essences, and perfumes. Some historians state that during the eighth or ninth century, Arab alchemists devised the alembic to obtain finer essences for perfumes while other Arab alchemists used the alembic to convert base metal into gold (copper-alembic.com) (Figure 1-2). The "alembics" derived from the Arabic term "al ambic," which in turn can be traced back to the Greek "Ambix", describing a container with a small hole (Sacher, García-Llobodanin, López, Segura, & Pérez-Correa, 2017).

Figure 1-2. Distillation description using an alembic by Arab alchemists in the 8th century.

Nowadays, distillation of alcoholic beverages must be carried out in batch copper Charentais alembics (French style) and in batch distillation columns (German style) (Figure 1-3). In fact, there are many research papers that study the impact of the distillation system on the aromatic and chemical characteristic in several kinds of distillates; melon fruit distillate using copper alembic and glass packed column (Hernández-Gómez et al., 2003), grappa distillation using tray and packed columns (Da Porto & Decorti, 2008), Cachaça distillation using copper alembic and stainless steel columns (Reche et al., 2007), copper Charentais alembic and packed column to obtain pear spirits (Arrieta-Garay et al., 2013; García-Llobodanin et al., 2011), kiwi spirits (Arrieta-Garay et al., 2014) and grape pomace spirits (Arrieta-Garay et al., 2014). Charentais alembics are widely used in small scale facilities since the operation is much simpler than batch columns and it better preserves the original fruit aroma (Arrieta-Garay et al., 2013). Nevertheless, traditional distillations with Charentais alembics allow limited control of the distillation process to improve the product. In this case, the heating power in the boiler is the only input variable that can be manipulated to modify the aromatic

composition of the distillate. Instead, are more flexible since they include two manipulated variables: heating power in the boiler and cooling flow rate in the partial condenser. In particular, batch distillations with packed columns allow fast and flexible control of the internal reflux rate, and this can be varied in a wide range (Matias-Guiu et al., 2016). Therefore, batch distillations with packed columns yield higher ethanol recovery (principal product) and productivity (Spaho, 2017). However, the process is less reproducible than traditional distillations in Charentais alembics. In both cases, the operation is subjected to many uncontrolled and unmeasured disturbances that generate variability in the distillate composition. For example, the environmental temperature influences the heat loss in the Charentais alembic swan neck (Sacher et al., 2013). This phenomenon is important since it defines the natural internal reflux rate that modifies the ethanol and congeners recoveries. Finally, the choice of distillation equipment depends mainly on the consumers' preferences for the typical flavor and aroma from the fruit that is distilled.
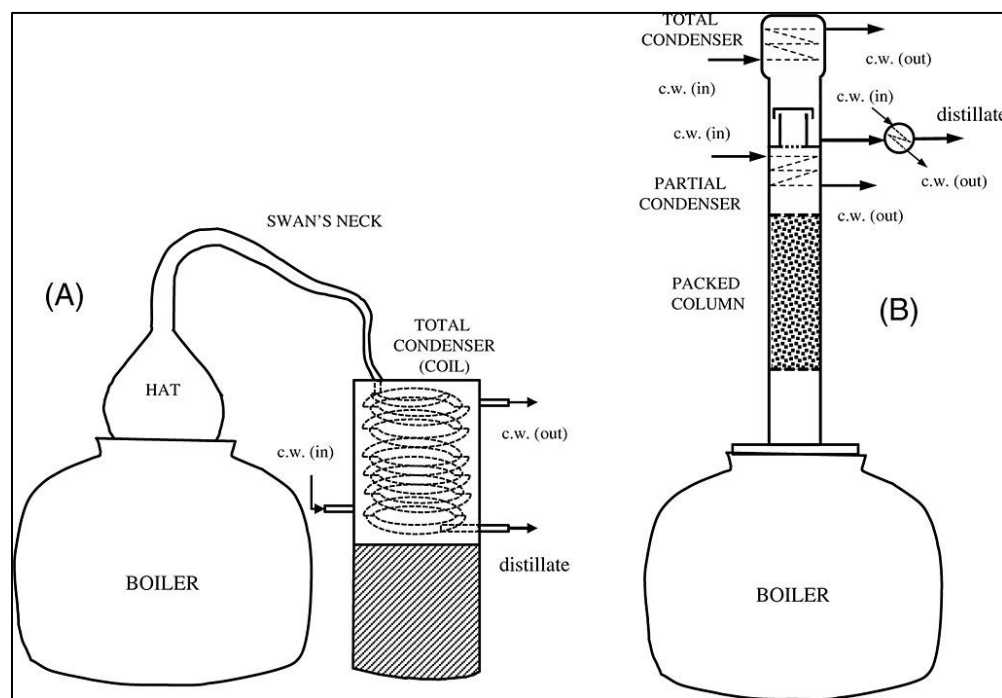
Figure 1-3. Schematic representation of distillation equipment. (A) Charentais alembic and (B) packed column from Arrieta-Garay *et al.* (2014).

1.5 Description of pisco distillation

Wine to distill is composed mainly of ethanol and water (97-99 %). However, the distinctive aroma is defined by over 300 compounds of low concentration called congeners. These compounds will distill differently depending on their boiling point, solubility in ethanol and water, and ethanol content in the vapor during distillation (Léauté, 1990). Some congeners are desirable like floral and fruity aromas; others should be removed as much as possible during distillation like fatty acids, methanol, acetaldehyde and furfural. Therefore, spirits distillations aim to concentrate ethanol and desirable aroma compounds like terpenes, esters and aromatic alcohols, while minimizing the recovery of negative compounds (off-flavors).

During the distillation process, the ethanol content in the vapor phase will define which volatile compounds will be more concentrated in the distillate (Figure 1-4).
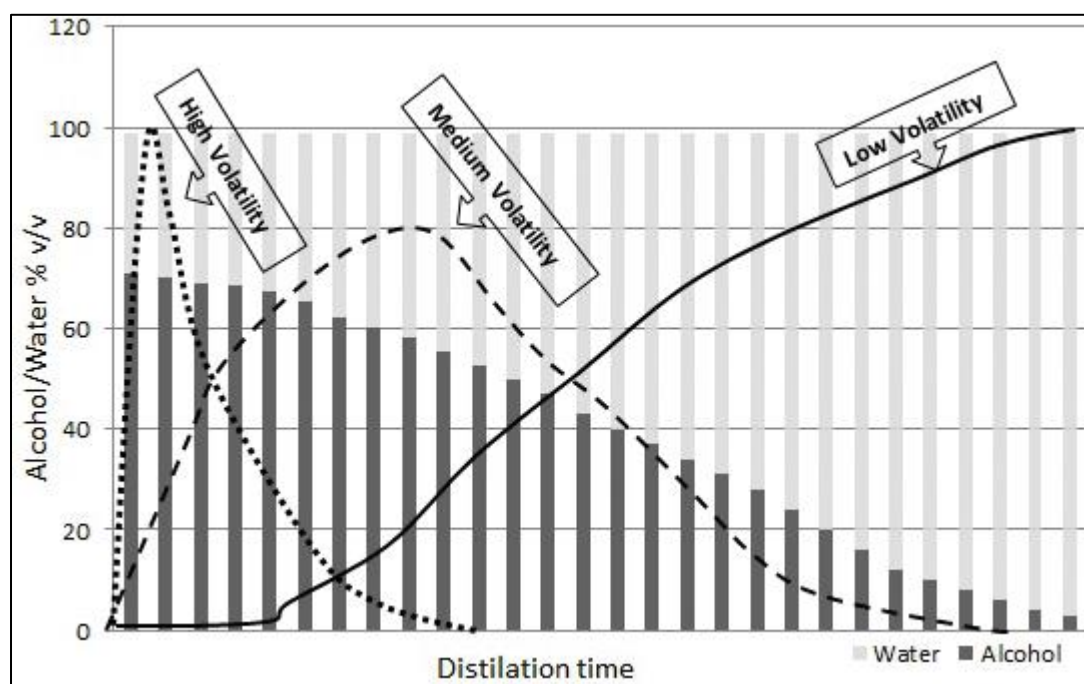
Figure 1-4. Distillation run of ethanol and congeners, distinguish by volatility (Spaho, 2017).

The first part of the distillate is rich in ethanol and in highly volatile compounds. Later, ethanol concentration decreases, and low volatile compounds increase. To separate the different congeners, the distillate is collected in three fractions: head, heart and tail. The head fraction is rich in congeners that present low boiling temperatures or are highly soluble in ethanol. Most of the times, head compounds are off-flavors like acetaldehyde, acetal and ethyl acetate. This fraction also includes fruity esters like ethyl butyrate, ethyl hexanoate, ethyl octanoate and ethyl decanoate. The head fraction is discarded to reduce in the final product the content of negative aromas and toxic compounds such as acetaldehyde (Christoph & Bauer-Christoph, 2007). The heart fraction should have a clean taste, corresponding to the alcohol base to make pisco. This fraction is rich in higher alcohols such as 1-propanol, 1-hexanol, 2-methyl-1-butanol and 3-methyl-1-butanol and in terpenes such as linalool and α-terpineol. At high concentrations, higher alcohols are known for their negative impact on the spirit's aroma (fusel-like flavors) (Matias-Guiu et al., 2018). In turn, terpenes are known for their high positive impact, providing the typical flowery notes from Muscat wines (Christoph & Bauer-Christoph, 2007). Finally, the tail fraction is rich in high boiling temperature or highly water soluble compounds. Most tail compounds are considered a defect in distilled spirits, especially fatty acids like octanoic and hexanoic acids. Usually, in the Chilean pisco industry, the head and tail fractions are collected and redistilled, since they contain significant amounts of alcohol and of some valuable congeners.

The art of spirits distillation is to balance productivity and distinctive flavor, ensuring a product free from off-flavors and toxic compounds. There are some different criteria to make the cut from heart to tail, e.g., a target ethanol recovery, a given alcoholic strength or a specified temperature of the vapor entering the total condenser (Spaho, 2017; Spaho et al., 2013). In many distilleries, experienced distillers do this very well by taste and smell. This method remains the most reliable method to define cuts. Alternatively, other methods like mathematical models have been developed for decision making and exploring new strategies.

1.6 Pisco flavor chemistry

Pisco flavor results from a unique mixture of volatile compounds originating mainly from the raw material (Muscat grape varieties) such as linalool, geraniol, nerol, among other. C_{13} norisoprenoids also contribute significantly to the fruity aroma of the distillate (Bordeu, Agosín, and Casaubon 2012). However, several secondary compounds are formed during the alcoholic fermentation by yeast (*Saccharomyces cerevisiae*) called fermentative aromas. These volatile compounds include higher alcohols, medium and long chain volatile acids, acetate esters, ethyl esters, and aldehydes, among others (Bordeu et al., 2012; Delfini et al., 2001; Lambrechts and Pretorius 2000). Moreover, some compounds are formed from a short aging process (Lambrechts & Pretorius, 2000; Swiegers et al., 2005) to add caramel flavor. Finally, during distillation, several aroma compounds are also released or decomposed, due to the acidic hot environment with pH between 2.8 and 4.0 (Bordeu et al., 2012; Ribéreau-Gayon et al. 2006) and temperatures between 78 and 100 °C. There are several complex reactions occurring in this extreme environment, e.g., terpenic compounds such as geraniol and nerol transform into linalool and alpha terpineol (Ohta et al., 1991). Matias-Guiu *et al.* (2018) reported that low pH (acidic media) favors the decomposition of linalool and acetaldehyde to form α-terpineol and acetal, respectively. In addition, low pH favors the formation of ethyl esters such as ethyl acetate and fruity esters (ethyl hexanoate, ethyl octanoate, among others) by esterification.

Several congeners have a significant olfactory impact at low concentrations. The aromatic impact of these compounds is expressed in terms of odor activity values (OAV), defined as the ratio between the concentration of the compound in a given mixture and its detection threshold. Table 1-1 shows the most relevant congeners found in Chilean commercial piscos, their aromatic characteristics and their odor thresholds. The most important odorants in pisco are linalool (terpene), β-damascenone (C_{13} norisoprenoids), ethyl hexanoate, ethyl heptanoate and octanoate, isoamyl acetate (Bordeu, Agosín, and Casaubon 2012). To explain the aromatic differences between commercial distillates, principal component analysis (PCA) was applied to the composition of ten Chilean commercial piscos considering fifteen congeners (Figure 1-5). The first two principal components covered 63.6% of the total variance. Commercial samples were separated into three main groups: (i) piscos rich in fruity aromas (mostly singly distilled); (ii) piscos rich in floral and terpenic aromas (one tripled

distilled and one singly distilled); and (iii) piscos characterized by floral and burnt aromas (one lightly aged, one singly distilled and one doubly distilled). Therefore, aging and the number of distillation processes yield significant differences between the distillates. The variety of Muscat grape used to produce the wine is also a relevant factor affecting the distillate composition, since each grape variety contains different concentrations of free and bound aromatic compounds (Agosin et al., 2000). The distillation equipment also plays a relevant role, although in Chile almost all piscos are distilled with the same technology. In Perú, some commercial piscos are distilled in Charentais alembics and others in batch distillation columns.
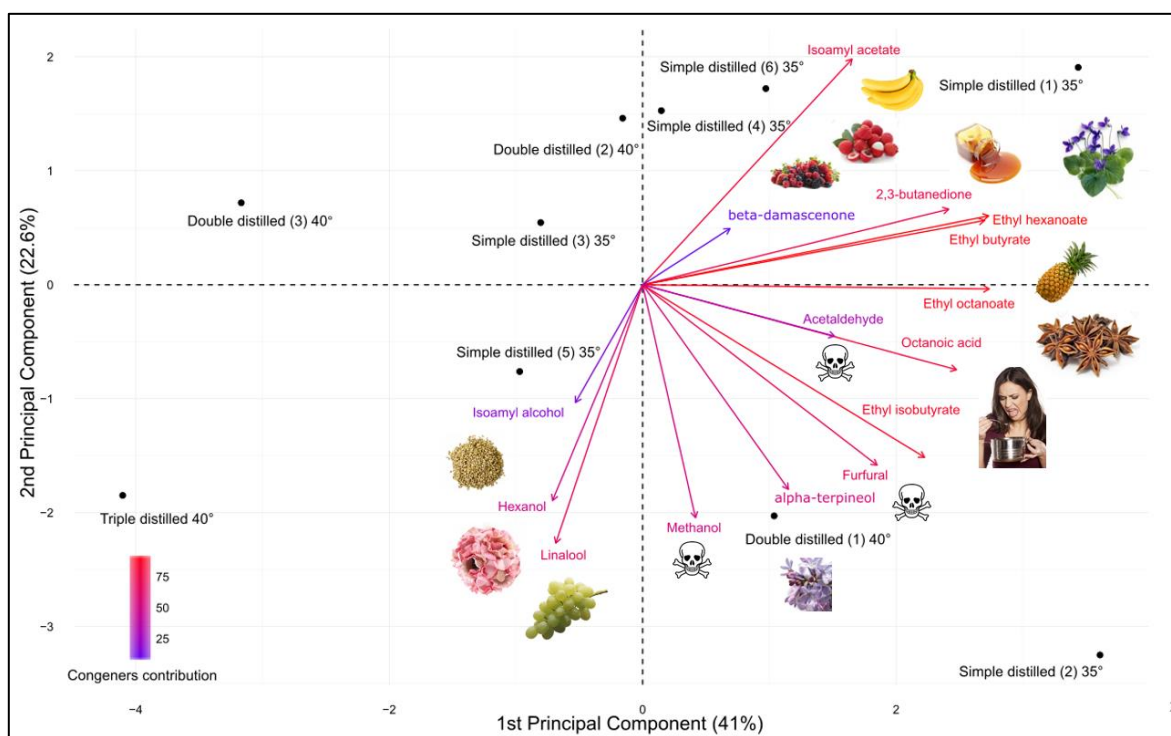
Figure 1-5. Principal component analysis of 10 commercial pisco considering 15 chemical markers.

Table 1-1. Concentration range and odor activity value of the most relevant aroma compound in Chilean commercial piscos.

Compounds	Odor description	Concentration (g/hL.a.a)[a]	Odor threshold (g/hL.a.a)	OAV[g]
Head compounds				
Acetaldehyde	Pungent	0-26	20.25[b]	0-1.3
2.3-butadione	Butter-like	0.07-0.3	4.7e-04[c]	149-638
β-damascenone	Cooked apple-like	0-0.11	6.6e-05[c]	0-1667
Fruity esters				
Ethyl acetate	Glue	12-20	25[d]	0.5-0.8
Ethyl hexanoate	Fruity	0.2-2	0.45[b]	0.4-4.4
Ethyl octanoate	Fruity	0.2-5	3[b]	0.1-1.7
Isoamyl acetate	Banana	0.3-3.2	0.02[e]	15-160
Terpenic compounds				
Linalool	Muscat, floral	0.08-1.4	0.25[f]	0.3-5.6
Geraniol	Citric, floral	0-0.1	0.75[f]	0-0.13
Nerol	Sweet, floral	0-0.18	10[f]	0-0.02
Alpha-Terpineol	Sweet, floral	0.12-2	75[f]	0.002-0.03
Higher alcohols				
2-methyl-1-butanol	Malty	14-35	91[b]	0.2-0.4
3-methyl-1-butanol	Malty	95-140	150.5[b]	0.6-0.9
Isoamyl alcohol	Whiskey, malt	55-80	20[e]	2.8-4
1-Hexanol	Green, flowery	1.8-8	6.8[c]	0.3-1.2

Table 1-1. Continued

Compounds	Odor description	Concentration (g/hL.a.a)[a]	Odor threshold (g/hL.a.a)	OAV[g]
Tail compounds				
Acetic acid	Vinegar	0-75	150[f]	0-0.5
Hexanoic acid	Rancid	0-0.9	2.5[b]	0-0.4
Octanoic acid	Fatty acid	0-3.8	0.625[b]	0-6.08
β-Phenylethanol	Roses, floral	0.03-15	5[f]	0.006-3
Methanol	Alcoholic, toxic	17-83	127.5[b]	0.1-0.7
Furfural	Smoky, burned	0-8	10.2[d]	0-0.8

[a] Commercial piscos analyzed: Gobernador, Fundo los nichos 40°, Alto del Carmen 40°, Artesanos del Cochiguaz, Capel 40°, Capel 35°, Capel DD 35°, Alto del Carmen 35°, Control, La serena, Valle del Limarí, Ruta Norte, Bauza 40°, Campanario, Mal paso.

[b] Mean values determined in 40% v/v ethanol reported in (Christoph and Bauer-Christoph 2007)

[c] Values determined in 60% v/v ethanol reported in (Willner, Granvogl, & Schieberle, 2013)

[d] Values determined in 20% v/v ethanol reported in (Clutton & Evans, 1978)

[e] Values determined in 10-15% v/v ethanol reported in (E Bordeu et al., 2012)

[f] Values determined in 40% v/v ethanol reported in (Cacho, Moncayo, Palma, Ferreira, & Culleré, 2012)

[g] Odor activity value expressed in units of aroma (u.a) were calculated by dividing the congeners concentrations by the respective odor threshold.

To analyze the sensory properties of different pisco distillates, Bordeu *et al.* (2004) developed the "pisco wheel" (Figure 1-6). This wheel is organized into three concentric levels, going from general to more specific descriptors in the outer ring. A total of 48 terms are proposed in this outer ring, far less than those proposed in other wheels. Several of the terms proposed are similar to those proposed for other spirits; however, some terms are specific for young spirits with Muscat aroma, like geraniol, linalool, raisin and honey (Bordeu, Agosín, and Casaubon 2012; Bordeu, Formas, and Agosin 2004). Descriptors like vanilla, oak and toasted are important even for lightly aged piscos. Vanilla, raisins, linalool, charcoal and prunes were

the most frequently used descriptors during the development of the pisco wheel (Bordeu et al. 2004).
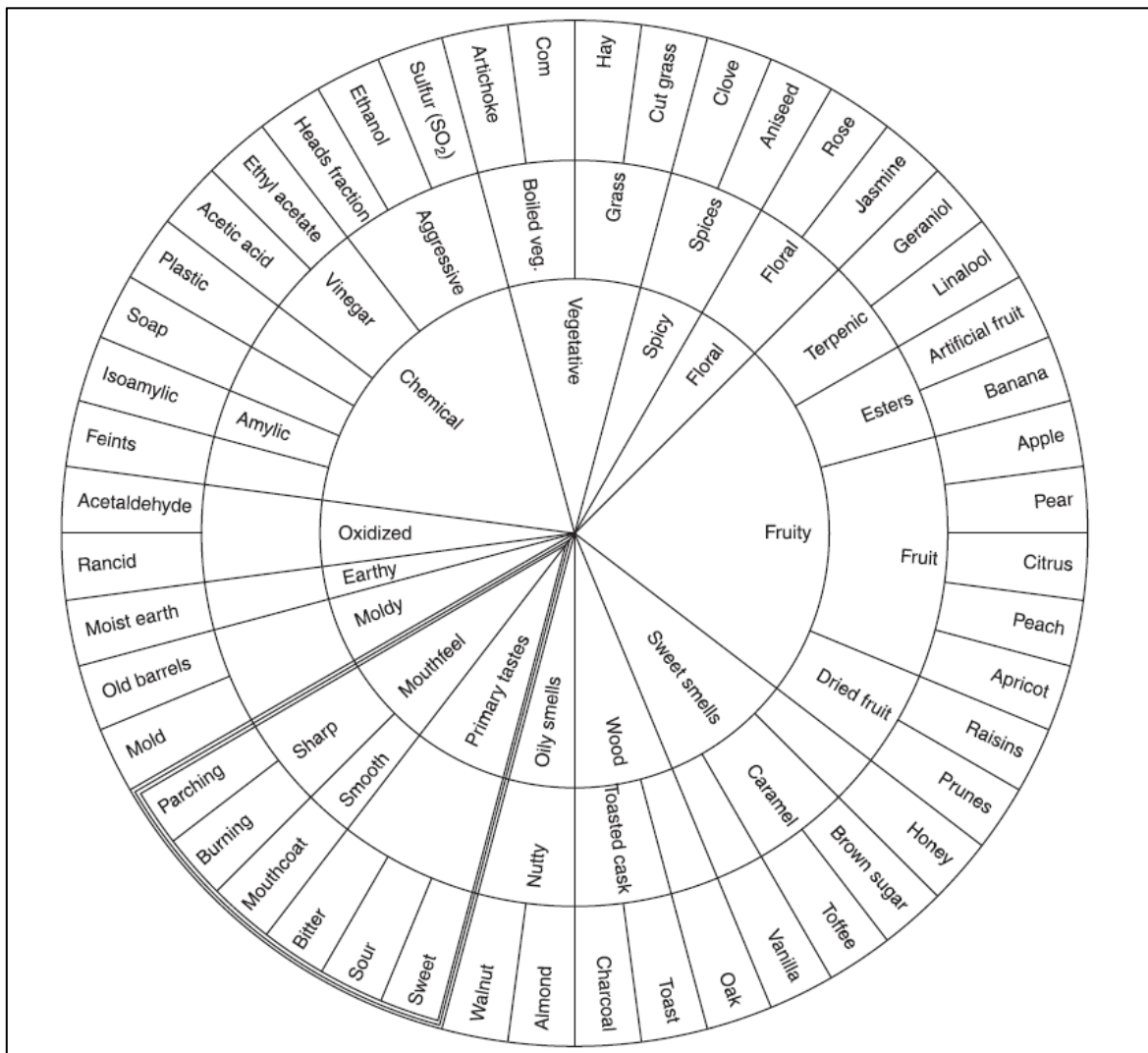
Figure 1-6. Pisco and mouth-feel Wheel, displaying its 48 outer-ring descriptors from Bordeu *et al.* (2004).

1.7 Modeling and simulation

Batch distillation is probably the oldest operation for separating liquid mixtures and became widely used for the production of fine chemicals and specialized products such as essential oils, perfume, pharmaceutical, petroleum products and alcoholic beverages. The main advantages of batch distillation over continuous distillation lie in the use of a single column as opposed to multiple columns and its flexible operation (Mujtaba, 2004).

Mathematical models have been used to design and better understand the operation of certain processes. To optimize batch distillation, a dynamic model should predict the behavior of the operation. Thus, key process variables (model outputs) such as chemical composition, productivity and energy consumption, should be predicted according to the specified manipulated and design variables (input variables). In the distillation of alcoholic beverages, much effort has been devoted to study the impact of operating strategies on the aromatic composition of the distillate. Experimental studies in a packed batch distillation column reported that low reflux rates at the beginning of the heart cut could produce distillates with an enhanced floral aroma (Matias-Guiu et al., 2016; Rodríguez-Bencomo et al., 2016). Nevertheless, these strategies were defined by trial and error, which is expensive and time consuming. Suitable operating strategies can be developed much faster and reliably using model-based design (Sacher et al., 2017). Mathematical models can be derived directly from experimental data (empirical models) or from fundamental relationships that rely on knowledge of the process (first principles, physics-based, phenomenological models). Sometimes, a combination of these two approaches (hybrid models) yields excellent results. Phenomenological models are preferred when few experimental data are available and when we need to predict in a wide range of operating conditions. In spirits distillation, first principles models include mass and energy balances, hydraulic model, physical properties and thermodynamic equilibrium relationships. For dynamic operation and batch distillations, these models are described by a set of differential and algebraic equations (DAEs). Several phenomenological models have been developed to explore new operating strategies for wine batch distillations in tray columns (Osorio et al., 2004), in packed rectification column (Carvallo et al., 2011), in alembics (Scanavini et al., 2012; Scanavini et al., 2010) and in copper Charentais alembics (Sacher et al., 2013). In Chapters III and IV of this thesis, a Charentais alembic model has been developed and validated with ternary (ethanol-water-

methanol) (Luna et al., 2018) and multi-component experimental data (ethanol-water plus six congeners) (Luna et al., 2019).

1.7.1 Thermodynamic modeling of congeners in wine
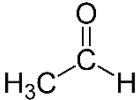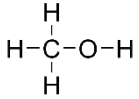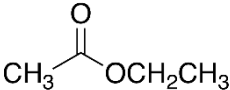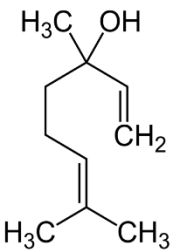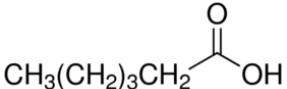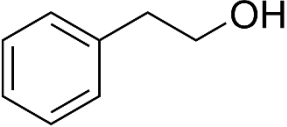
Thermodynamically, wine is a highly non-ideal solution that contains several hundred minority volatile components. These compounds are affected by their solubility in water and ethanol during distillation, as well as by their relative volatility and their chemical interactions. To estimate the relative volatility of each congener, several non-ideal thermodynamic approaches have been applied to model the vapor liquid equilibrium (VLE) properties of the mixtures. Most of these are either correlating models or semi-predictive models. NTRL, Wilson and UNIQUAC are correlating models widely used in the literature (Prausnitz, Lichtenthaler, & de Azevedo, 1998), where model parameters are calibrated using experimental data from binary systems (Valderrama et al., 2001; Valderrama et al., 2000). Semi-predictive models such as SAFT (Statistical Associating Fluid Theory), PSRK (Predictive Soave Redlich Kwong) and UNIFAC (Universal Functional Activity Coefficient), can be used to predict the behavior of new compounds, but these should belong to the same family of previously studied compounds or at least contain the same functional groups of previously studied molecules. Still, model parameters (applicable to a broader range of molecules) should be calibrated with experimental data. Purely empirical models, like artificial neural networks (ANN), have been also used to model VLE properties (Faúndez, Quiero, & Valderrama, 2010, 2011).

According to Valderrama *et al.* (2012), most of the times the NTRL model gives the best result and it is the one recommended for modeling and simulation of alcoholic beverage distillation. Nevertheless, in several cases no experimental data is available to obtain the binary or ternary interactions parameters required by the NTRL model. A good alternative is the UNIFAC model which corresponds to the group contribution version of the UNIQUAC model (Fredenslund, 1977). This model only needs to identify the functional subgroups present in each molecule by means of the UNIFAC group. Then, the activity coefficient for each species is calculated as the sum of a combinatorial part and residual part, both evaluated by the group contribution method. Using UNIFAC in predictions of Muscat wine distillations have been accurate for some congeners, such as methanol, ethyl hexanoate, octanoic acid and

linalool (Osorio et al., 2004). Sacher et al. (2013) developed a quasi-binary model of ethanol-water plus congeners, using a UNIFAC model to calculate the activity coefficients. The quasi-binary model assumed infinite dilution of each congener in the water-ethanol mixture (given the extremely low concentrations of the congeners); hence, these congeners do not influence the equilibrium temperature, enthalpy or physical properties of the mixture. This model obtained accurate predictions for seven compounds (acetaldehyde, ethyl acetate, ethyl hexanoate, methanol, 2-methyl-1-propanol, 2-methyl-1-butanol and 3-methyl-1-butanol) during an alembic distillation of pear wine (Sacher et al., 2017).

In our research, we applied Sacher approach to predict the behavior in Muscat wine distillations of six congeners: acetaldehyde, ethyl acetate, methanol, linalool, β-Phenylethanol and hexanoic acid (Luna et al., 2019). Table 1-2 shows the functional subgroups of each congener included in this study. Accurate predictions were obtained, and this model supports the multi-objective optimization method we developed to improve the aromatic quality of Muscat wine distillates (Chapter IV of this thesis).

Table 1-2. Thermodynamic properties of congeners used in Luna *et al.* (2018).

Congener	Structure	UNIFAC groups	Antoine parameters		
			A (mmHg)	B (mmHg K)	C (K)
Acetaldehyde		1 CH3 1 CHO	16.248	2465.148	-37.150[a]
Methanol		1 CH3OH	18.533	3600.017	-35.171[a]
Ethyl acetate		1 CH3 1 CH2 1 CH3COO	16.182	2763.631	-60.926[a]
Linalool		3 CH3 3 CH2 2 CH 2 C 1 OH	19.705	6110.099	-2.32[b]
Hexanoic acid		1 CH3 4 CH2 1 COOH	23.662	7825.227	-9.0018[b]
β-Phenylethanol		5 ACH 1 AC 2 CH2 1 OH	21.753	7273.03	0[a]

[a] Data from Sacher *et al.* (2013).
[b] Chemical ecology database (Byers, 1997).

1.8 Dynamic optimization

In the batch distillation process, usually the optimization problem considers different goals for solving the problem such as to minimize distillation time, maximize the amount of distillate, maximize a key component that defines the quality in a fixed time and maximize economic profit or minimize energy consumption along the distillation (Diwekar, 1995; Mujtaba, 2004). In the distillation of spirits, the aim is to obtain a distillate rich in fruity and floral aromas and free of off-flavors and toxic compounds. Additionally, distillers look for higher yields and less energy consumption. The reflux rate and the heating power rate in the boiler are the most common optimization variables in batch distillations.

To solve numerically optimization problems, a reliable model of the process is required. In particular, dynamic optimization requires process models that are usually described by differential and algebraic equations (DAE). A dynamic optimization problem involving lumped parameter models can be formulated as follows:

$$\min_{u(t)} J\left(\frac{dz}{dt}, z(t), u(t)\right) \qquad (1\text{-}1)$$

$$y\left(\frac{dz}{dt}, z(t), u(t)\right) = 0 \qquad (1\text{-}2)$$

$$g\left(\frac{dz}{dt}, z(t), u(t)\right) \geq 0 \qquad (1\text{-}3)$$

where J is the cost function, $z(t)$ is the state variables, y is the algebraic variables, g is the inequality constraints and $u(t)$ is the decision variables (manipulated variable of the process). The optimization of DAE systems can be solved by different discretization approaches such as sequential and simultaneous. The sequential approach solves the objective function (Eq. 1-1) and model equations (Eq. 1-2) in successive evaluations

(Safdarnejad et al., 2015). This means that the differential equations are solved independently from the optimization routine. Each optimization iteration is solved sequentially, until the optimization routine converges to given tolerances for the objective function and constraints (Beal et al., 2018; Hedengren et al., 2014) (Figure 1-7). The sequential approach is relatively easy to code and is most useful when a reliable process model is already available or when the solution of the DAE system is extremely difficult (Beal et al., 2018; Luna et al., 2018).
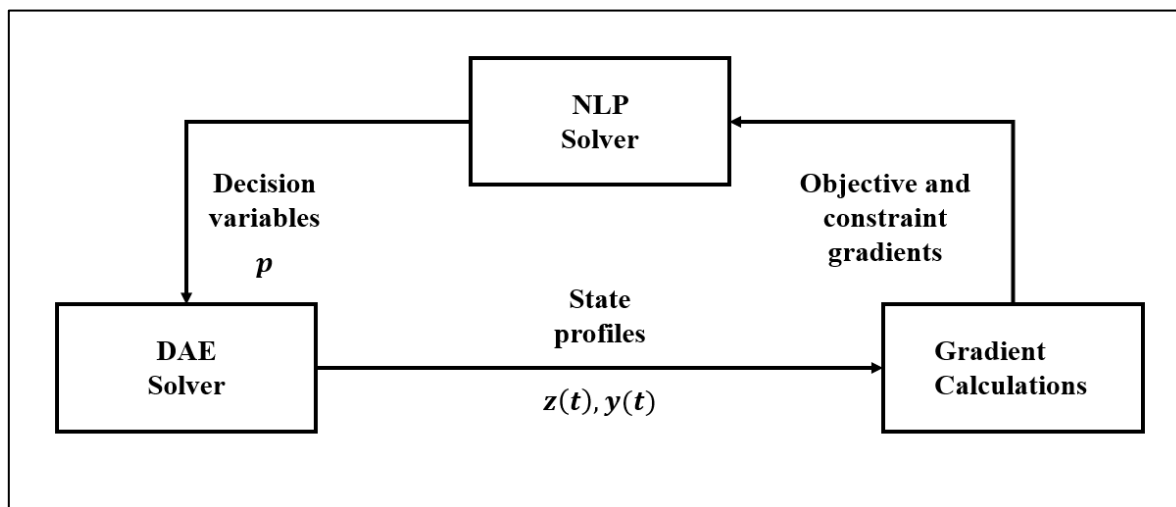
Figure 1-7. Scheme of the sequential dynamic optimization approach. Adapted from Biegler (2010).

In the simultaneous approach or direct transcription method, the objective function and all the equations (equality and inequality constraints) are solved simultaneously (Eqs. 1-1, 1-2 and 1-3). The differential equations are discretized and translated into algebraic equations through orthogonal collocation on finite elements to solve the objective function and the model equations simultaneously (Kameswaran & Biegler, 2006). In orthogonal collocations the state and control variables inside each finite element are described with polynomials (Figure 1-8). To perform well, simultaneous methods require efficient large-scale NLP solvers and accurate problem information, such as exact second derivatives (Beal et al., 2018). Nonlinear solvers such as IPOPT (Interior Point OPTimizer) (A. Waechter & Biegler, 2006) and APOPT/BPOPT (for Advanced Process OPTimizer) (APMonitor, 2018) are well suited for this task. In addition, there are software packages particularly suitable to solve dynamic optimization problems using the simultaneous approach, such as AMPL (Fourer et

al., 1990), GAMS (Bisschop & Meeraus, 1982) and GEKKO (Beal et al., 2018) where exact first and second derivatives can be obtained.
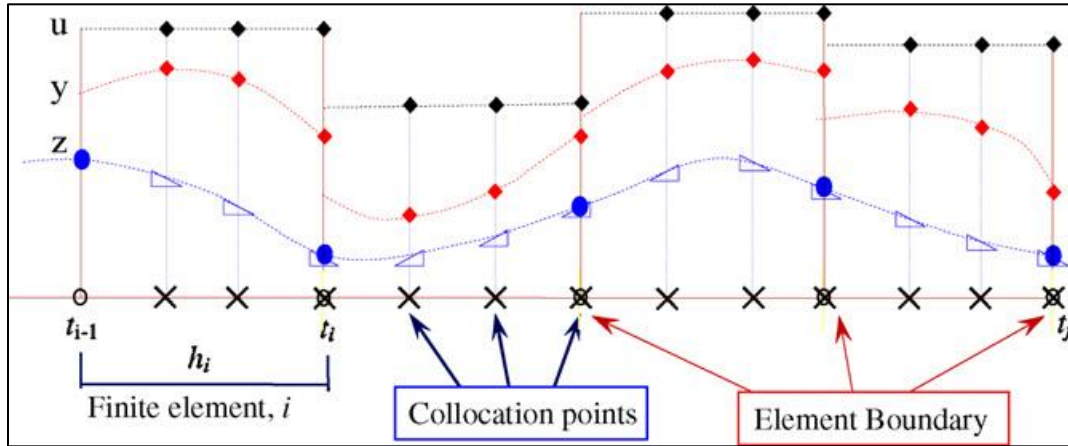
Figure 1-8. Collocation on finite elements. The diamonds represent u and y at collocation points. The triangles represent $\frac{dz}{dt}$ at collocation points and the circles represent z at element boundaries (Biegler, 2007).

In this thesis, sequential and simultaneous approaches for multi-objective dynamic optimization in Charentais copper alembic batch distillations were applied (Chapter III and IV). In Chapter III, both approaches were used and compared for distillation of a ternary mixture of water-ethanol-methanol. Here, the sequential approach was applied using MATLAB with a metaheuristic algorithm for global optimization called scatter search (Egea et al., 2007). Whereas, the simultaneous approach was applied using AMPL with IPOPT solver. Both methods generated the same Pareto front despite different techniques and algorithms of optimization. In Chapter IV, the sequential method was applied using MATLAB and scatter search for a multi-component mixture using two multi-objective functions based on the weighting approach and PCA decomposition.

1.9 Automatic control

Automatic control in the process industries helps to improve productivity, economic profit, security and quality, among others. Most of the times, these objectives must be attained simultaneously. Developing process control strategies may be challenging, depending on the

process specification, for example the control accuracy needed, the kind of the process and their mode of operation.

In batch mode, the process has no steady states and usually presents time-varying and nonlinear dynamics. In batch distillation of alcoholic beverages, the operation of the process is subjected to several uncontrolled and unmeasured disturbances, such as raw material composition and environmental temperature (Luna, Duarte-Mermoud et al., 2018). Hence, automatic control is fundamental to ensure reproducible product quality and high productivities (Valenzuela, 2002). Usual controlled variables are boiler temperature, partial condenser temperature, and ethanol concentration in the distillate. Reflux rate in the partial condenser and heating power in the boiler are the most used manipulated variables.

Feedback control is a widely applied strategy in all engineering areas (Bennett, 1996) (Figure 1-9). In this strategy, the control effort $u(t)$ works to compensate the differences between the controlled variable $y(t)$ and the set-point $sp(t)$ caused by process disturbances $d(t)$.
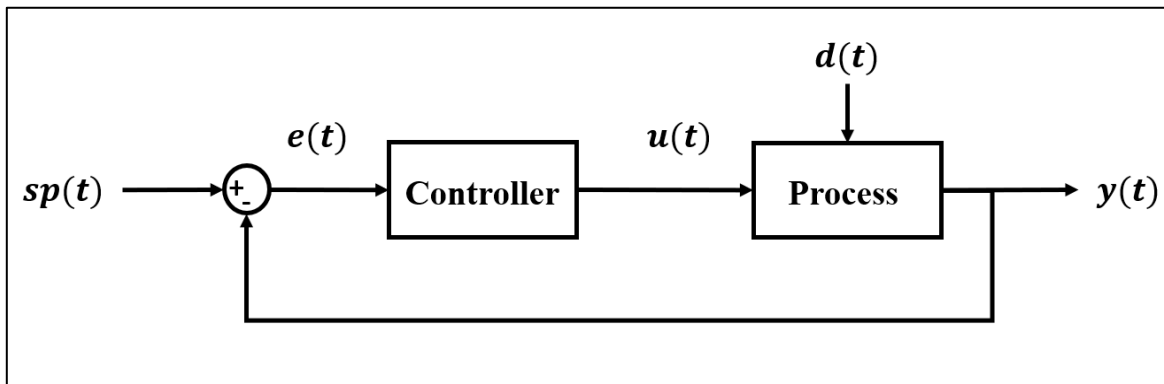
Figure 1-9. Classical feedback control strategy.

There are several control algorithms to design the controller. The PID (proportional-integral-derivative) controller is the most widely used in the industry since it is simple to code and apply, and there are many useful tuning methods (Ang, Chong, & Li, 2007; Li, Ang, & Chong, 2006). In the process industries, model based controllers such as internal model control (IMC) (Brosilow & Joseph, 2002), model predictive control (MPC) and nonlinear model predictive control (NMPC) (Camacho & Alba, 2013) are applied in special cases where PID yields unsatisfactory results. Nonlinear, interactive and time-varying dynamics

are particularly difficult to handle effectively with PID controllers. However, in many cases model-based controllers are difficult to design, code and tune.

Fractional order proportional-integral-derivative control (FOPID) and fractional order proportional-integral control (FOPI) have been widely investigated in the last decade since they usually provide good performance. These controllers are an extension of the classical PID and PI controllers plus two parameters that corresponds to the order of integration and order of differentiator. These extra tuning parameters add more flexibility that explain the improve performance (Shah & Agashe, 2016). Figure 1-10 shows that FOPID moves in the tuning plane continuously, instead of jumping between four fixed points like a standard PID (Hamamci, 2007; Shah & Agashe, 2016). Many applications have shown improved control with FOPID in the presence of disturbances, noisy environments and time-varying dynamics (Aguila-Camacho & Duarte-Mermoud, 2013).
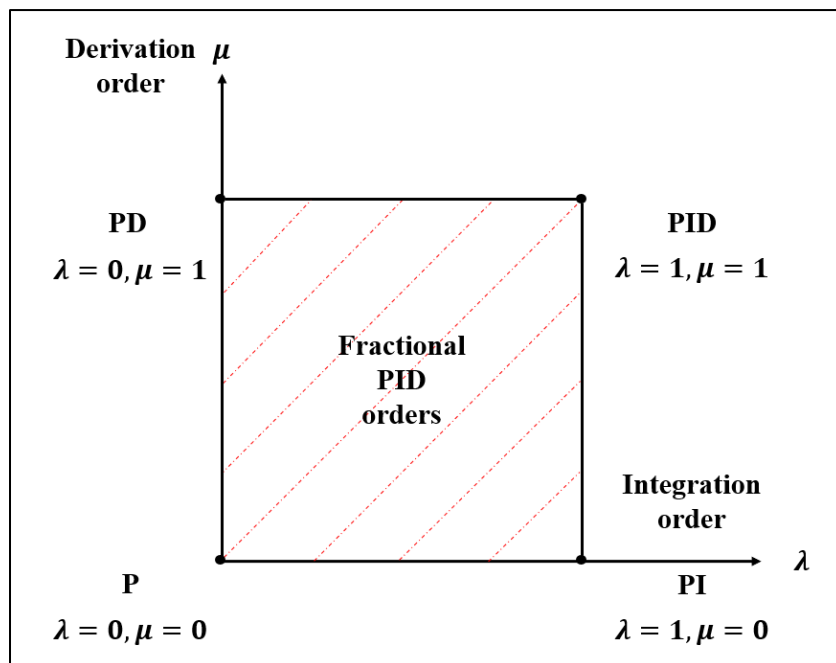
Figure 1-10. Convergence plane of fractional PID controller. Adapted from Shah *et al.* (2016)

Alembics in spirits distillations are normally operated manually in medium and small-scale distilleries. This operation is subjected to many uncontrolled and unmeasured disturbances that generate variability in the aromatic composition of the spirits (Luna et al., 2018; Luna et

al., 2019). In this study, an automatic distillation process control system was applied in a lab-scale alembic. Chapter 2 of this thesis reports the application of several controllers such as PI, PID, IMC and FOPID. These were designed, tuned, compared and simulated in several disturbance scenarios in (Luna, Duarte-Mermoud, et al., 2018). IMC control was validated and implemented in a Charentais alembic lab-scale, obtaining a reproducible operation despite disturbances in the environmental temperature and in the heating power (Chapter 3 and 4 of this thesis).

1.10 Hypothesis and objectives

Using a model-based optimal operation strategy in spirits distillations, it is possible to obtain reproducibly distillates with a predefined aromatic composition.

General objective

Develop and implement experimentally optimal operating strategies using a Charentais alembic that yield distillates rich in fruity and floral aromas and low in off-flavors and toxic compounds.

The specific objectives are:

- Develop, simulate and calibrate dynamic models to describe spirits distillations in a Charentais alembic.
- Develop a robust automatic control strategy for distillations in a Charentais alembic.
- Design optimal operating strategies for spirits distillations in Charentais alembics.

1.11 Approach of the thesis

Details regarding the specific objectives above are given in the different chapters of this doctoral thesis; each chapter is associated with a journal manuscript that have been submitted or already published (Figure 1-11).

Chapter II describes in detail the binary distillation model developed. This chapter focuses on the development and application of different control algorithms in a simulated Charentais copper alembic. Traditional controllers such as PI, PID and IMC are compared with FOPI

and FOPID. The controllers were tuned with simple rules and evaluated under different disturbance scenarios of environmental temperature and heating power. An automatic control system is proposed to ensure a reproducible operation in a real plant.

Chapter III describes in detail the ternary distillation model developed. This chapter focuses on the simultaneous optimization of ethanol recovery and methanol concentration in distillates produced in Charentais copper alembics. The sequential and the simultaneous dynamic optimization techniques were compared. The optimal strategy was validated experimentally using an automatic control system with an IMC controller.

Chapter IV describes in detail the multicomponent distillation model developed. This chapter focuses on a model-based methodology to generate operating recipes for Muscat wine distillations in Charentais alembics. The recipes were obtained by dynamic multi-objective optimization. Two multi-objective functions were developed, one including three chemical markers characteristic of each distillation cut (head, heart and tail), and the other applied principal component analysis (PCA) to reduce the composition dimensionality.

Modeling and Optimal Operation of Traditional Alembics to Distill Fruit Wines

Motivation
International sales of Chilean pisco are much smaller than national sales (1% of total production). Therefore, initiatives and strategies must be developed to allow for improvements in the production quality to diversify products and consolidate its presence in the international markets. The application of modern engineering tools would be a fundamental support to attain these goals.

General Objective
Develop and implement operating strategies for Charentais alembics to obtain reproducibly distillates rich in fruity and floral aromas and low in off-flavors and toxic compounds.

Hypothesis
Using a model-based optimal operation strategy in spirits distillations, it is possible to obtain reproducibly distillates with a predefined aromatic composition.

Objectives

How?

Develop and implement experimentally optimal operating strategies using a Charentais alembic that yield distillates rich in fruity and floral aromas and low in off-flavors and toxic compounds.

Optimization distillation strategies in Charentais alembics:

Minimize the relative methanol concentration and maximize the ethanol recovery in the distillate.

Minimize the toxic compounds and off-flavors and maximize terpenic compounds in the distillate.

Methodology

Automatic control

Modeling & Simulation

Model calibration

Congeners selection

Dynamic optimization

Experiment Distillation

Chapter II:
Fractional order control in Charentais alembic distillations

Chapter III:
Minimizing methanol content in experimental Charentais alembic distillations

Chapter IV:
Modeling and multi-objective optimization of synthetic Muscat wine distillations

Figure 1-11. Thesis general overview

CHAPTER 2: FRACTIONAL ORDER CONTROL IN CHARENTAIS ALEMBIC DISTILLATION

Ricardo Luna, Manuel A. Duarte-Mermound, José R. Pérez-Correa.

2.1 Introduction

Alembics have been used for many centuries in the production of several kinds of distilled alcoholic beverages, medicines and perfumes. In spirits distillation, alembics operating in batch mode are most commonly used in small-scale productions, where, compounds of different volatility need to be separated. Spirits mainly contain water and ethanol, but the distinctive aroma of these spirits is defined by minority compounds, called congeners. Spirits of high quality should be rich in fruit and floral aromas and low in off-flavours and toxic compounds.

Alembics are normally operated manually, subjected to the experience of the operator and to many uncontrolled and unmeasured disturbances such as raw material composition, cuts criteria during distillation, room temperature and time-varying parameters. All these disturbance generate variability in the composition of the final product (Luna et al., 2018). Consumers look for new spirits that are safe and have distinctive aromas, although it is hard and time consuming to adapt the distillation recipe to these demands and obtain a new product consistently. Mathematical models have been developed for exploring new operating recipes in wine distillations to produce spirits with defined characteristics in plate columns (Osorio et al., 2004), packed columns (Carvallo et al., 2011) and copper Charentais alembics (Sacher et al., 2013). To yield a defined product with reproducible aromatic characteristics, automatic control systems for Charentais alembics have been developed and implemented. Control of alembic distillation systems is challenging since they are nonlinear and present time-varying dynamics (batch process). Few papers have been published on the control of alembic batch distillation systems. Fernandez *et al.* (2016) developed a novel strategy based on the Hill repressor equation (Goutelle et al., 2008) to operate automatically a copper Charentais alembic and its performance was compared with an internal model control (IMC) algorithm (Brosilow & Joseph, 2002). The control system aimed to track a predefined optimal path of

the alembic's head temperature (set-point), by manipulating the heating power of the boiler. Both, Hill and IMC controllers achieved good performance in tracking the set-point employing similar control efforts, although the Hill controller was much easier to tune. IMC needs a good process model, while the Hill controller (Pérez-Correa, Lefranc, & Fernández-Fernández, 2015) does not require any model and good tuning can easily achieved by trial and error. Luna *et al.* (2018) assessed experimentally an automatic control system for a Charentais alembic using an IMC control algorithm. This control system tracked closely the predefined variable set-point in the alembic's head temperature despite disturbances like room temperature. Small variations in the manipulated variable compensated these disturbances efficiently.

PID controllers have been commonly and widely used in several industries since they are simple and easy to tune, although they usually cannot handle adequately time-varying and non-linear dynamics (Aguila-Camacho et al., 2017). Since there are not many papers dealing with the control of Charentais alembics, which present time-varying and non-linear dynamics (Luna et al., 2018), it is worth exploring the suitability of PID controllers and compare its performance with more advanced algorithms. Fractional order proportional integral derivative control (FOPID) and fractional order proportional integral control (FOPI) based on derivative and integral fractional operators have shown to be a good option to achieve robust control in the presence of strong disturbances, noise and time-varying dynamics (Aguila-Camacho & Duarte-Mermoud, 2013). In the last two decades there has been much interest in applying fractional order operators (FOO) to model and control dynamical linear and nonlinear systems. By fractional order control (FOC) it is understood the used of integral or derivative operators whose order are not integer but real numbers, expanding the space where the controller parameters can be tuned to achieve better performance. Numerous applications of FOC have been reported in the technical literature informing some advantages of using FOC control schemes compared to the traditional integer order controllers (IOC).

In Jauregui *et al.* (2016b) the experimental level control of a conical tank is addressed using IOPI and IOPID control strategies and compared with their FO counterparts (FOPI/FOPID). The results are compared with a PI control strategy whose parameters are tuned using the Root Locus (RL) method considering a linearized model of the tank around three different

operating points. The parameters of the IOPI/IOPID and the FOPI/FOPID were obtained using the Particle Swarm Optimization (PSO) method, considering as a performance index the integral of the absolute error (IAE), and taking into account the information provided by the nonlinear model without approximations around operating points. The same analysis but with simulations was reported in Jauregui *et al.* (2016a). Ortiz-Quisbert *et al.* (2018) extended the results obtained in Aguila-Camacho & Duarte-Mermoud (2013), where the control strategies for fractional order model reference adaptive control (FOMRAC) and FOPID control applied to an automatic voltage regulator (AVR). The gains and orders of the controllers FOPID and FOMRAC, were obtained using three different tuning methods; sequential quadratic programming (SQP), particle swarm optimization (PSO), and genetic algorithms (GA), considering IAE as performance index. The performance of the proposed controllers was compared with those obtained with PID and MRAC controllers optimized by GA. By means of suitable performance criteria it was concluded that FOC optimized by PSO improve the behaviour of the controlled system, specifically the robustness against model uncertainties and the speed of convergence.

Other successful applications of FOC include simulations of level and pH control (Aguiar, Franco, Leonardi, & Lima, 2018), experimental pH control (Meenakshipriya, Prakash, & Maheswari, 2015), bioreactors control (Vali, Rezaei Estakhrouiyeh, & Gharaveisi, 2016; Vinopraba, Sivakumaran, Narayanan, & Radhakrishnan, 2013) and experimental and magnetic levitation plant (Gole, Barve, Kesarkar, & Selvaganesan, 2014; Swain, Sain, Mishra, & Ghosh, 2017).

In this paper we present a comparison among IOPID, IOPI, FOPID and IMC controllers, in a simulated Charentais alembic distillation system. The control system aims to track the alembic head temperature, whose evolution has been predefined by dynamic optimization to ensure a standard quality of the distillate. IOPI, IOPID and FOPID controllers were tuned by a simple rule-based on the minimization of the integrated absolute error. IMC control was tuned using the IMCTUNE software (Brosilow & Joseph, 2002). Controllers performance was assessed using standard cost functions such as IAE, ITAE, ISE, IAI and ISI in six simulation scenarios with different kinds of disturbances.

The paper is organized as follows: Section 2.2 describes the distillation process of the Charentais alembic copper, the nonlinear model used for alembic's simulations, their conditions and operating variables. Section 2.3 introduces the design of controllers, tuning methods and their implementation. Whereas Section 2.4 describes the different simulation cases and their corresponding results. Finally, Section 2.5 presents the main conclusions of this work.

2.2 Alembic distillations

2.2.1 Model description

The dynamic phenomenological nonlinear model validated by Luna *et al.* (2018) and Luna et al. Luna *et al.* (2019) is used to apply the proposed FOC algorithms. The model describes the laboratory scale distillation batch of an alembic copper Charentais. The model includes two inputs: electric heating power $\dot{Q}_{Cal}$ (manipulated variable) and room temperature T_{env} (disturbance). The model outputs are the head temperature of the alembic T_c (controlled variable), the distilled volume V, the alcohol strength in the distillate and the congeners concentration in the distillate. The temperature in the alembic´s head T_c is related to the liquid-vapor equilibrium that defines the ethanol recovery curve. In turn, the relative volatility of each congener (i.e., its tendency to evaporate) is defined by the ethanol concentration in the boiler. In this work, we consider only the binary model (ethanol-water mixture) to simulate the different controllers. To ensure the reproducibility of the process, the control objective is to track the head temperature of the alembic T_c by manipulating the electric heating power $\dot{Q}_{Cal}$, considering disturbances in the room temperature T_{env} and the heating power $\dot{Q}_{Cal}$ (Figure 2-1). The model includes two dynamic mass balances (total mass and ethanol) and a dynamic energy balance in the boiler, as well as two steady state mass balances (total mass and ethanol) and a stationary energy balance in the partial condenser. Several constitutive equations were included to describe the heat loss to the environment and empirical correlations to describe the vapor/liquid equilibrium of the ethanol-water mixture. The model is described in detail in what follows. The nomenclature of the variables and their units are presented in Table 2-1.

Table 2-1. Model nomenclature and variables description.

Variable	Units	Description
M_B	mol s^{-1}	Molar hold-up in the bottom
L	mol s^{-1}	Liquid natural reflux flow
V_B	mol s^{-1}	Vapor flow from the bottom
V_D	mol s^{-1}	Distillate flow
x_B	mol mol^{-1}	Ethanol molar fraction in the bottom
x_L	mol mol^{-1}	Ethanol molar fraction in the liquid reflux
y_B	mol mol^{-1}	Ethanol molar fraction in the vapor flow from the bottom
y_D	mol mol^{-1}	Ethanol molar fraction in the distillate flow
H_B	J mol^{-1}	Molar specific enthalpy in the vapor flow
H_D	J mol^{-1}	Molar specific enthalpy in the distillate flow
h_B	J mol^{-1}	Molar specific enthalpy in the bottom
h_L	J mol^{-1}	Molar specific enthalpy in the liquid reflux
u_B	J mol^{-1}	Molar specific internal energy in the bottom
T_B	K	Boiler temperature
T_C	K	Head temperature (controlled variable)
T_{env}	K	Room temperature
$\dot{Q}_B$	W	Net heat rate to the alembic bottom
$\dot{Q}_C$	W	Heat loss to the environment from the neck
$\dot{Q}_{Cal}$	W	Electric heating power (manipulated variable)
ρ	kg m^{-3}	Density of the liquid mixture
ρ_W	kg m^{-3}	Water density
ρ_E	kg m^{-3}	Ethanol density
Mw_W	g mol^{-1}	Water molar weight
Mw_E	g mol^{-1}	Ethanol molar weight
$Mw_{mixture}$	g mol^{-1}	Water-Ethanol weight
ϕ	mL mol^{-1}	Apparent molal volume
F	mL min^{-1}	Distillate flow rate
V	mL	Distillate volume
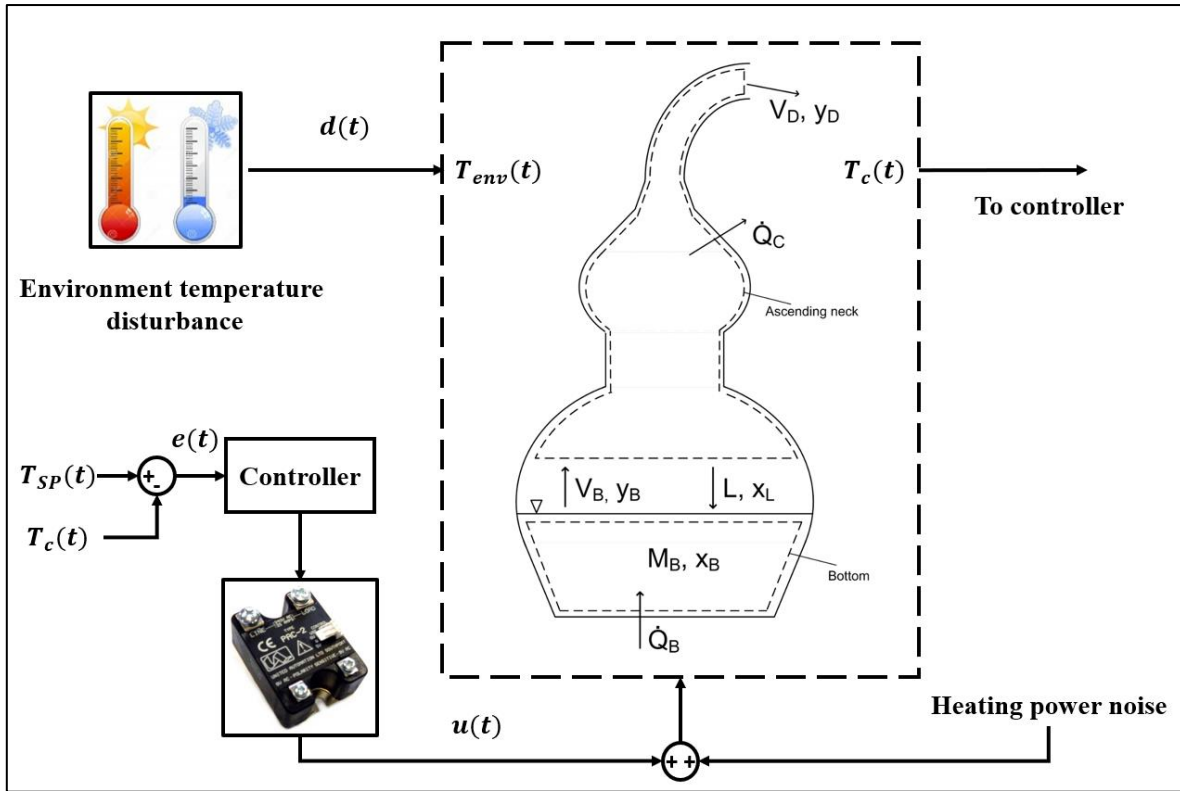
Figure 2-1. General diagram of automatic alembic distillation system.

a) Dynamic balances in the boiler,

$$\frac{d(M_B)}{dt} = L - V_B \tag{2-1}$$

$$\frac{d(M_B \cdot x_B)}{dt} = L \cdot x_L - V_B \cdot y_B \tag{2-2}$$

$$\frac{d(M_B \cdot u_B)}{dt} = L \cdot h_L - V_B \cdot H_B + \dot{Q}_B \tag{2-3}$$

b) Steady state balances in the partial conderser,

$$V_B - L - V_D = 0 \tag{2-4}$$

$$V_B \cdot y_B - L \cdot x_L - V_D \cdot y_D = 0 \tag{2-5}$$

$$V_B \cdot H_B - L \cdot h_L - V_D \cdot H_D - \dot{Q}_C = 0 \tag{2-6}$$

c) Heat transfer model

$$\dot{Q}_B = \dot{Q}_{cal} - UA_b \cdot (T_B - T_{env}) \tag{2-7}$$

$$\dot{Q}_C = UA_c \cdot (T_C - T_{env}) \tag{2-8}$$

$\dot{Q}_{cal}$ is the heat input in the boiler, T_{env} is the room temperature, UA_b is the global heat transfer coefficient multiplied by the heat transfer area in the boiler, and UA_c is the global heat transfer coefficient multiplied by the heat transfer area in the partial condenser. After fitting with experimental distillations, the following correlations were obtained,

$$UA_b = \frac{(0.349 - 0.840)\left(\dot{Q}_{cal} - 230\right)}{(400 - 230)} + 0.840 \tag{2-9}$$

$$UA_c = \frac{(1.49 - 0.804)\left(\dot{Q}_{cal} - 230\right)}{(400 - 230)} + 0.804 \tag{2-10}$$

d) Thermodynamic equilibrium L-V for ethanol-water

$$\begin{aligned} y_{B,D} &= -59.6868501 - 89.4037240 \cdot x_{B,L} - \\ &\quad 39.8552042 \cdot x_{B,L}^{1.5} + 81.47664393 \cdot e^{x_{B,L}} \\ &\quad -21.7897938 \cdot e^{-x_{B,L}}, x_{B,L} \leq 0.1161 \end{aligned} \tag{2-11}$$

$$T_{B,C} = \begin{cases} 273.15 + \left(\begin{matrix} -0.02214517 - 0.05785120 \cdot x_{B,L}^{1.5} + \\ 0.032146591 \cdot e^{x_{B,L}} \end{matrix}\right)^{-1}, x_{B,L} \leq 0.1661 \\ 273.15 + \left(\begin{matrix} 278.3854921 - 141.465178 \cdot x_{B,L} + \\ 49.67113604 \cdot x_{B,L} \cdot \ln(x_{B,L}) + \\ 9.159930587 \cdot x_{B,L} - 184.225674 \cdot e^{-x_{B,L}} \end{matrix}\right), x_{B,L} \geq 0.1661 \end{cases} \tag{2-12}$$

$$h_{B,L} = \left(55.678 \cdot x_{B,L} + 75.425\right) \cdot T_{B,C} - 15208.44 \cdot x_{B,L} - 20602.34 \qquad \text{(2-13)}$$

$$H_{B,D} = 36172.03 - 2919.83 \cdot y_{B,D} +$$
$$\left(31.461 - 11.976 \cdot y_{B,D}\right) \cdot T_{B,C} + \left(4.063 \cdot 10^{-4} + 0.0734 \cdot y_{B,D}\right) \cdot T_{B,C}^2 \qquad \text{(2-14)}$$

e) Model simulation

The steady state balances in the partial condenser are reordered,

$$V_B = \frac{\dot{Q}_C}{(H_B - H_D) + \dfrac{(y_B - y_D)}{(x_L - y_D)} \cdot (H_D - h_L)} \qquad \text{(2-15)}$$

$$L = -\frac{-\dot{Q}_C}{(h_L - H_D) + \dfrac{(x_L - y_D)}{(y_B - y_D)} \cdot (H_D - H_B)} \qquad \text{(2-16)}$$

$$V_D = V_B - L \qquad \text{(2-17)}$$

The volume of the distillate is obtained from an empirical density correlation (Neuburg & Perez-Correa, 1994),

$$\rho = \frac{Mw_{mixture}}{\phi \cdot y_D + (1 - y_D) \cdot Mw_W / \rho_W} \qquad \text{(2-18)}$$

$$Mw_{mixture} = y_D \cdot Mw_E + (1 - y_D) \cdot Mw_W \qquad \text{(2-19)}$$

$$\phi = 10^3 \cdot \left(5.1214 \cdot 10^{-2} + 6.549 \cdot 10^{-3} \cdot y_D + 7.406 \cdot 10^{-5} \cdot (T - 273.15)\right) \qquad \text{(2-20)}$$

The distilled volume, V, and the accumulated ethanol, M_D, are given by,

$$F = \frac{V_D \cdot Mw_{mixture}}{\rho} \tag{2-21}$$

$$\frac{dV}{dt} = F \tag{2-22}$$

$$\frac{dM_D}{dt} = y_D \cdot V_D \tag{2-23}$$

V and M_D are the distilled volume and the ethanol moles in the accumulated distillate, respectively.

Dynamic balances in the boiler are rearranged,

$$\left(L(x_L - x_B) - V_B(y_B - x_B)\right)\left(\frac{\partial h_B}{\partial x_B} + \frac{\partial h_B}{\partial T_B}\frac{dT_B}{dx_B}\right) = L(h_L - h_B) - V_B(H_B - h_B) + \dot{Q}_B \tag{2-24}$$

This implicit function in x_L is solved iteratively at each integration step using MATLAB's *fsolve* routine.

2.2.2 Optimal operating condition

The defined operating conditions of the alembic were derived using a multi-objective dynamic optimization procedure Luna *et al.* (2019). The dynamic optimization problem looked for decision variables, such as heating power path and volume cuts in the distillate, that satisfied three objectives simultaneously. These correspond to chemical markers, characteristics of each cut in wine distillations. The heating power varied between 230 and 400 W and the final time of distillation was 59.1 min. However, dynamic optimization problem does not consider disturbances in the distillation system such as room temperature variations and noise in the heating power signal. Therefore, as shown in Figure 2-2, we designed a control system to track the optimal temperature (servo control), despite room temperature and heating power disturbances.
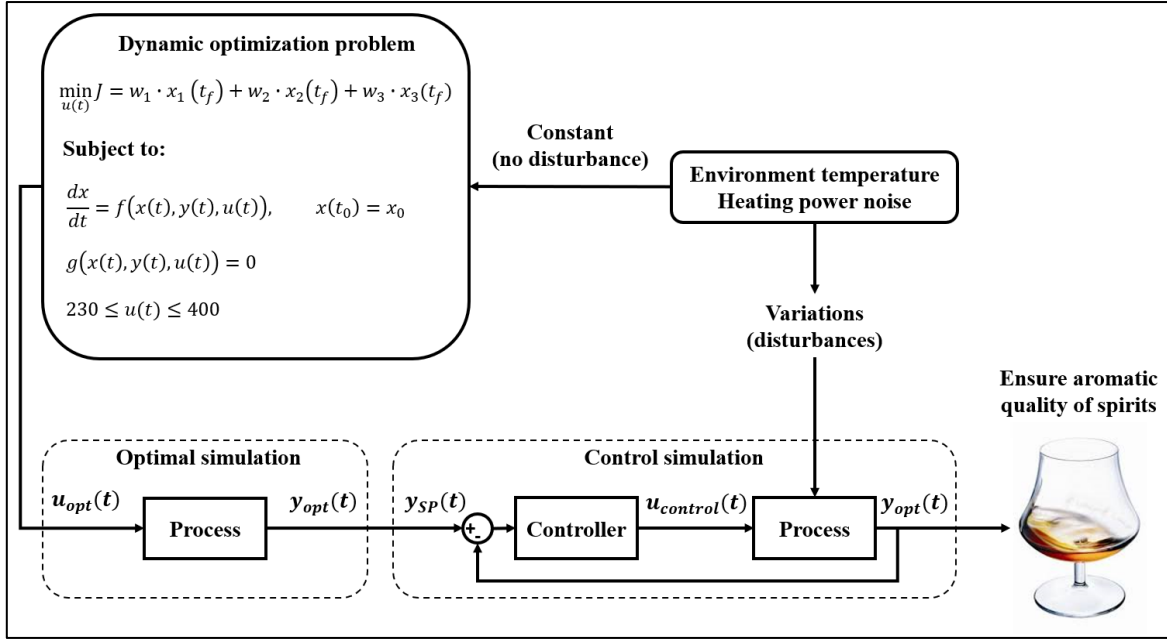
Figure 2-2. Optimal operating scheme and automatic control of Charentais alembic distillation.

2.3 Design, tuning and implementation of controllers

2.3.1 Integer and fractional PID controllers

A Standard FOPID controller in ideal (noninteracting) form is defined as (Padula & Visioli, 2015)

$$C_{FOPID}(s) = K_p \left(1 + \frac{1}{T_i s^\lambda} + T_d s^\mu \right) \frac{1}{T_f s + 1} \tag{2-25}$$

K_p, T_i and T_d are the standard PID tuning parameters, while λ and μ are the non-integer orders of the integral and derivative terms, respectively. In the case of IOPID controllers, λ and μ are equal to one (Shah & Agashe, 2016). To make the controller proper and filter high frequency noise, a first-order filter is used. A good choice for the time constant, T_f, is (Padula & Visioli, 2015)

$$T_f = min\left\{\frac{T_i^{\frac{1}{\lambda}}}{10}, \frac{T_d^{\frac{1}{\mu}}}{10}\right\} \tag{2-26}$$

2.3.2 IMC controller for an FOPDT process

Following Brosilow & Joseph (2002), the imc controller for a first order plus time delay plant (FOPDT) is given by,

$$C_{IMC}(s) = \frac{Ts + 1}{K \cdot (\varepsilon \cdot s + 1)^\alpha} \tag{2-27}$$

ε is the tuning parameter and α is the relative order of the inverse of the plant (in this case $\alpha = 1$).

2.3.3 Controller tuning

For tuning the controllers, the dynamics of the process plus sensor were fitted to a FOPTD transfer function as in Åström & Hägglund (2006),

$$P(s) = \frac{K}{Ts + 1} e^{-Ls} \tag{2-28}$$

This transfer function is defined as a representative nominal plant by linearizing the plant model around a wide range of operating points between 89 and 95°C at different times. Table 2-2 shows the fitted parameters and their ranges of variation.

Table 2-2. Transfer function parameters of the process model

Parameters	Minimum	Maximum	Average	units
K	0.006	0.015	0.010	K/W
L	8.00	8.53	8.13	s
T	40.8	49.5	45.0	s
τ	0.16	0.15	0.15	-

2.3.3.1 Tuning rules for IO/FO and PI and PID controllers

We used a tuning rule for optimal IOPID and FOPID controllers based on a first order plus dead time process. The tuning rules have been derived in order to minimize the integral of the absolute error (IAE) with a constraint on the maximum sensitivity. For IOPID controllers, we compared the tuning rules proposed by Murril and Smith (Smith & Corripio, 1985), Madhuranthakam *et al.* (2008) and Padula & Visioli (2011) in servo control. For FOPID controller the tuning rules proposed by Padula & Visioli (2011) were used, where the dynamic of the process is characterized by a normalized dead time defined as

$$\tau = \frac{L}{L + T} \tag{2-29}$$

which represents a measure of the difficulty in controlling the process. The rules were validated between $0.05 \leq \tau \leq 0.8$. The FOPID controller parameters were obtained by tuning rules designed in ideal form structure. Tuning rules for IOPID controller parameters were obtained from Padula & Visioli (2015) in series form structure. The values of the parameters for IOPID controller in ideal form (Eq. 2-25 with λ and μ equal one) can be obtained from a conversion proposed in Åström & Hägglund (2006). In this work, we used the setpoint following tuning and the maximum sensitivity value was $M_s = 2.0$ (aggressive control) for IOPID and FOPID controllers. The values of a, b, c and d are given in Padula & Visioli (2015) for each control parameter in FOPID ideal form and IOPID series form. Thus, the following expressions for the controller parameters are used (the proportional gain has the same expression for FOPID in ideal form and IOPID in series form),

proportional constant

$$K_p = \frac{1}{K}(a\tau^b + c) \tag{2-30}$$

integral and derivative time constants for FOPID in ideal form

$$T_i = T^\lambda (a\tau^3 + b\tau^2 + c\tau + d) \tag{2-31}$$

$$T_d = \mathrm{T}^\mu (a \cdot e^{b\tau} + c \cdot e^{d\tau}) \tag{2-32}$$

$$\lambda = 1 \tag{2-33}$$

$$\mu = a\tau^3 + b\tau^2 + c\tau + d \tag{2-34}$$

integral and derivative time constants for IOPID in series form

$$T_i = \mathrm{T}\left(a \left(\frac{L}{\mathrm{T}}\right)^b + c \right) \tag{2-35}$$

$$T_D = \mathrm{T}\left(a \left(\frac{L}{\mathrm{T}}\right)^b + c \right) \tag{2-36}$$

2.3.3.2 Tuning IMC controller

IMC controller was tuned using the IMCTUNE MATLAB toolbox (Brosilow & Joseph, 2002). The process model considered uncertain parameters for the gain, time constant and dead time between the minimum and maximum values given in Table 2-2. The IMC controller was designed with the average FOPTD model parameter values given in Table 2-2 and the order of the filter was defined equal to 1. The IMCTUNE results gave a filter constant equals to 2.5 seconds.

2.3.4 Performance indices

Five different performance criteria were used to assess the alembic control system; Integral of the absolute error (IAE), Integral of the squared error (ISE), Integral of the absolute input (IAI), Integral of the squared input (ISI) and Integral of the time weighted absolute error (ITAE) (Smith & Corripio, 1985). In addition, the error of the temperature and the control effort were standardized according to the maximum values of the temperature set-point and the heating power, respectively,

$$\hat{e}(t) = \frac{y(t) - y_{SP}(t)}{\max(y_{SP}(t))} \tag{2-37}$$

$$\Delta\hat{u}(t) = \frac{u(t) - u_o}{\max(u(t))} \tag{2-38}$$

IAE: Integral of the absolute error

$$IAE = \int_0^T |\hat{e}(t)| \cdot dt \tag{2-39}$$

ISE: Integral of the square error

$$IAE = \int_0^T \hat{e}(t)^2 \cdot dt \tag{2-40}$$

IAI: Integral of the absolute input

$$IAI = \int_0^T |\Delta\hat{u}(t)| \cdot dt \tag{2-41}$$

ISI: Integral of the square input

$$ISI = \int_0^T \Delta\hat{u}(t)^2 \cdot dt \tag{2-42}$$

ITAE: Integral of the time weighted absolute error

$$ITAE = \int_0^T |\hat{e}(t)| \cdot t \cdot dt \tag{2-43}$$

2.3.5 Implementation of controllers

IOPI, IOPID, FOPID and IMC controllers were implemented in MATLAB/Simulink. For the FO controllers the Ninteger Toolbox for Matlab/Simulink (Valerio & Da Costa, 2004) was used. Figure 2-3 shows the block diagram used to implement IMC and FOPID controllers where the NID block simulates a fractional derivate in the case of FOPID. The specifications of NID block were chosen as N=8 and frequency interval [0.001, 1000], according to tuning

rules in Padula & Visioli (2015), and Crone approximation (Oustaloup, 1991). Parameters T_i and T_d for IO and FO controllers were changed to K_i and K_d as follows

$$K_i = \frac{K_p}{T_i} \tag{2-44}$$

$$K_d = K_p \cdot T_d \tag{2-45}$$
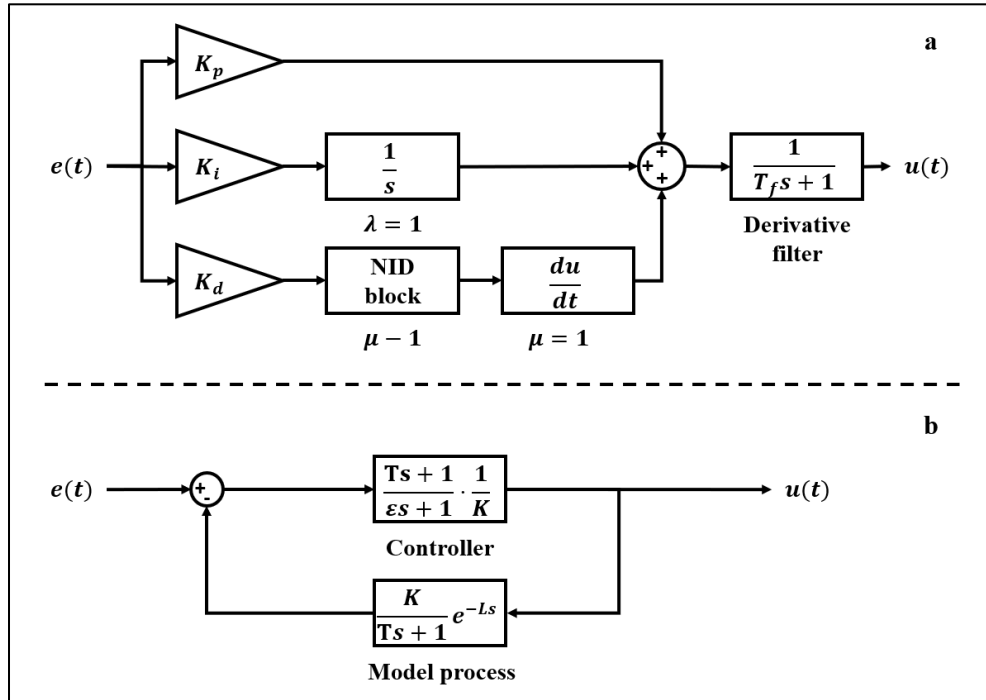
Figure 2-3. Blocks diagram for implementation of FOPID (a) and IMC (b) controllers.

2.4 Simulation results

2.4.1 Simulation environment

As mentioned in Section 2.2.2, we evaluated the controllers under several disturbance cases. The main disturbances are the room temperature and the heating power. We added white noise to the temperature and the heating power signals, where the noise power (NP) is defined as follows

$$NP = std^2 \cdot T_0 \tag{2-46}$$

where std is the standard deviation and T_0 is the sample time. The standard deviation of the white noise in the room temperature $w_{T_{env}}(t)$ and the heating power $w_{HP}(t)$ was set at $0.1°C$ and 15 W respectively, and the sample time was set at 10 seconds for both noises. The room temperature variations were constant, sinusoidal and colored noise (white noise passed through a first-order transfer function). The latter intended to simulate a non-periodic evolution of the room temperature. Six disturbance cases were simulated with a distillation time of 59.1 min,

i) Constant room temperature at 30°C plus white noise (case DT1).

ii) Sinusoidal round temperature around 30°C with amplitude of 2°C, plus white noise $w_{T_{env}}(t)$ (case DT2).

iii) Sinusoidal room temperature around 30°C with amplitude of 4°C, plus white noise $w_{T_{env}}(t)$ (case DT3).

iv) Sinusoidal room temperature around 30°C with amplitude at 4°C, plus white noise $w_{T_{env}}(t)$ and heating power plus white noise $w_{HP}(t)$ (case DT4).

v) Colored noise room temperature plus white noise $w_{T_{env}}(t)$ (case DT5).

vi) Colored noise room temperature plus white noise and heating power plus white noise $w_{HP}(t)$ (DT6).

2.4.2 Comparison of integer-order PID tuning rules

Table 2-3 shows the comparison of control parameters of IOPID controllers using rule-based on minimization the IAE proposed by Murril & Smith (1985), Madhuranthakam *et al.* (2008), and Padula & Visioli (2011). These tunings were evaluated in four disturbances cases; DT1, DT2, DT3, and DT4. Padula tuning obtained the best performance for IAE and ITAE indices in all cases. The relative indices of IAE and ITAE were calculated dividing the indices of Murril-Smith and Madhuranthakam by the indices of Padula to facilitate the comparison.

When the room temperature disturbance changed from purely white noise (DT1) to sinusoidal of moderate amplitude plus white noise (DT2), Padula tuning improved its relative

performance. For DT1, Padula tuning reduced the IAE and ITAE relative values in 15% and 13.5%, respectively, compared with Murril-Smith and Madhuranthakam tuning. In turn, for disturbance DT2, Padula tuning reduced the IAE and ITAE relative values by 17% and 19%, respectively. If the room temperature disturbance gets more aggressive (DT3), Padula tuning relative performance drops significantly (8% better in IAE and 5% better in ITAE). Finally, when noise was added to the heating power (DT4), the relative performance of Padula tuning decreased a little (6.5% better in IAE and 4.5% better in ITAE).

Figure 2-4 shows the simulations of IOPID controllers with the three tuning rules for the DT2 disturbance case. The control effort obtained with the Murril-Smith tuning was smoother and presented fewer peaks than the Padula and Madhuranthakam tunings. Similar behavior was observed in the DT3 case (Figure 2-5), although here the control effort was saturated for long periods. This explains why the Padula tuning was less effective under these strong disturbances.

Since Padula tuning presented better overall control performance, it was chosen to compare IOPID controller with FOPID and IMC controllers.

Table 2-3. IOPID parameters for tuning rules based on minimization of IAE and their control performance in different disturbances scenarios.

Tuning rules	Parameters			DT1		DT2		DT3		DT4	
	K_p	K_i	K_d	ITAE[*]	IAE[*]	ITAE	IAE	ITAE	IAE	ITAE	IAE
Murril-Smith	480	7.65	1575	244 (1.16)	0.501 (1.18)	729 (1.24)	0.723 (1.21)	3445 (1.06)	1.99 (1.09)	3680 (1.05)	2.11 (1.07)
Madhuranthakam	500	7.70	1285	242 (1.15)	0.495 (1.17)	721 (1.22)	0.719 (1.20)	3401 (1.05)	1.97 (1.08)	3647 (1.04)	2.10 (1.07)
Padula	454	9.50	1507	210 (1.00)	0.423 (1.00)	587 (1.00)	0.596 (1.00)	3245 (1.00)	1.82 (1.00)	3496 (1.00)	1.97 (1.00)

[*] Relative ITAE and IAE values in parentheses were calculated dividing by ITAE and IAE obtained from Padula respectively in each disturbance scenarios.
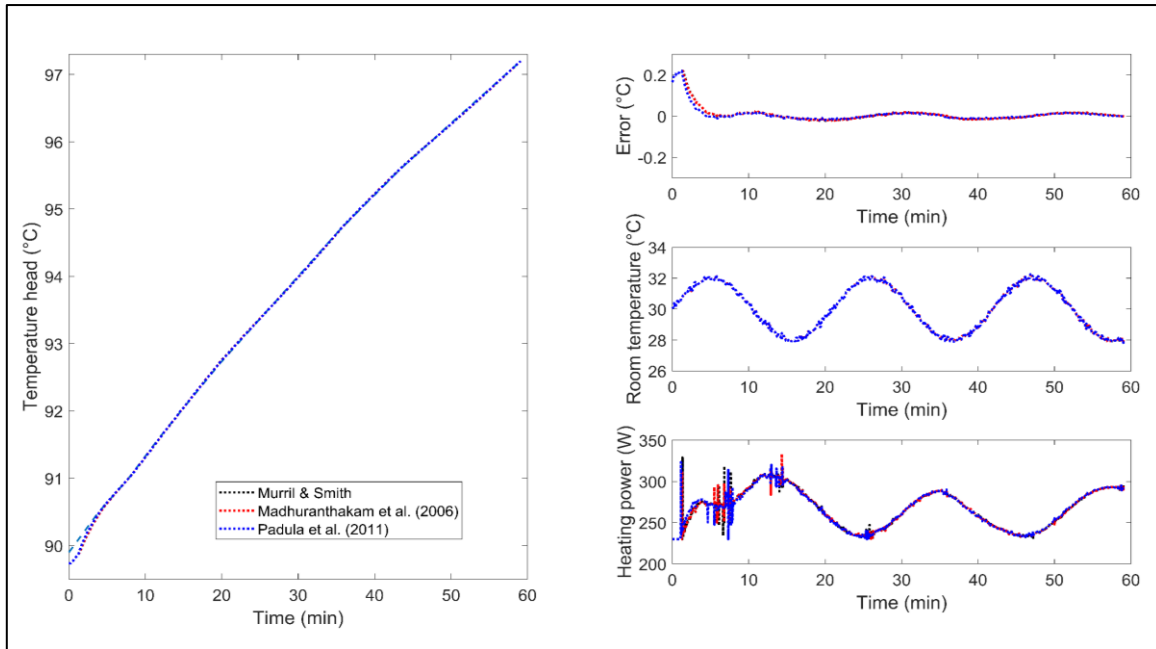
Figure 2-4. Behavior of the controlled variable and manipulated variable in the presence of sinusoidal disturbance (amplitude 2°C) in room temperature (DT2) for three tuning rules of IOPID controllers.
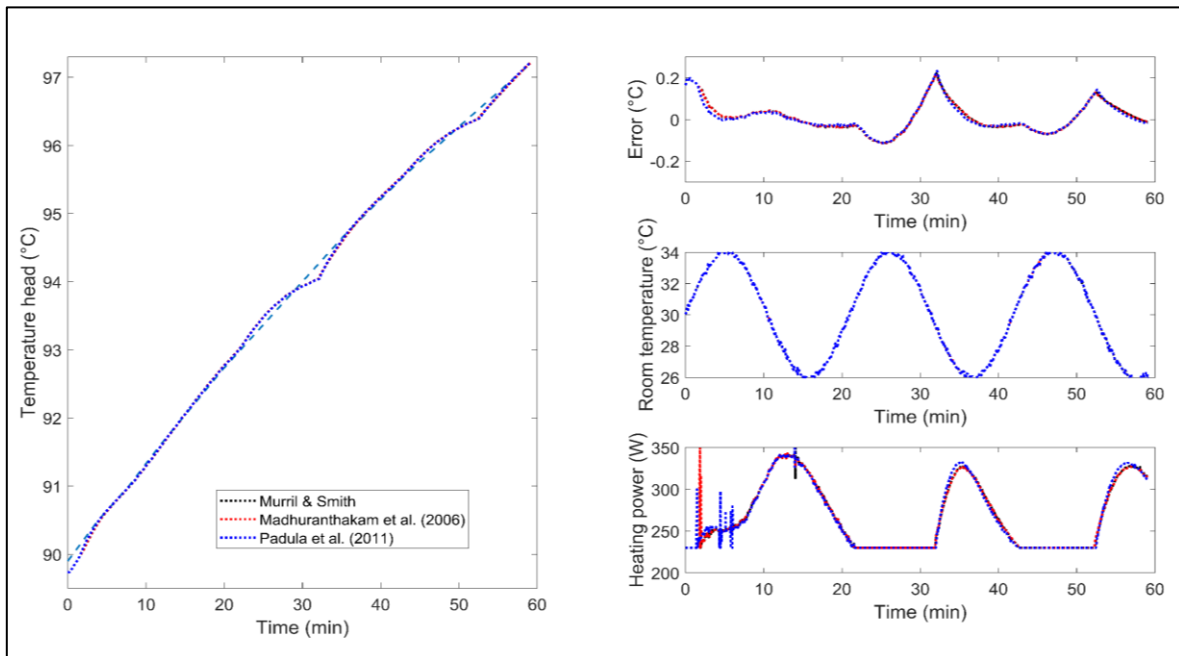
Figure 2-5. Behavior of the controlled variable and manipulated variable in the presence of sinusoidal disturbance (amplitude 4°C) in room temperature (DT3) for three tuning rules of IOPID controllers.

2.4.3 Comparison of integer/fractional order controllers

Table 2-4 shows the control parameters for IOPI, IOPID, FOPID and IMC controllers obtained for each tuning rule-based method (see Section 2.3.3). In all disturbance cases, FOPID obtained the best performance according to IAE and ITAE; hence, relative indices were calculated dividing the respective indices with those of the FOPID controller. Table 2-5 shows the absolute and relative IAE and ITAE values obtained by IOPI, IOPID, FOPID and IMC controllers for the six disturbance cases.

In DT1 and DT2 cases, FOPID controller improved the IAE and ITAE values in 8%, 10% and 24% as compared with IOPID, IMC and IOPI, respectively. Instead, for DT3 and DT4 disturbance cases, the FOPID controller improvement was smaller (5%, 6% and 14%, respectively) because the control effort saturated for long periods.Figure 2-6 shows that under disturbance DT3, IOPI, IMC and FOPID controllers presented a control effort with no peaks and smoother than that of IOPID.

Table 2-4. Parameters fitted for IOPI, IOPID, FOPID and IMC controllers.

Controller	K_p	K_i	K_d	λ	μ	T_f	ε
IOPI	366.3	7.9	0	1	-	-	-
IOPID	453.8	9.5	1507.4	1	1	0.33	-
FOPID	510.4	10.3	2432.8	1	1.14	0.39	-
IMC	-	-	-	-	-	-	2.5

Table 2-5. Performance indices values for all controllers with different room temperature and heating power noise disturbances.

Disturbance type	IOPI		IOPID		FOPID		IMC	
	ITAE[*]	IAE[*]	ITAE	IAE	ITAE	IAE	ITAE	IAE
DT1	256 (1.32)	0.509 (1.31)	210 (1.08)	0.423 (1.09)	194 (1.00)	0.389 (1.00)	216 (1.11)	0.435 (1.12)
DT2	721 (1.34)	0.720 (1.32)	587 (1.10)	0.596 (1.09)	536 (1.00)	0.548 (1.00)	605 (1.12)	0.613 (1.12)
DT3	3592 (1.16)	2.04 (1.18)	3245 (1.05)	1.82 (1.05)	3093 (1.00)	1.73 (1.00)	3290 (1.06)	1.85 (1.07)
DT4	3892 (1.16)	2.22 (1.18)	3496 (1.05)	1.97 (1.04)	3344 (1.00)	1.89 (1.00)	3550 (1.06)	2.01 (1.06)
DT5	671 (1.30)	0.704 (1.28)	562 (1.09)	0.596 (1.08)	516 (1.00)	0.550 (1.00)	576 (1.12)	0.610 (1.11)
DT6	1293 (1.26)	1.08 (1.27)	1076 (1.05)	0.899 (1.06)	1025 (1.00)	0.851 (1.00)	1098 (1.07)	0.920 (1.08)

[*] Relative ITAE and IAE values in parentheses were calculated dividing by ITAE and IAE obtained from FOPID controller respectively in each disturbance scenarios.
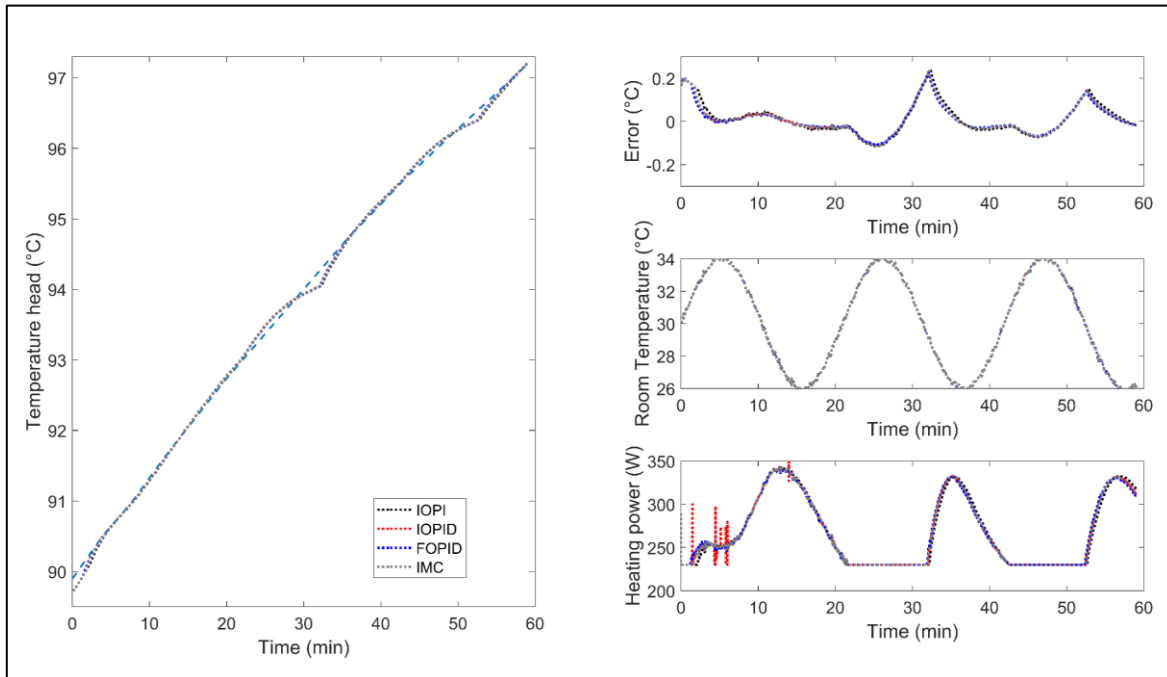
Figure 2-6. Behavior of the controlled variable and manipulated variable in the presence of sinusoidal disturbance (amplitude 4°C) in room temperature (DT3) for IOPI, IOPID, FOPID and IMC controllers.

Under a more realistic room temperature disturbance simulation (DT5), no control saturation was observed Figure 2-7 and the FOPID controller reduced the relative IAE and ITAE values in 8%, 11% and 23% compared to IOPID, IMC and IOPI controllers, respectively. In this case, the FOPID controller presented a control effort without peaks and smoother than the IOPID. When noise was added to the heating power (DT6), the relative improvement of the FOPID controller decreased a little (6%, 7% and 21%, respectively), since, as shown in Figure 2-8, the control effort became saturated between 44 and 48 min.

The improvement in control performance of the FOPID with respect to IOPID observed here (between 5 and 8%) agrees with that observed in other nonlinear plants. For example, in a conical tank level control, the FOPID controller reduced the relative IAE compared to the IOPID controller in 1.4% in simulations (Jauregui et al., 2016a) and in 1.05% in an experimental implementation (Jauregui et al., 2016b).
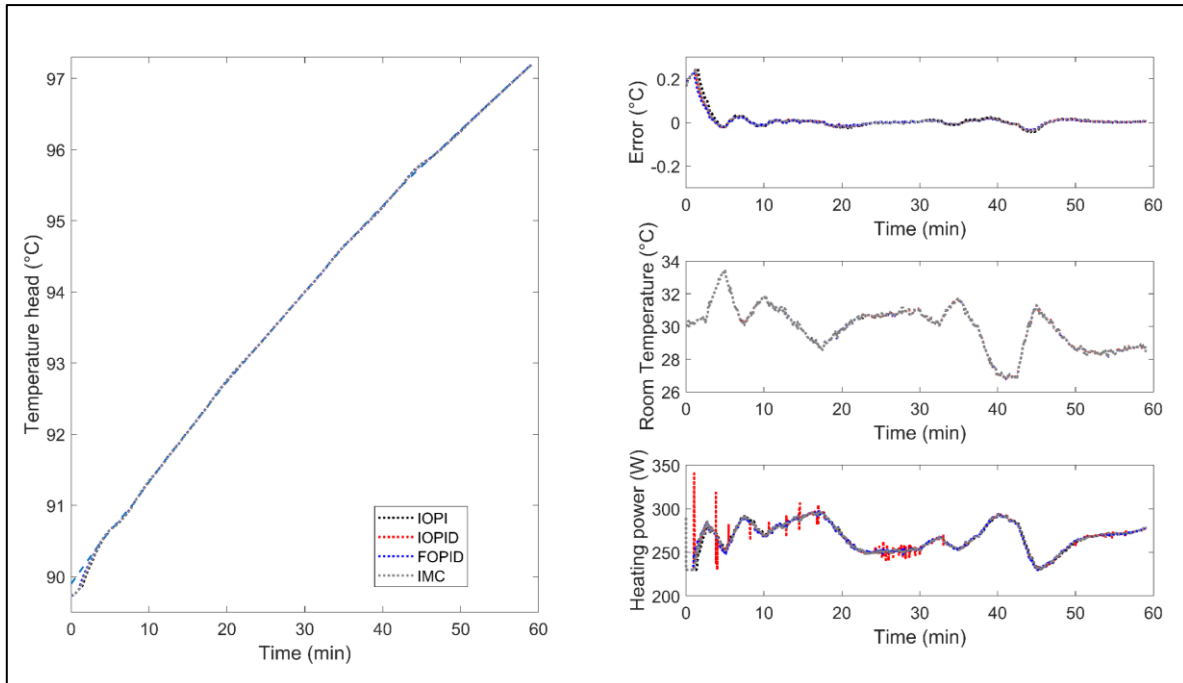
Figure 2-7. Behavior of the controlled variable and manipulated variable in the presence of colored noise disturbance in room temperature (DT5) for IOPI, IOPID, FOPID and IMC controllers.
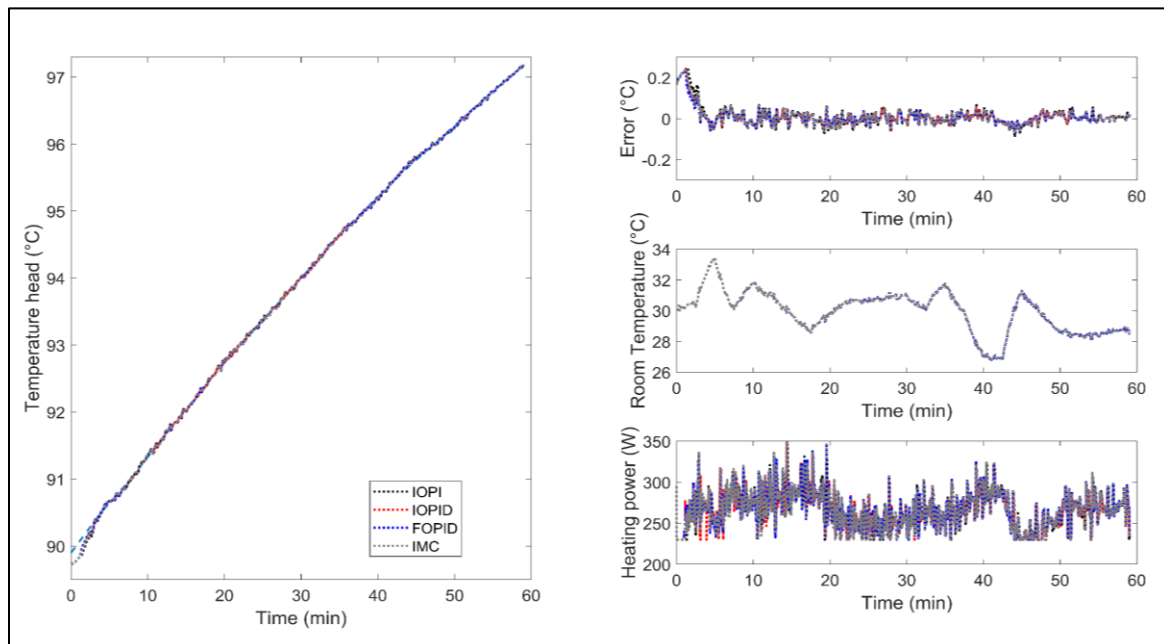
Figure 2-8. Behavior of the controlled variable and manipulated variable in the presence of colored noise disturbance in room temperature plus heating power white noise (DT6) for IOPI, IOPID, FOPID and IMC controllers.

2.5 Conclusions

Simple tuning rules based on the minimization of the IAE index were applied to compare IO and FO controllers in a nonlinear model of a Charentais alembic distillation system. Using an IOPID controller, Padula tuning rules provided better performance than classical tuning rules such as Murril-Smith and Madhuranthakam. The FOPID controller performed better than IOPI, IOPID and IMC controllers in all the disturbance scenarios simulated, showing lower IAE and ITAE indices and a smoother control effort without peaks. Even though the FOPID controller has two more tuning parameters (λ, μ) than the IOPID controller, this work shows how a simple tuning rule like Padula, yields effective and robust control for a time-varying and nonlinear process.

2.6 Acknowledgements

CHAPTER 3: MINIMIZING METHANOL CONTENT IN EXPERIMENTAL CHARENTAIS ALEMBIC DISTILLATIONS

Ricardo Luna, Francisco López, José R. Pérez-Correa.

3.1 Introduction

Distilled alcoholic beverages are produced worldwide from local raw materials. For example, whisky (UK, Ireland) is produced from cereals, cachaça from cane juice (Brazil), tequila from agave (Mexico), cognac/brandy (France, Spain) and pisco (Peru, Chile) from grapes (Small et al., 2011). Young distillates are characterized by a delicate aroma that resembles the original fruit. In addition, high quality spirits should be free from off-flavors and toxic compounds. In spirits production processes, distillation plays a key role to ensure that the standards of quality of the product are met. This is an operation already used by ancient cultures to produce medicines and perfumes, and nowadays are used in almost every chemical processing plant. Distillation is a method for separating substances of different volatility. Most spirits production processes use either batch distillation columns or Charentais alembics. The latter are most frequently used in small-scale production facilities. In this system, three cuts (head, heart and tail) are collected sequentially; high quality spirits are produced from the heart cut. Even though the operation of alembics is relatively simple compared to batch distillation columns, it is subjected to many uncontrolled and unmeasured disturbances that generate variability in the composition of the final product. Hence, it is still difficult to ensure that the produced spirit consistently meets a defined quality criterion. It is even more difficult to adapt the production process to meet changing market trends.

There are many published studies dealing with the production of fruit distillates in Charentais alembics and distillation columns (Arrieta-Garay, et al., 2014; Arrieta-Garay et al., 2014b; Arrieta-Garay et al., 2013; Claus & Berglund, 2005; Da Porto & Decorti, 2008; García-Llobodanin et al., 2011; Hernández-Gómez et al., 2003; Reche et al., 2007). Many of these studies were concerned with the impact of the fruit variety or the distillation equipment on the aroma composition of the spirit. In addition, in these studies distillation strategies were

not changed and were defined heuristically. Recent studies have explored the impact of different operating strategies on the composition of Muscat wine distillates obtained in a packed batch distillation column (Matias-Guiu et al. 2016; Rodríguez-Bencomo et al. 2016). It was found by trial and error that low reflux rates at the beginning of the heart cut could produce distillates with an enhanced floral aroma. Although establishing suitable alembic distillation strategies by trial and error is a valid option that has been used for centuries in the production of spirits, medicines and perfumes, these strategies can be developed much faster and reliably using model based optimization (Osorio et al., 2005; Sacher et al., 2017).

Several techniques have long been applied to design optimal operating strategies for batch distillation processes relevant in chemical engineering. Most of these methods transform the strategy design into an optimal control problem, where the usual goals are to minimize time, maximize distillate, maximize concentration of a key component or maximize profit (Diwekar, 1995; Mujtaba, 2004). As a result, most of the time, difficult nonlinear programing problems (NLP) should be solved numerically, either by the sequential approach (partial discretization) or the simultaneous approach (full discretization) (Kameswaran & Biegler, 2006). The sequential approach is relatively easy to code and apply, especially if a reliable process model is already available. In this formulation, the control variables are discretized as piecewise polynomials and optimization is performed with respect to the polynomials' coefficients (Barton et al., 1998; Vassiliadis et al., 1994a, 1994b). Alternatively, the simultaneous approach is faster and can handle many more decision variables and constraints than the sequential approach. This method does nevertheless require sophisticated optimization routines for handling large-scale problems as well as additional techniques to avoid numerical difficulties and to guarantee convergence. In this formulation, the control and state variables are discretized in time, using for example collocation on finite elements.

Although the sequential approach (Kim, 1999; Jain, Kim, & Smith, 2012; Mujtaba & Macchietto, 1993; Mujtaba & Macchietto, 1997) and the simultaneous approach (Biegler, 2007; Biegler et al., 2002; Logsdon et al., 1990; Mujtaba & Macchietto, 1996; Zavala & Coronado, 2008) have been widely used to solve batch distillation optimization problems, few of these studies include experimental validation. Previous studies with experimental validation involve distillation of binary mixtures (Elgue et al., 2004; Li et al., 1998;

Safdarnejad et al., 2016), distillation of ternary mixtures (Bonsfills & Puigjaner, 2004) and reactive distillation (Noeres et al., 2004). Nevertheless, studies involving optimization with experimental validation in the distillation of alcoholic beverages are scarce. Fruit wines are complex mixtures where water and ethanol represent around 96% of the total mass, and the delicate aroma of the spirit is defined by the remaining 4% made up of hundreds of volatile compounds (Osorio et al., 2004). Osorio *et al.* (2005) solved a multi-objective optimal control problem for the distillation of a spirit in a tray column, finding a suboptimal path for the cooling flow rate in the partial condenser that simultaneously maximized the recovery of terpenes (floral aroma in Muscat wines) and minimized the recovery of fatty acids (off-flavors). The process model was complex, with many differential and implicit algebraic equations; therefore, the formulation and solution of a full optimization problem was difficult. To simplify the numerical solution of the optimization problem, the control path was parametrized using a smooth time-varying function with variable coefficients. With their method, Osorio *et al.* (2005) were able to experimentally obtain a distillate with three times more linalool (floral aroma) than commercial piscos (Muscat grape brandies) and six times more linalool than a distillate obtained by applying a standard distillation policy to the same batch distillation column. In addition, the optimum distillate contained on average four times less octanoic acid (off-flavor) than commercial and standard distilled piscos. More recently, De Lucca *et al.* (2013) explored by simulation several operating policies to minimize the methanol content in the distillate obtained in a batch packed bed column (Carvallo et al., 2011). These authors used the same predefined function with variable coefficients of Osorio *et al.* (2005) to find an optimal cooling flow rate path. Simulations showed that the best operating strategy could not reduce the relative methanol concentration in the distillate more than 23% compared with the relative methanol concentration in the wine.

Our long-term aim is to apply model-based techniques to design and implement batch distillation strategies to produce young fruit distillates that consistently meet a given standard of quality, i.e., rich in fruity and floral aromas and low in off-flavors and toxic compounds. Specifically, in this paper we focus on designing a distillation strategy that minimizes the methanol content in a distillate obtained in a Charentais alembic, without sacrificing ethanol recovery. Methanol metabolizes slowly in the human body, producing formaldehyde and formic acid, which are extremely toxic in high concentrations. Excessive intake of methanol

generates various ailments such as fatigue, thirst, headache, stomachache, nausea, vomiting, sensitivity to light and noise, lack of concentration and attention, tremors, excessive sweating and hypertension (Swift & Davidson, 1998). Hence, in many countries, methanol content in alcoholic beverages is regulated.

First the calibration procedure of a dynamic alembic model adapted from Sacher *et al.* (2013) is described. Then, a suitable multi-objective dynamic optimization problem is formulated and solved using both the sequential and simultaneous approaches. Finally, the obtained experimental results are shown and discussed.

3.2 Materials and Methods

3.2.1 Distillation system

The automatic Charentais copper alembic (Figure 3-1) used in our experiments consists of a 4.8 L capacity boiler, a natural convection partial condenser (head), a swan neck and a total condenser. PT100 sensors measured the boiler, head and room temperatures. The heating power (1200 W) applied to the boiler was manipulated using a PAC2 regulator module that controls the phase angle of the AC supply. A S7-200 Siemens PLC (Programmable Logic Controller) received the temperature data from the PT100 sensors and sent the controller output to the PAC2 module to adjust the heating power. The human-machine interface (HMI) and the control algorithms were coded in MATLAB$^®$/Simulink$^{™}$ using the OPC Toolbox in a PC (Intel® Core™ 2 Hewlett-Packard). A cascade control system was applied: the primary controller (outer loop) read the head temperature and provided the heating power set point for the secondary controller; the secondary controller (inner loop) adjusted the applied heating power to follow the set point provided by the primary controller. Both controllers used an internal model control (IMC) algorithm (Brosilow & Joseph, 2002).
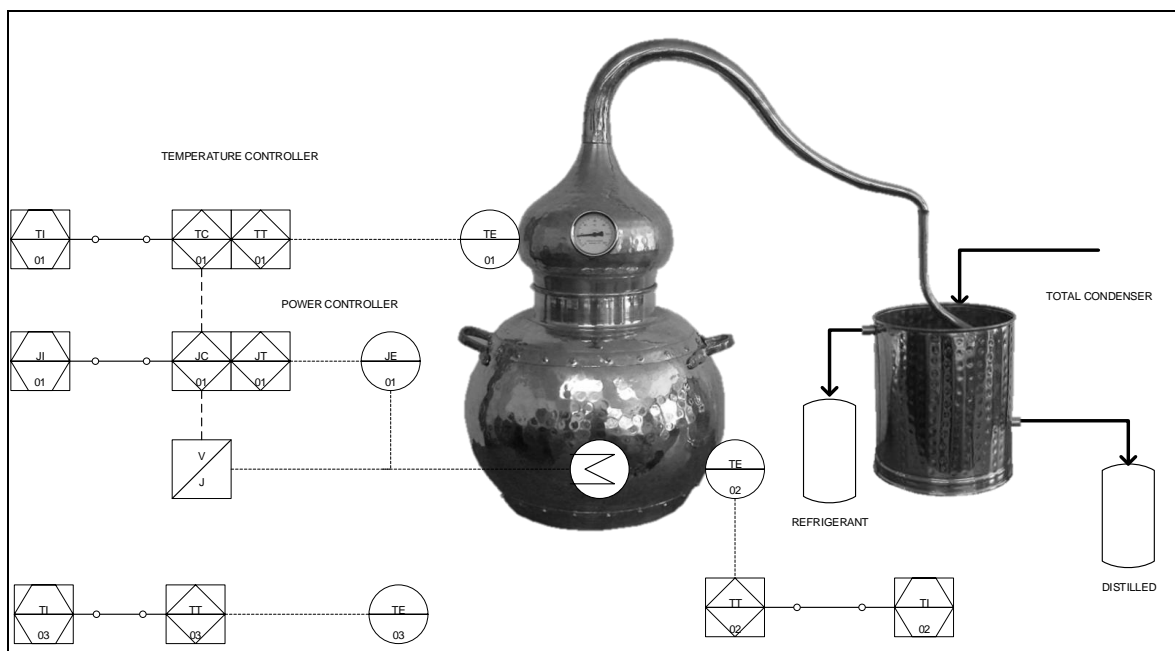
Figure 3-1. P&ID of the distillation system.

3.2.2 Experiments

In this study, a synthetic ternary mixture was prepared with a composition usually found in wine, i.e., 13% v/v of ethanol and 1.37 g/L.a.a. of methanol (grams of methanol per liter of absolute alcohol). The solution was prepared once and in sufficient amount before all the experimental distillations. The Alembic was initially loaded with 1.8 L of synthetic wine in each experiment. Distillation strategies were defined in terms of the heating power applied to the boiler. Three strategies (performed in triplicate) were assessed: i) slow distillation at constant low heating power (230 W); ii) fast distillation at constant high heating power (400 W); and iii) optimal distillation applying a variable heating power. The first two strategies are common practice in small-scale spirits production facilities: slow distillations tend to increase spirits quality while fast distillations tend to increase ethanol recovery. The third strategy was defined to balance two objectives; low methanol content and high ethanol recovery (see section 3.2.7). In all distillation runs, three fractions were collected according to predefined volumes: 85 mL of head, 375 mL of heart and 115 mL of tail. The corresponding total distillation times were 168, 67 and 87 min for the slow, fast and optimal distillations respectively.

3.2.3 Chemical analysis

Ethanol content was determined (in triplicate) with a pycnometer, correcting the density to 20°C. Methanol content was determined (in duplicate) using the method proposed by the International Organization of Vine and Wine (OIV) (Wine, 2009). Distillate samples were diluted up to an ethanol content of 5% v/v and the methanol in the diluted samples was oxidized to formaldehyde with a solution of 3% w/v potassium permanganate and 15% v/v phosphoric acid. Then, the diluted oxidized samples were bleached with dry sodium bisulfite. The amount of formaldehyde was defined by the intensity of the violet color followed by the reaction of 5% w/w chromotropic acid in a sulfuric medium. This intensity was determined by spectrophotometry UV-VIS (T70 UV/VIS spectrometer PG Instruments) at 575 nm. All reagents were analytical grade. We used these low cost analytical techniques instead of gas chromatography (GC) or high-pressure liquid chromatography (HPLC), since these are too expensive to be implemented in small-scale distilleries.

3.2.4 Data reconciliation

Total mass, alcoholic strength and methanol concentrations were measured in the synthetic wine initially charged in the boiler, in all the distillate samples and in the residue left in the boiler after distillation. Discrepancies were found in the global mass balances due to measurement errors. Therefore, measurements were corrected with a standard data reconciliation procedure normally applied in the process industries (Narasimhan & Jordache, 2000). Hence, reconciled values closed the global mass balances (total mass, ethanol and methanol).

3.2.5 Modelling

A simplified version of the model presented in Sacher *et al.* (2013) is used here, which considers a mixture of water, methanol and ethanol. The model comprises total mass, ethanol and energy dynamic balances in the boiler, as well as total mass, ethanol and energy stationary balances in the partial condenser. Several constitutive equations were included to describe the heat loss to the environment and the vapor/liquid equilibrium. The complete model is given in the appendix and further details and specific assumptions can be found in Sacher *et al.* (2013).

3.2.6 Model calibration

The data obtained in the constant heat rate distillations (see section 3.2.2) were used to calibrate the dynamic alembic model. The fitting parameters were:

$$\theta = [UA_b, UA_c, M_0, x_0^e, x_0^m] \tag{3-1}$$

where UA_b and UA_c represent the global heat transfer coefficient multiplied by the corresponding heat transfer area in the boiler and head respectively. M_0, x_0^e and x_0^m are the initial total moles, ethanol molar fraction and methanol molar fraction in the boiler just at the moment when the first drop of distillate is recovered. These unmeasured values were different from those of the initial mixture. For the optimal strategy, the heat transfer parameters (UA) were not fitted; instead, they were modeled as linear functions of the heat transfer parameters fitted with the constant heating experiments.

The calibration cost function was:

$$J(\theta) = \sum_{j}^{n_{var}} \sum_{i=1}^{n_{obs}} \left(\frac{\hat{y}_{ij}(u,\theta,t) - y_{ij}(u,t)}{\max(y_{ij})} \right)^2 \tag{3-2}$$

where index j represents the measured variables and index i the sample times. The measured variables were: alcoholic strength GA, methanol concentration M_{eth}, distilled volume V and head temperature T_c. $\max(y_{ij})$ corresponds to the maximum measured value of variable j during the distillation run. The optimization problem was solved within MATLAB® R2015a with the scatter search metaheuristic code (SSM) (Egea et al., 2007).

Equations A.3-20, A.3-21 and A.3-22 in the appendix, that represent the instant concentration of ethanol, methanol and relative methanol respectively, were modified. Hence, eqs. 3-3, 3-4 and 3-5 represent the average concentration of the distillate stream leaving the system at the corresponding time interval where the sample was collected:

$$GA_i = \frac{\Delta GA}{\Delta V} = \left(\frac{M_D^e(t_{exp,i}) - M_D^e(t_{exp,i-1})}{V(t_{exp,i}) - V(t_{exp,i-1})} \right) \cdot PM_E \cdot \frac{1}{\rho_e} \cdot 100 \tag{3-3}$$

$$M_{et,i} = \frac{\Delta M_{et}}{\Delta V} = \left(\frac{M_D^m(t_{exp,i}) - M_D^m(t_{exp,i-1})}{V(t_{exp,i}) - V(t_{exp,i-1})} \right) \cdot PM_M \cdot 1 \cdot 10^{-6} \qquad (3\text{-}4)$$

$$C_{meth,i} = \frac{\Delta C_{meth}}{\Delta V} = \left(\frac{M_D^m(t_{exp,i}) - M_D^m(t_{exp,i-1})}{\left(V(t_{exp,i}) - V(t_{exp,i-1})\right) \cdot (GA_i/100)} \right) \cdot PM_M \cdot 1000 \qquad (3\text{-}5)$$

Finally, the heart cut of the three distillation strategies were compared. In model calibrations, the cut times of head/heart and heart/tail for each strategy were defined by the volumes collected, i.e., 85 mL of head and 375 mL of heart (see section 3.2.2).

3.2.7 Dynamic optimization

A multi-objective cost function, $J(u)$, was defined to get a good compromise between low relative methanol concentration in the distillate and high ethanol recovery.

$$\min_u J(u) = \alpha \cdot \frac{C_{meth}(t_f)}{1.5} - (1 - \alpha) \cdot \frac{Rec_{eth}(t_f)}{100} \qquad (3\text{-}6)$$

here, α is an arbitrary positive scalar (≤ 1) that defines the relative weight of each objective (Bhaskar, Gupta, & Ray, 2000; Miettinen & Hakanen, 2009) and C_{meth} is the relative methanol concentration. Ethanol recovery was defined by:

$$Rec_{eth} = \frac{\int_{t0}^{tf} \left(V_D(t) \cdot x_{eth}(t) \right) dt}{M_0 \cdot x_{eth}(t_0)} \qquad (3\text{-}7)$$

where V_D is the molar flow rate of distillate, x_{eth} is the ethanol mole fraction, M_0 is the initial mass, and finally, t_0 and t_f are the initial and final distillation times respectively. Both objectives were scaled by their maximum values: the maximum methanol concentration in spirits allowed in the Chilean law (Biblioteca del Congreso Nacional de Chile & Ministerio de Agricultura, 2012) is 1.5 g/L.a.a, while the maximum ethanol recovery is 100%.

The only input variable that could be manipulated in the alembic was the heating power. Hence, the optimization problem looked for a heating path that minimized the relative methanol concentration in the distillate and simultaneously maximized ethanol recovery. Only the heart cut was considered in computing the cost function (Eq. 3-6). Based on experience, the head/heart cut was fixed at 5.5 min and the heart/tail cut was set at 120 min. Additional optimization constraints were: (i) the heating power varied between 230 and 400 W; (ii) the minimum distillate flow rate was 2 mL/min.

Two numerical methods were applied to solve the optimization problem (Srinivasan, Bonvin, Visser, & Palanki, 2003): the sequential solution/optimization method (SEM) and the simultaneous solution/optimization method (SIM). In SEM, the control variable was discretized into 18 equally spaced time steps where the control value was kept constant:

$$u(\Delta t_i) = a_i \tag{3-8}$$

where index i represents the 18 time intervals and a_i represents the value of the control u in the i-th time interval. The scatter search code mentioned above was used to solve the resulting optimization problem within MATLAB® R2015a. The dynamic model of the alembic was solved with MATLAB's solver *ode15s* (Shampine & Reichelt, 1997). In turn, in SIM, the control and state variables were discretized in time using 3 Radau collocation points on 18 finite elements (Biegler, 2007; Kameswaran & Biegler, 2006). The resulting optimal control problem was:

$$\min_u J(u) \tag{3-9}$$

Subject to,

$$\forall\, i = 1 \dots ne, j = 1 \dots ncp$$

$$x_{i,j} = x_{i-1} + h_i \sum_{j=1}^{ncp} \Omega_j(\tau_j) \cdot \frac{dx}{dt_{i,j}} \tag{3-10}$$

$$g(x_{i,j}, y_{i,j}, u_{i,j}, \theta) = 0 \tag{3-11}$$

$$u_L \le u_{i,j} \le u_U; \; x_L \le x_{i,j} \le x_U; \; y_L \le y_{i,j} \le y_U; \theta_L \le \theta \le \theta_U \qquad (3\text{-}12)$$

$$\frac{dx}{dt_{i,j}} = f(x_{i,j}, y_{i,j}, u_{i,j}, \theta) \qquad (3\text{-}13)$$

where ne represents the number of finite elements (18), ncp the number of collocation points (3), x the state variables, y the algebraic variables, u the control variables, θ the model parameters vector, h_i the length of the finite elements (total process time divided by the number of finite elements), and finally, Ω the interpolation polynomial functions in each finite element. The optimization problem was coded in AMPL (R. Fourer, Gay, & Kernighan, 2003) and solved with the IPOPT code (A. Waechter & Biegler, 2006).

3.3 Results

3.3.1 Model calibration

Figures 3-2 and 3-3 show measured values and model outputs of the head temperature, alcoholic strength, methanol concentration, distillate volume and distillate flow rate of the three replicates of the constant high heating rate distillation. The 95% confidence intervals shown in the figures were obtained by simulation, considering the standard deviation in the estimated parameter set ($\theta \pm 2\sigma_\theta$). Table 3-1 shows the fitted parameters for the two constant heating distillations (230 W and 400 W); for the optimal strategy, the initial concentrations were fitted only, since heat transfer parameters were defined by linear functions (see section 3.2.6).
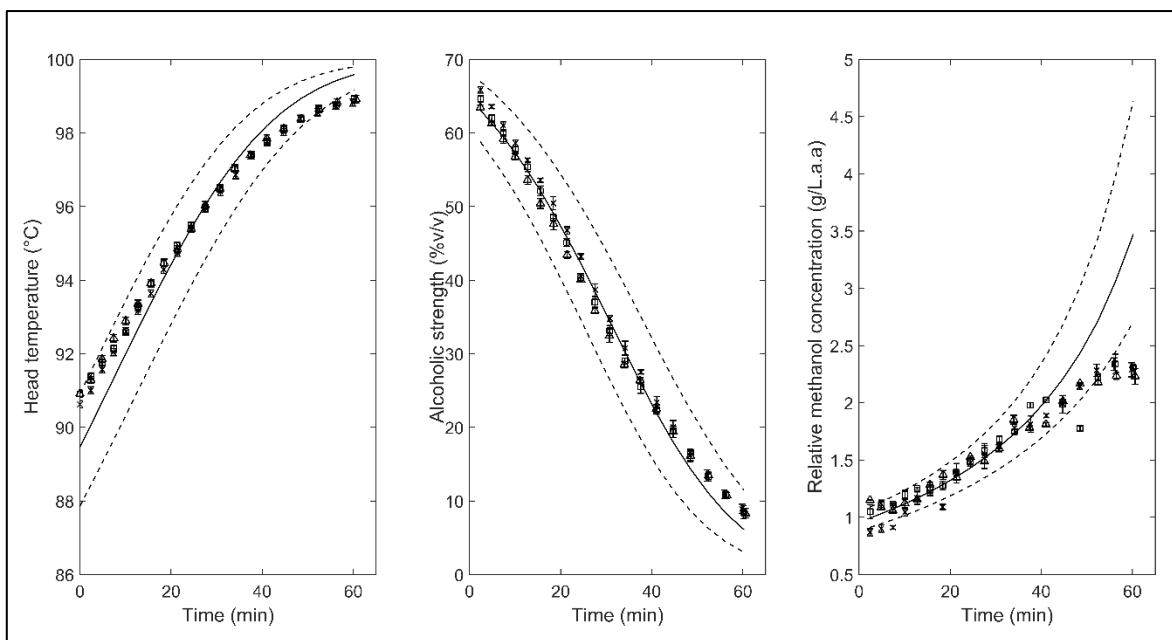
Figure 3-2. Head temperature, alcoholic strength and relative methanol concentration for a constant heating power rate of 400 W. Experimental data: run 1 (×), run 2 (□) and run 3 (Δ). Simulation (solid line) and confidence interval (dashed line).
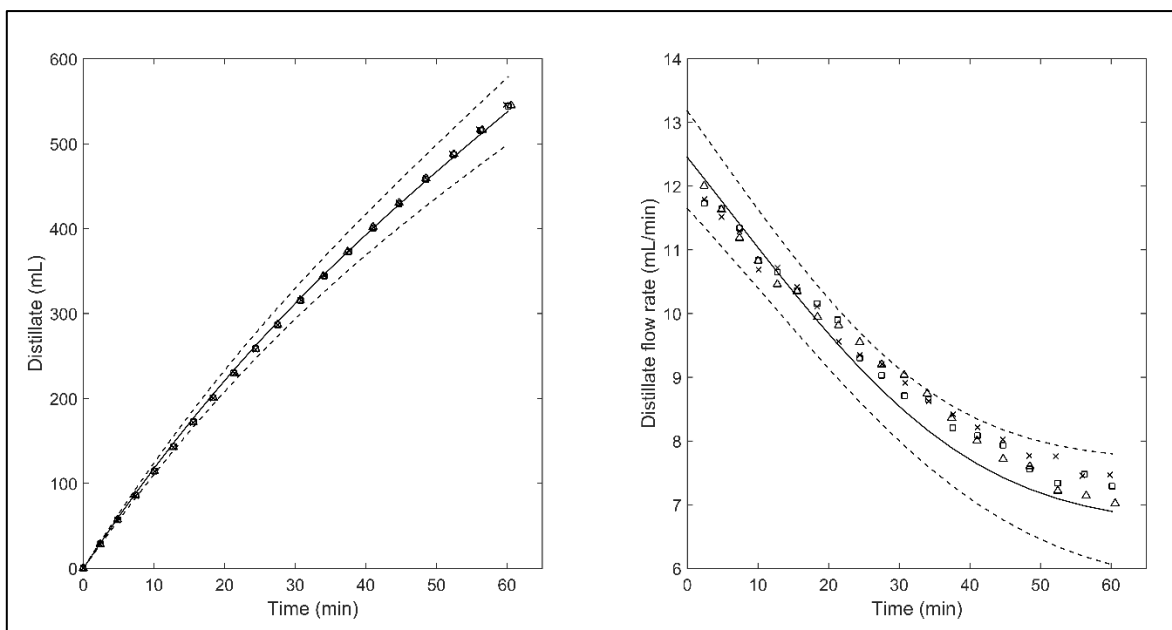
Figure 3-3. Distillate volume and distillate flow rate for a constant heating power rate of 400 W. Experimental data: run 1 (×), run 2 (□) and run 3 (Δ). Simulation (solid line) and confidence interval (dashed line).

Model fitting was better for the high heating rate distillation (Figs. 3-2 and 3-3) than for the low heating rate distillation (Figs. 3-4 and 3-5). At low heating, distillate flow rates were extremely low (less than 6 mL^{-1}) and distillation times were high (180 min); consequently, measurements were more sensitive to disturbances. The alcoholic strength and the distilled volume were the best-fitted variables in both distillation experiments. Simulated values did not represent well the measurements of relative methanol concentrations at the end of the distillation, especially for low heating operation. In this case, low concentration and flow rate values were observed. Absolute errors of these measurements were approximately constant; hence, relative errors were higher at low concentration and flow rate values.
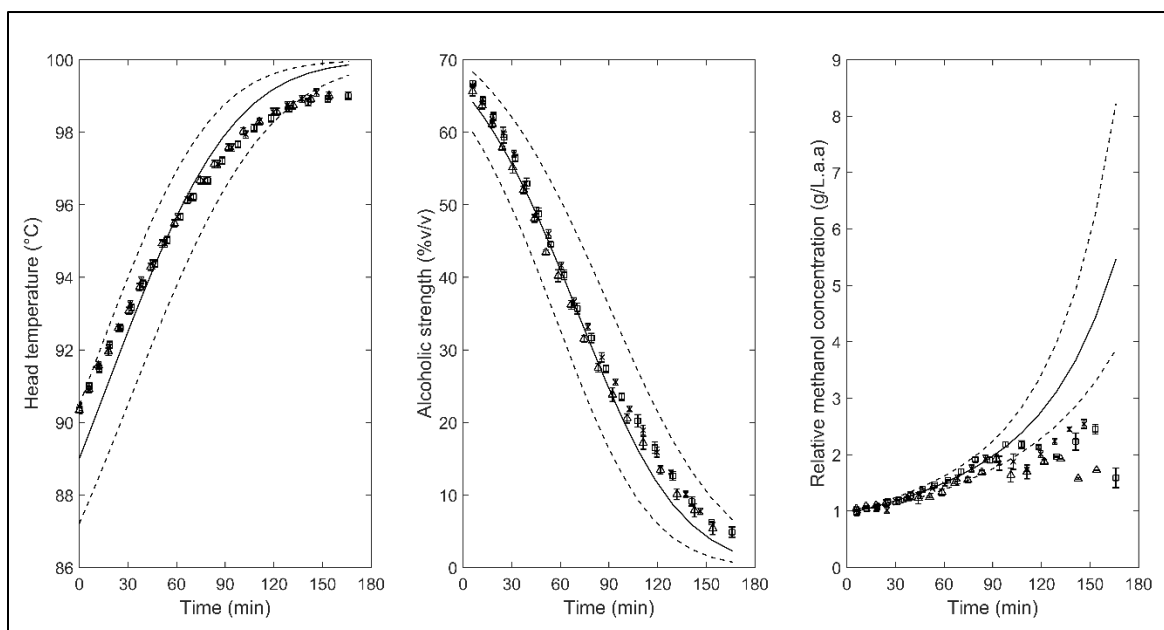
Figure 3-4. Head temperature, alcoholic strength and methanol concentration curves for constant heating power rate 230 W. Experimental data: run 1 ($\times$), run 2 ($\square$) and run 3 (Δ). Simulation (solid line: $-$) and confidence interval (dashed line: - - -).
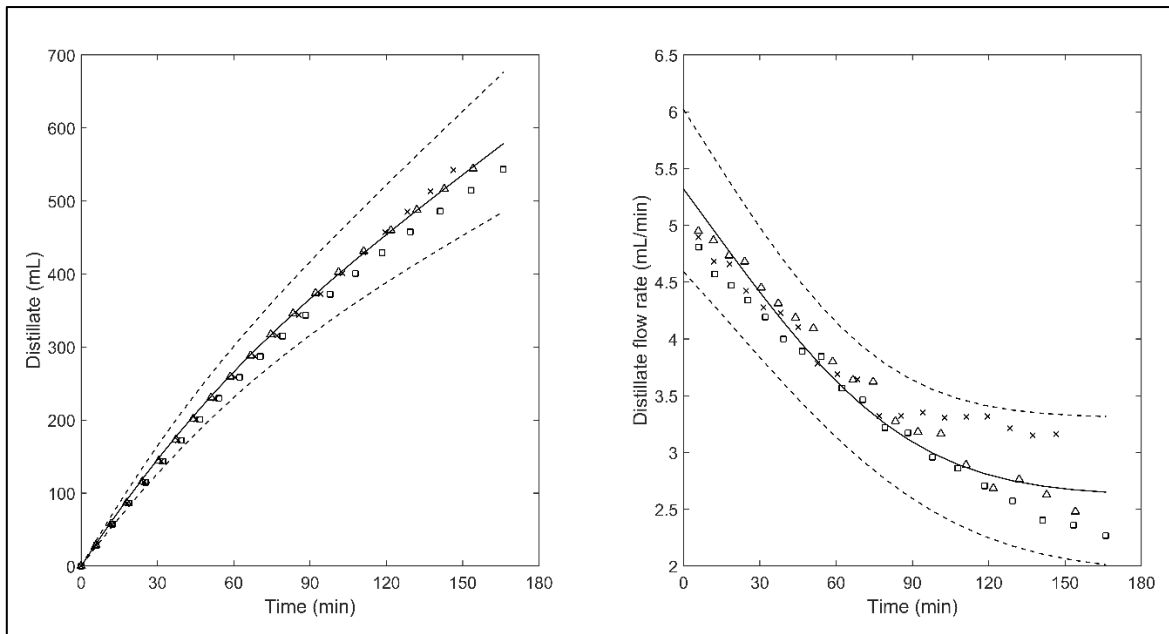
Figure 3-5. Distillate volume and distillate flow rate curves for constant heating power rate 230 W. Experimental data: run 1 (×), run 2 (□) and run 3 (Δ). Simulation (solid line: −) and confidence interval (dashed line: - - -).

Table 3-1 shows that under low heating, the heat transfer parameters (UA) were practically the same for the boiler and the partial condenser. In turn, under high heating, the heat transfer parameter of the head was higher than that of the boiler. Sacher *et al.* (2013) found the same behavior in a similar system; however, our heat transfer parameters were higher due to differences in the heating methods used. Sacher *et al.* (2013) applied a hot plate to heat the boiler; hence, they could not measure the effective heat supplied, which was estimated instead. They argue also that low heating powers induced low convective air streams, reducing the heat transfer in the head. This explains why we observed a low heat transfer parameter of the head at low heating powers. The heat transfer parameter of the boiler was less dependent on the heating power in our case, since the heating element is inside the boiler.

Table 3-1. Fitted parameters for distillation strategies.

Strategy	UA_b (W/°C)	UA_c (W/°C)	M_0 (mol)	x_0^e (mol/mol)	x_0^m (mol/mol)
230 W	0.82 ± 0.06	0.81 ± 0.10	90.4 ± 1.2	37.1e-3 ± 0.7e-3	10.12e-5 ± 0.13e-5
400 W	0.37 ± 0.10	1.48 ± 0.13	90.4 ± 0.9	38.5e-3 ± 2.0e-3	10.41e-5 ± 0.16e-5
Optimal	a	b	89.5 ± 1.7	36.6e-3 ± 1.4e-3	9.40e-5 ± 0.53e-5

[a] Linear function between UA_b values obtained from 230 and 400 W.

[b] Linear function between UA_c values obtained from 230 and 400 W.

3.3.2 Optimal operation

Tables 3-2 and 3-3 show the optimization results with the SEM and SIM methods respectively, including the optimal values of relative methanol concentration (C_{meth}), ethanol and methanol recoveries (Rec_{eth}, Rec_{meth}), as well as alcohol strength (GA_d) for different values of the weight of the cost function ($0 \leq \alpha \leq 0.5$). For values of $\alpha \geq 0.5$, the same results were obtained, where the heating power was the lower limit. In the case of SIM, the optimization routine did not converge for some α values. Figure 3-6 shows the optimum trajectories of the heating power, the head temperature and alcoholic strength variation for α = 0.05 and α = 0.06 obtained by SEM and SIM respectively. Figure 3-7 shows the optimum trajectories of the heating power, the head temperature and alcoholic strength variation for α = 0.2 obtained by SEM and SIM. Figure 3-8 shows the Pareto front yielded by both dynamic optimization methods.

Table 3-2. Results obtained with the sequential solution/optimization method (SEM) for head/heart cut at 5 min and heart/tail cut at 120 min.

adjustable weight (α)	objective function (J)	relative methanol concentration (C_{meth})	ethanol recovery (Rec_{eth})	methanol recovery (Rec_{meth})	alcohol strength (GA)
0	-0.915	1.40	91.5	94.3	24.8
0.05	-0.823	1.40	91.5	94.1	26.7
0.10	-0.730	1.39	91.4	93.5	29.9
0.15	-0.638	1.38	91.4	92.8	32.0
0.20	-0.547	1.37	91.2	91.9	34.2
0.25	-0.456	1.36	91.0	90.9	36.1
0.30	-0.365	1.35	90.6	89.5	38.2
0.35	-0.276	1.33	90.2	88.2	40.0
0.40	-0.186	1.31	89.5	86.3	42.0
0.45	-0.0985	1.30	88.5	84.2	44.1
0.50	-0.0116	1.27	86.7	80.5	47.1

Table 3-3. Results obtained with the simultaneous solution/optimization method (SIM) for head/heart cut at 5 min and heart/tail cut at 120 min.

adjustable weight (α)	objective function (J)	relative methanol concentration (C_{meth})	ethanol recovery (Rec_{eth})	methanol recovery (Rec_{meth})	alcohol strength (GA)
0.06	-0.805	1.40	91.5	94.0	27.6
0.10	-0.731	1.39	91.5	93.5	29.9
0.15	-0.639	1.38	91.4	92.8	32.4
0.20	-0.547	1.37	91.2	91.9	34.5
0.25	-0.456	1.36	91.0	90.8	36.6
0.30	-0.366	1.35	90.7	89.6	38.5
0.36	-0.258	1.33	90.1	87.8	40.8
0.40	-0.187	1.31	89.5	86.3	42.4
0.43	-0.134	1.30	89.0	85.1	43.6
0.45	-0.0987	1.29	88.6	84.2	44.4
0.48	-0.0465	1.28	87.8	82.7	45.6
0.50	-0.0120	1.27	87.2	81.5	46.5

Both optimization methods provided different heating trajectories, where the SIM heating trajectories were easier to implement in real time experiments since they were much smoother. Even though different evolutions of head temperature and distillate alcoholic strengths were obtained for the same values of α, both methods yielded practically the same values of relative methanol concentration and ethanol recovery (Figure 3-8, and Tables 3-2 and 3-3). Therefore, the optimal solutions found were reliable, since both methods, using different discretization techniques and optimization solvers, reached the same objective values. In addition, SEM was easier to apply than SIM, since the model was already coded in MATLAB® and the DAE system was efficiently solved with the *ode15s* routine. Therefore, we only had to add the optimization routine, code the multi-objective cost function and discretize the control variable. For the SIM approach, the code was adapted to AMPL language (which was rather difficult) and the model was fully discretized, generating many equations, variables and inequality constraints in the state variables and the control variable. SEM solved the optimization problem much slower than SIM (5 to 10 h for SEM and 1 to 5 s for SIM). The SEM approach solved the numerical integration of the DAE system at each iteration step. Instead, SIM solved the optimization problem once at the optimal point. However, in many cases the SIM method could not solve the optimization problem since the model did not converge due to numerical limitations.
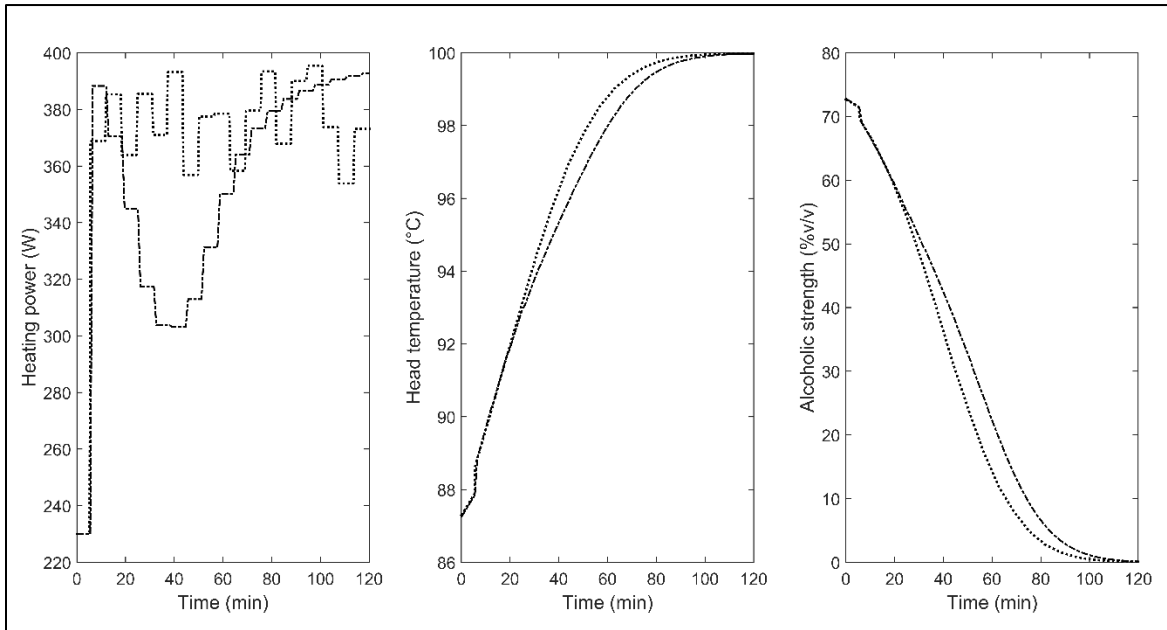
Figure 3-6. Heating power, head temperature and instant alcoholic strength optimal curves obtained by SEM ($\alpha = 0.05$, dotted line) and SIM ($\alpha = 0.06$, dash-dot line).
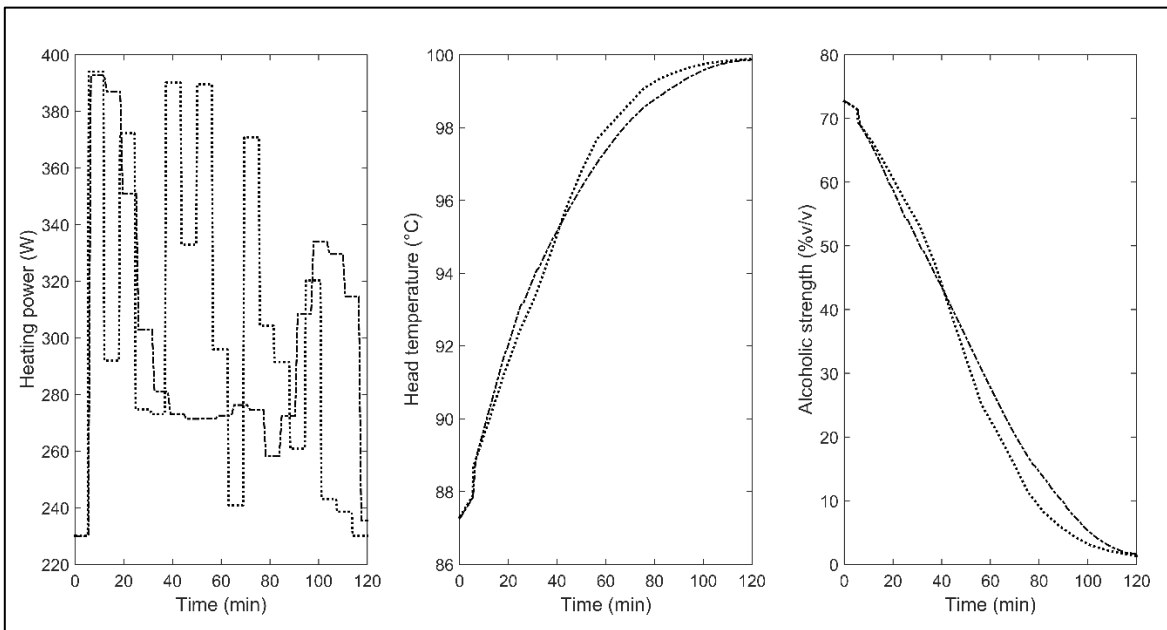
Figure 3-7. Heating power, head temperature and instant alcoholic strength optimal curves obtained by $\alpha = 0.2$. SEM (dotted line) and SIM (dash-dot line).

For $\alpha = 0.06$ for SEM and 0.05 for SIM, the high-limit heating rate (400 W) was obtained, resulting in the highest ethanol recovery (objective 1) at the expense of the highest methanol concentration (objective 2). In turn, for $\alpha \geq 0.5$, the low-limit heating rate (230 W) was obtained, yielding the lowest ethanol recovery and lowest methanol concentration. In this case, it was possible to reduce the relative methanol concentration 7.3% compared to the concentration in the initial mixture (1.37 g/L.a.a.), recovering 87.2% of the ethanol (Table 3-3). De Lucca *et al.* (2013) were able to reduce the relative methanol concentration in the distillate by 22.7% in relation to the initial mixture, recovering 75% of the ethanol in a simulated packed column. In addition, these authors observed that smaller head/heart and heart/tail cut times yielded lower methanol concentrations, independently of the distillation strategy. Thus, to compare both distillation methods (Charentais alembic and packed distillation column) in their ability to reduce the distillate methanol content, we solved the optimization problem with $\alpha = 1$, reducing the head/heart cut time and fixing the ethanol recovery at 75%. We were able to reduce the methanol content in the distillate by 16.8% (1.14 g/L.a.a) in relation to the initial mixture. A batch packed column distillation system has a much higher rectification capacity than a Charentais alembic; therefore, it can reduce the methanol concentration in the distillate 35% more than the Charentais alembic.
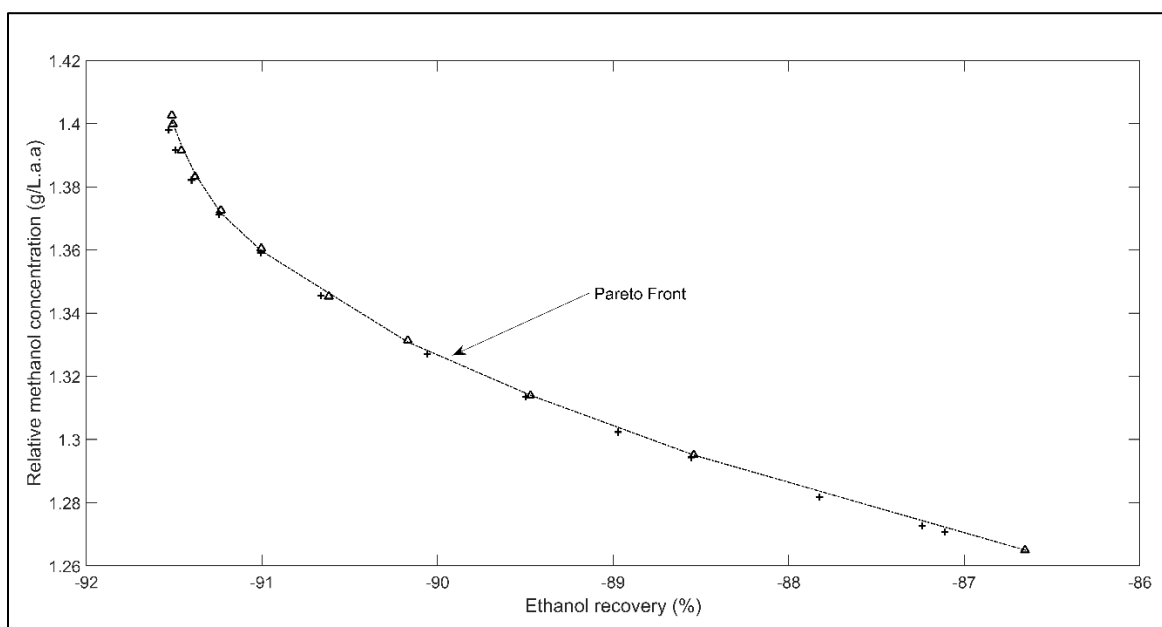
Figure 3-8. Relative methanol concentration (objective 1) vs ethanol recovery (objective 2). Sequential method (Δ) and simultaneous method (+).

3.3.3 Experimental validation

A good compromise between both optimization objectives was achieved with α = 0.2, where the methanol concentration was below the legal limit without sacrificing ethanol recovery. Hence, we performed the validation experiments (in triplicate) with this solution, using the SIM head temperature as a variable set point to be tracked by the control system. Figure 3-9 shows the temperature set point (optimal path), the measured head temperature, the room temperature (disturbance) and the heating power (manipulated variable).
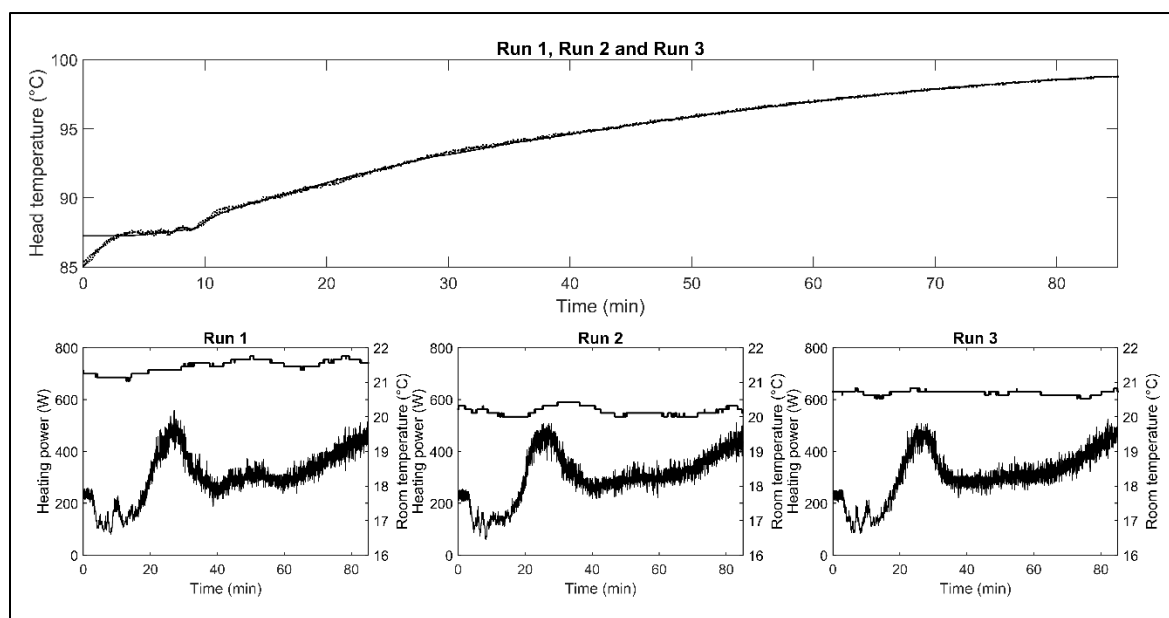
Figure 3-9. Experimental optimal strategy in triplicate. Top figure: head temperature set point (solid line) and measured temperatures (dotted lines). Bottom figures: room temperature (thin lines) and heating power (thick lines).

The measured head temperature evolutions were the same in the three experimental runs, closely tracking the optimal path despite the different evolutions of the room temperature. Small variations in the manipulated variable efficiently compensated these disturbances. It is worth noticing that the optimal experiment finished earlier than predicted by the model. In the experiments, the cuts were defined by the recovered volumes, in order to simplify the comparison with the constant heating strategies (see section 3.2.2). Moreover, the final distillate corresponds to the tail fraction cut which was not part of the optimization objective.

Figures 3-10 and 3-11 show a good agreement between simulations and measured values, where most of them lie within the confidence interval. Like in the model calibration experiments, alcoholic strength and distilled volume were the best-fitted variables.
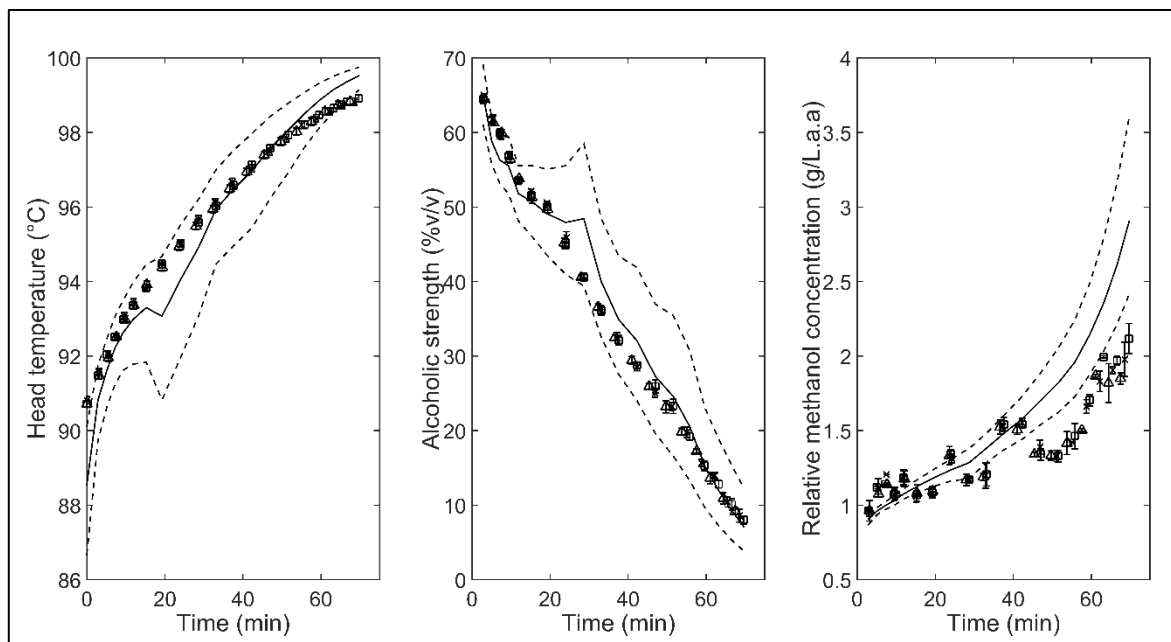
Figure 3-10. Experimental optimal strategy: head temperature, alcoholic strength and methanol concentration. Experimental data: run 1 (×), run 2 (□) and run 3 (Δ). Simulation (solid line) and confidence interval (dashed line).
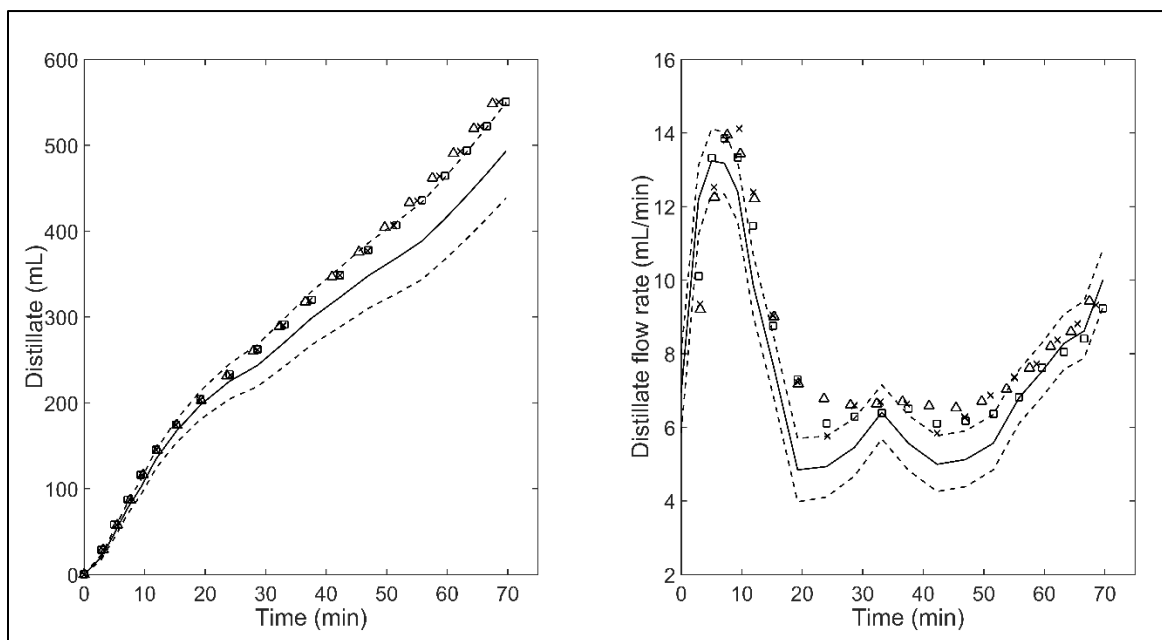
Figure 3-11. Experimental Optimal strategy: distillate volume and distillate flow rate. Experimental data: run 1 (×), run 2 (□) and run 3 (Δ). Simulation (solid line) and confidence interval (dashed line).

We compared the heart cut ethanol recovery and relative methanol concentration obtained in the three distillation strategies. Simulations of all strategies considered 85 mL of head and 375 mL of heart (see section 3.2.2), and these were compared with experimental values (Figure 3-12). Experiments confirmed that the optimal strategy achieved the lowest methanol concentration in the heart cut (1.23 g/L.a.a.).
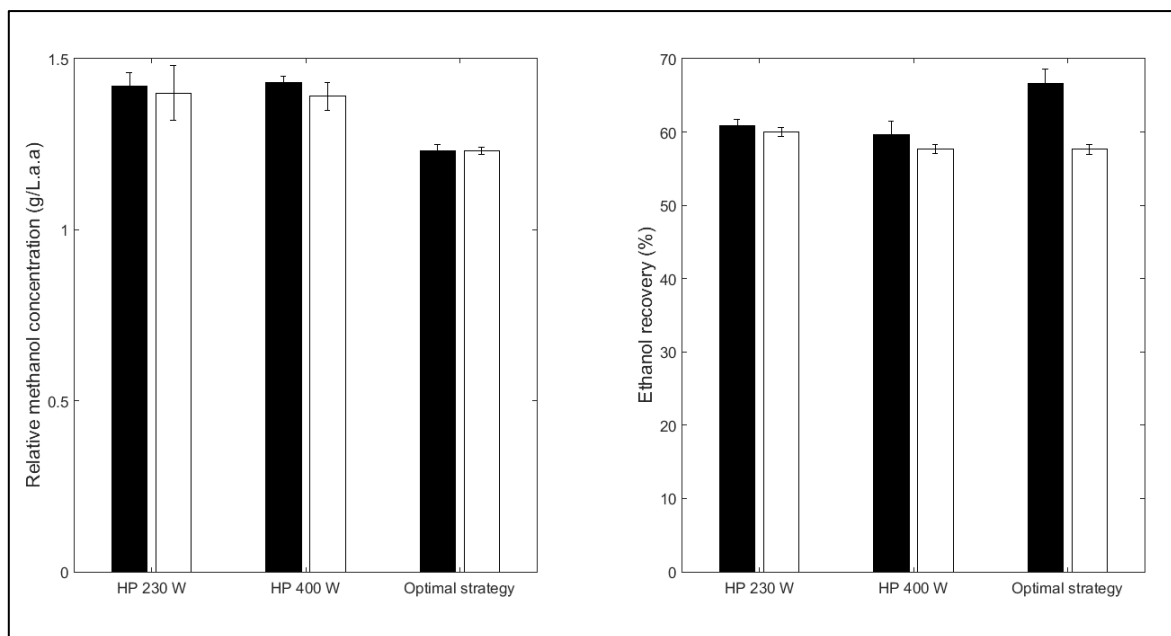
Figure 3-12. Relative methanol concentration and ethanol recovery in the heart cut for each distillation strategy: predicted values (■) and experimental data (□).

The experimental relative methanol concentrations were practically the same for high and low heating power strategies, while simulated values (based on cut times) were significantly different (see Tables 3-2 and 3-3). In the experiments, for simplicity, the fractions were defined by volume, while in the simulations the fractions were defined by fixed cut times. Nevertheless, simulations of methanol concentrations in the heart fractions based on volumes were quite accurate in all experiments (see Figure 3-12). Simulations of ethanol recovery were inaccurate only for the optimal heating strategy, which was overestimated by 9%. This overestimation can be due to differences between simulated and experimental heating, where the latter covered a wider range of values (0-500 W) to provide the control system more flexibility to cope with unmeasured disturbances. In addition, our model included several approximations regarding the energy balances: (i) the heat transfer parameters in the optimal strategy (UA) were a linear function of the heating power applied in the boiler between 230-400 W; (ii) the energy balances did not consider the thermal inertia contribution of the 2.5 kg of copper of the alembic; and (iii) the accumulation term in the energy balance in the head of the alembic (partial condenser) was neglected. Since ethanol content in the distillate depends strongly on the equilibrium temperature and varied widely in all distillation runs (between 5 and 65%), simulations of the heart cut ethanol recovery were quite sensitive to

the small errors in the simulated instantaneous values due to the assumptions above. In turn, relative methanol concentrations were less dependent on the equilibrium temperature and varied in a much narrower range (between 1.23 and 1.45); hence, those small errors due to the energy balance assumptions had much less impact on the predictions of the relative methanol concentration in the heart cut. Nevertheless, by applying the methodology described above, we were able to reproducibly obtain in experimental runs a distillate with 12% less methanol than standard strategy distillates, with a moderate reduction (2.4%) in the ethanol recovery.

3.4 Conclusions

A reliable method was presented to develop optimal operating strategies for Charentais alembics that simultaneously achieved high ethanol recoveries and low methanol concentrations in the distillate. The developed model accurately reproduced the experimentally observed methanol concentrations in the optimal strategy. Experimental ethanol recoveries were 9% lower than simulated for the optimal strategy, due to model approximations and the wider operating range of the control variable of the experimental system. With the optimal strategy tested experimentally, we were able to reduce the methanol concentration in the distillate by 12% compared with standard operating strategies (constant heating rates), without a significant reduction in the ethanol recovery. In particular, our results showed that a volatile impurity such as methanol could be reduced in the spirit by applying a low heating power during the head cut. In addition, increasing the heating power at the beginning of the heart cut will favor the recovery of ethanol. Much better distilled spirits can be obtained by applying model-based engineering tools than those achieved by trial and error experimentation or intuitively. In addition, the methodology proposed in this study could be easily applied to tackle objectives that are more challenging. For example, to produce spirits with enhanced floral aroma and reduced off-flavors. This technology can be applied in small and medium distilleries since the system implementation is relatively simple and low cost.

3.5 Appendix A. Alembic model

Mass (total, ethanol, methanol) and energy balances in the boiler,

$$\frac{d(M_B)}{dt} = L - V_B \tag{A.3-1}$$

$$\frac{d(M_B \cdot x_B^e)}{dt} = L \cdot x_L^e - V_B \cdot y_B^e \tag{A.3-2}$$

$$\frac{d(M_B \cdot x_B^m)}{dt} = L \cdot x_L^m - V_B \cdot y_B^m \tag{A.3-3}$$

$$\frac{d(M_B \cdot u_B)}{dt} = L \cdot h_L - V_B \cdot H_B + \dot{Q}_B \tag{A.3-4}$$

Mass (total, ethanol, methanol) and energy balances in the partial condenser (negligible liquid holdup),

$$V_B - L - V_D = 0 \tag{A.3-5}$$

$$V_B \cdot y_B^e - L \cdot x_L^e - V_D \cdot y_D^e = 0 \tag{A.3-6}$$

$$V_B \cdot y_B^m - L \cdot x_L^m - V_D \cdot y_D^m = 0 \tag{A.3-7}$$

$$V_B \cdot H_B - L \cdot h_L - V_D \cdot H_D - \dot{Q}_C = 0 \tag{A.3-8}$$

Thermodynamic equilibrium relationships for methanol,

$$y_D^m = K_C^m \cdot x_L^m \tag{A.3-9}$$

$$y_B^m = K_B^m \cdot x_B^m \tag{A.3-10}$$

$$K_{B,C}^m(x_B^e, x_L^e) = \frac{y_{B,D}^m}{x_{B,L}^m} = \frac{P_m(x_B^e, x_L^e) \cdot \gamma_m(x_B^e, x_L^e)}{P} \qquad \text{(A.3-11)}$$

The activity coefficient for methanol γ_m is estimated using the UNIFAC contribution groups method. Given the assumption of a quasi-binary mixture, the activity coefficient only depends on the ethanol concentration since an infinite dilution of methanol in a mixture of water-ethanol is assumed.

Heat transfer model

$$\dot{Q}_B = \dot{Q}_{cal} - UA_b \cdot (T_B - T_{env}) \qquad \text{(A.3-12)}$$

$$\dot{Q}_C = UA_c \cdot (T_C - T_{env}) \qquad \text{(A.3-13)}$$

Where $\dot{Q}_{cal}$ and T_{env} are input variables corresponding to the control variable and disturbance of the system respectively. This model has only one empirical parameter, $U \cdot A$, which can be easily fitted with data normally available in commercial distillation facilities (J.R. Pérez-Correa et al., 2013).

Simulation

To simulate the model, a reordering of equations is convenient. The distillate molar flow rate is obtained from mass and energy balances in the partial condenser (Eqs. A.3-5, A.3-6 and A.3-8)

$$V_D = \frac{\dot{Q}_C}{(H_B - H_D) + \frac{(y_B^e - y_D^e)}{(x_L^e - y_D^e)} \cdot (H_D - h_L)} - \frac{-\dot{Q}_C}{(h_L - H_D) + \frac{(x_L^e - y_D^e)}{(y_B^e - y_D^e)} \cdot (H_D - H_B)} \qquad \text{(A.3-14)}$$

To calculate the volume of distillate, an empirical correlation which calculates the density of the mixture from ethanol composition is used (Neuburg & Perez-Correa, 1994),

$$\rho_L(y_D^e) = \frac{y_D^e \cdot PM_E + (1 - y_D^e) \cdot PM_W}{\phi \cdot y_D^e + (1 - y_D^e) \cdot PM_W/\rho_W} \tag{A.3-15}$$

$$\phi = f(y_D^e, T_D) \tag{A.3-16}$$

To simulate the model outputs, the distilled volume (V), as well as the accumulated ethanol and methanol, must be calculated by three differential equations.

$$\frac{dV}{dt} = \frac{V_D \cdot (y_D^e \cdot PM_E + (1 - y_D^e) \cdot PM_W)}{\rho_L(y_D^e)} \tag{A.3-17}$$

$$\frac{dM_D^e}{dt} = y_D^e \cdot V_D \tag{A.3-18}$$

$$\frac{dM_D^m}{dt} = y_D^m \cdot V_D \tag{A.3-19}$$

where M_D^e and M_D^m are the ethanol and methanol moles in the accumulated distillate, respectively. However, the ethanol concentration was measured in alcoholic strength (GA), the methanol concentration in mg/L (M_{eth}) and relative methanol concentration in g/L.a.a (C_{meth}).

$$GA = \frac{M_D^e \cdot PM_E \cdot (1/\rho_E)}{V} \cdot 100 \tag{A.3-20}$$

$$M_{eth} = \frac{M_D^m \cdot PM_M}{V} \cdot 1 \cdot 10^{-6} \tag{A.3-21}$$

$$C_{meth} = \frac{M_D^m \cdot PM_M}{V \cdot (GA/100)} \cdot 1000 \tag{A.3-22}$$

Finally, to calculate the composition of ethanol in the partial condenser, a rearrangement of the energy balance (Eq. A.3-4) from mass balances in the boiler (Eqs. A.3-1 and A.3-2) is required,

$$\left(L(x_L^e - x_B^e) - V_B(y_B^e - x_B^e)\right)\left(\frac{\partial h_B}{\partial x_B} + \frac{\partial h_B}{\partial T_B}\frac{dT_B}{dx_B}\right) = L(h_L - h_B) - V_B(H_B - h_B) + \dot{Q}_B \qquad \text{(A.3-23)}$$

This equation is an implicit function that depends on the value of x_L^e. This equation was solved iteratively using MATLAB's *fsolve* routine (in the sequential method) and in the AMPL code was included as an additional constraint in the optimization problem (in the simultaneous method).

3.6 Acknowledgements

CHAPTER 4: MODELING AND MULTI-OBJECTIVE DYNAMIC OPTIMIZATION OF MUSCAT WINE BATCH DISTILLATIONS

Ricardo Luna, Pau Matias-Guiu, Francisco López, José R. Pérez-Correa

4.1 Introduction

Distilled spirits, normally produced from the surplus of cereals and fruits available in a given region, are characterized by a distinctive aroma. Barley is used in both Scotch Whisky and Irish Whiskey. Barley, corn and rye are used to produce bourbon in USA. Cane juice is used to produce rum in the Caribbean and cachaça in Brazil, while agave is used to produce tequila in Mexico. Grapes are used to produce several kinds of distillates, like brandy in Spain, cognac in France, as well as pisco in Chile and Peru (Small et al., 2011). These beverages are mainly composed of water and ethanol, representing 97-99 % of the total content of the spirits. However, the distinctive aroma of these spirits is defined by hundreds of low concentration compounds called congeners. These compounds explain the difference in flavor and aroma between 2 spirits, such as whisky and pisco. The concentration of these congeners depends on many variables such as growing conditions, fermentation variables, yeast strain, distillation equipment, distillation variables, as well as maturation and aging conditions. Distillation plays a key role in preserving the distinctive aroma of young spirits (López, Rodríguez-Bencomo, Orriols, & Pérez-Correa, 2017).

Traditional systems, like copper Charentais alembics (French style) and batch distillation tray-columns (German style), are normally used to produce young spirits like pisco and cachaça. Charentais alembics are widely used in small scale facilities since its operation is much simpler than batch columns and are more suitable to preserve the original fruit aroma (Arrieta-Garay et al., 2013). It has been observed that batch distillation packed-columns allow fast and flexible control of the internal reflux rate (Matias-Guiu et al., 2016, 2018), although the process is much less reproducible than distillations with Charentais alembics (García-Llobodanin et al., 2011). Nonetheless, alembics are subjected to many uncontrolled and unmeasured disturbances that also generate variability in the composition of the final product (Luna et al., 2018). In these systems, three cuts are collected sequentially: head, heart

and tail. There are different criteria to define the cuts during the distillation, such as ethanol recovery, alcoholic strength (Spaho et al., 2013) or the temperature of the vapor before it enters the condenser (Spaho, 2017). Distillers, based on experience and on-line tasting and smelling, define the cut-times to balance the congeners to attain spirits with good aroma and no off-flavors. This remains the most reliable method to determine cut-times. Alternatively, distillation mathematical models have been developed for decision making and exploring new strategies. Wine distillation models have been developed for batch distillations in plate columns (Osorio et al., 2004), packed columns (Carvallo et al., 2011) and copper Charentais alembics (Sacher et al., 2013). These models are constituted by a set of differential and algebraic equations (DAEs) and have been applied to define cut-times and to find optimal operating strategies (De Lucca, Munizaga-Miranda, Jopia-Castillo, Gelmi, & Pérez-Correa, 2013b; Luna et al., 2018; Osorio, Pérez-Correa, Biegler, & Agosin, 2005).

Model based design have many advantages such as being much faster and cheaper than experimental trial and error. To design optimal operating strategies for batch distillations, dynamic optimization techniques, using the sequential or the simultaneous approach (Srinivasan et al., 2003), can be applied. In the sequential method, the model equations and the objective function are calculated in successive evaluations, i.e., the DAEs are solved independently of the objective function (Safdarnejad et al., 2015). In this case, only the manipulated variable is discretized as a piecewise polynomial and the decision variables of the optimization problem are the polynomial coefficients (Barton et al., 1998; Vassiliadis et al., 1994a, 1994b). In the simultaneous approach, the model equations and the optimization problem are solved together (Hedengren et al., 2014). In this formulation, manipulated variables and state variables are both discretized, therefore differential equations are transformed into algebraic equations, for example using orthogonal collocation on finite elements (Kameswaran & Biegler, 2006). For problems with a moderate number of state variables, the simultaneous approach is faster and can handle more decision variables and constraints than the sequential approach (Hedengren et al., 2014). However, for problems with a small number of decision variables and a large-scale model with many state variables, sequential methods perform better.

Dynamic optimization problems in batch distillation usually consider goals, such as minimize process time, maximize the amount of distillate or of a key component, and maximize economic profit (Diwekar, 1995; Mujtaba, 2004). In batch distillation of alcoholic beverages, dynamic optimization problems have been formulated through multi-objective functions since there are some objectives that should be minimized (off-flavors and toxic compounds) and other maximized (terpenes and fruity esters). Osorio *et al.* (2005) used a multi-objective dynamic optimization weighting method to maximize ethanol and linalool recoveries and minimize the octanoic acid recovery of wine spirit in a tray column. *Luna et al.* (2018) used a weighting method in the dynamic optimization of an alembic distillation to maximize the ethanol recovery and minimize the methanol concentration. Matias-Guiu *et al.* (2018) used a multi-objective optimization based on the desirability approach, using a response surface model to improve the aroma of a Muscat spirits distilled in a batch packed column. In the desirability approach, the conflicting objectives are transformed into a range of acceptability values between 0 and 1, ranging from an undesirable to a desirable objective respectively. When the number of objectives is high, solving the multi-objective problem is difficult, since many conflicting objectives appear that complicates the visualization and interpretation of the solution space, hampering the decision-making process (Pozo, Ruíz-Femenia, Caballero, Guillén-Gosálbez, & Jiménez, 2012). An alternative approach is to use dimension reduction methods that allow omitting redundant metrics from the problem to keep it at a manageable size.

In this study, we used Principal component analysis (PCA) to reduce the dimensionality of a multi-objective dynamic distillation optimization problem. We focused on a model-based design and assessed experimentally the optimal distillation strategies for young Muscat spirits in a Charentais alembic. The aim was to obtain a distillate rich in fruit and floral aromas and low in off-flavors and toxic compounds. A dynamic model (DAEs) of a Charentais alembic developed by Luna *et al.* (2018) was extended to include six congeners representing reliable markers of each distillate cut. In addition, principal component analysis (PCA) was applied to analyze Chilean commercial piscos. Two dynamic optimization problems with two objectives each were formulated and solved using the sequential approach. To reduce the problem's dimensionality, the objectives were a weighting function based on chemical markers and a weighting function based on PCA decomposition.

Experimental computer-controlled distillations were carried out to calibrate the model and to compare standard distillation strategies with optimum operation. The decision variables were the heating power path, the head volume cut, and the heart volume cut.

4.2 Materials and methods

4.2.1 Distillation system

The Charentais copper alembic with automatic control used in our experiments consists of a 4.8 L capacity boiler, a natural convection partial condenser (head), a swan neck and a total condenser. PT100 sensors measured the boiler, head and room temperatures. The heating power (750 W) applied to the boiler was manipulated using an RG solid state controller (Carlo Gavazzi, RGC1P series, Italy). A Programmable Logic Controller (PLC) (S7-1200 Siemens, Germany) received the temperature data from the PT100 sensors and sent the controller output to the RG solid state. A human-machine interface (HMI) and an internal model control (IMC) algorithm were coded in MATLAB®/Simulink™ using the TCP/IP communication protocol with TIA Portal V14 SP1 in a PC (Intel® Core™ i5 7th Gen Hewlett-Packard ProDesk 400MT, USA). In the main control loop, the measured variable was the alembic´s head temperature and the manipulating variables was the heating power in the alembic´s boiler.

4.2.2 Synthetic Muscat wine and experiments

Wines

Model calibration and validation were carried out using data from distillations with a synthetic wine consisting of a mixture of water-ethanol (11.4 % of alcoholic strength, pH 3.2) and six congeners that were adjusted to obtain a composition similar to a Muscat wine (2016 vintage year) (Matias-Guiu et al., 2018). This mixture was prepared once and enough for all the experimental distillations. In each distillation run, the alembic was initially loaded with 1.8 kg of synthetic wine, equivalent to 95 moles (M_0) and 0.038 ethanol molar fraction (x_0). Table 4-1 shows the congener composition of both the synthetic and Muscat wines.

1   Table 4-1. Congeners concentration and their properties in synthetic and Muscat wines.

N_{cong}	Congener	Molar Weight (g/mol)	Synthetic wine		Muscat wine		Odor	Odor threshold (g/hL.a.a.)
			Concentration (mg/L)	Molar fraction (mol/mol)	Concentration (mg/L)	Molar fraction (mol/mol)		
			Head compounds					
1	Acetaldehyde	44.1	162	7.16e-05	179	7.87e-05	Pungent	25[a]
2	Methanol	32.0	88.9	5.39e-05	82.7	5.01e-05	Toxic	167[a]
3	Ethyl acetate	88.1	70.4	1.55e-05	81.3	1.79e-05	Glue	12.5[b]
			Terpenic compound					
4	Linalool	154	1.01	1.27e-07	1.11	1.39e-07	Muscat	0.25[c]
			Tail compounds					
5	Hexanoic acid	116	8.01	1.34e-06	6.57	1.10e-06	Rancid	2[a]
6	β-Phenylethanol	122	31.5	5.00e-06	26.8	4.26e-06	Roses, floral	5[c]

2   [a] Referenced in (Christoph & Bauer-Christoph, 2007).

3   [b] Referenced in (Clutton & Evans, 1978).

4   [c] Referenced in (Cacho et al., 2012).

Model fitting experiments

Two distillation strategies were performed in triplicate, applying different heating powers in the boiler: (i) slow distillation at constant low heating power (250W) and (ii) fast distillation at constant high heating power (450 W). In all distillation runs, three fractions were collected according to predefined volumes: 85 mL of head (sub-fractions 1-2), 375 mL of heart (sub-fractions 3-11) and 115 mL of tail (sub-fractions 12-15). The total amount collected was 640 mL. The corresponding total distillation times were 170 and 68 min for the slow and fast distillations respectively.

Optimization experiments

Two optimal strategies, obtained by multi-objective dynamic optimization, were carried out in triplicate. The first strategy, called w13, was obtained by a weighting function based on chemical markers (MO1) (see section 4.2.9.1). The second strategy, called PCh6, was obtained by a weighting function based on PCA decomposition (MO2) (see section 4.2.9.2). Optimal distillation runs finished when the heart fraction was collected. The head and heart fractions were collected according to the corresponding multi-objective dynamic optimization strategy. For w13, the head and heart fractions were 81.6 and 245.4 mL respectively (see section 4.3.3). For PCh6, the head and heart fractions were 157.3 and 460.1 mL respectively (see section 4.3.4).

4.2.3 Chemical analysis

The ethanol content of wine and distillation residues were determined by ebulliometry (electronic ebulliometer, GAB instruments, Moja-Olèrdola, Spain), wine pH was measured with a pH-meter (Crison Basic 20, L'Hospitalet de Llobregat, Spain) and ethanol content of distilled samples was measured with an electronic density meter (Anton Paar DSA 5000M, Graz, Austria).

Volatile compounds of wines and distillation residues were extracted in duplicate with dichloromethane for further chromatographic analysis, using a methodology adapted from Ferreira et al. (Ferreira, López, Escudero, & Cacho, 1998). Thus, 10 mL of wine were added to a 12-mL glass tube with 50 µL of the internal standard solution (400 mg/L of 2-octanol, Sigma-Aldrich, Saint Louis, USA), 2.5 g of ammonium sulfate (PanReac Química, S.A.U.

Castellar del Vallès, Spain) and 0.5 mL of dichloromethane (PanReac Química, S.A.U. Castellar del Vallès, Spain). Liquid-liquid extractions were carried out for 1 h in an orbital shaker at 110 rpm.

To perform the analysis of distilled samples, 50 µL of the internal standard solution (400 mg/L of 2-octanol, Sigma-Aldrich, Saint Louis, USA) were added to 1 mL of distilled sample (previously adjusted to an alcoholic strength by volume of 40 % v/v to avoid matrix effects during chromatographic analysis). All analyses were performed 21 days after each distillation.

4.2.4 Chromatographic analysis

Chromatographic analyses were performed using a gas chromatograph equipped with a flame ionization detector (GC-FID) (Agilent 6890, Agilent Technologies, Waldbronn, Germany), an autosampler (Agilent 7683, Agilent Technologies, Waldbronn, Germany) and a capillary polar column (MetaWAX, 60 m length, 0.25 mm ID and 0.5 µm phase thickness) from Teknokroma (Barcelona, Spain). Injection (2 µL) was done in split mode (1:5). Injector and detector temperatures were 250 °C and 260 °C, respectively. Oven temperature program was: 40 °C (5 min), 7 °C/min up to 100 °C (15 min), 3 °C/min up to 140 °C and 2 °C/min up to 200 °C (16 min). Column-head flow was initially set at 0.5 mL/min (28 min) and increased with a rate of 5 mL/min^2 up to 1.1 mL/min using helium as carrier gas. Quantifications were carried out by interpolation of calibration curves built with a synthetic hydro-alcoholic solution (40% v/v of ethanol) spiked with the selected compounds at different levels. Reagents' CAS, supplier companies, purity and Kovats retention indices are shown in Table S4-1. Detection and quantification limits were determined by signal-to-noise ratios (S/N) of 3 and 10, respectively.

4.2.5 Principal component analysis

Principal component analysis (PCA) (Jolliffe, 2002) was performed with nine Chilean commercial piscos (number of observations) and six congeners (number of variables) selected for the phenomenological model in section 2.6. The Chilean piscos were analyzed using GC-FID (see section 4.2.4). Table S4-2 shows the congener concentrations of the commercial piscos. Each variable was standardized according to the maximum concentration

observed, and then normalized considering that the measured data follows a normal distribution,

$$Z = \frac{X - \mu}{\sigma} \tag{4-1}$$

where X corresponds to the PCA standardized variables, μ is the mean of the sample of the respective variable and σ is the corresponding standard deviation. The PCA method was coded in MATLAB® R2015a using the *statistics toolbox*. Figure S4-1 shows the PCA results, where the congeners were distributed in three quadrants; (i) acetaldehyde and hexanoic acid, (ii) ethyl acetate, methanol and β-phenylethanol, and (iii) linalool.

4.2.6 Modeling

The original ternary model of the alembic, developed by Luna *et al.* (2018), was expanded to include five new congeners characteristic of the different distillation cuts:

i) *Head cut*: acetaldehyde and ethyl acetate provide negative impact aromas in the final product; to reduce the content of these compounds in the heart cut, they should be recovered as much as possible in the head cut (Christoph & Bauer-Christoph, 2007).

ii) *Heart cut*: linalool is a terpenic compound characteristic of young Muscat wine distillates; it provides a desirable flowery note (Christoph & Bauer-Christoph, 2007).

iii) *Tail cut*: hexanoic acid provides a rancid aroma and is considered a defect in young spirits; β-phenylethanol, although provides a positive rose aroma, it is a an odor marker of tail compounds (Christoph & Bauer-Christoph, 2007).

In addition, PCA equations of these congeners in Chilean commercial piscos were added to the DAE system (see section 4.2.5). Then, the two principal components where compared between the congener simulations from the heart cut and the commercial Chilean pisco´s data.

4.2.7 Model calibration

The data obtained in the constant heat rate distillations with synthetic wine (see Section 4.2.2) were used to calibrate the dynamic alembic model. The fitting parameters were:

$$\theta = [UA_b, UA_c, M_0, x_0, x_{0,cong}] \tag{4-2}$$

Where UA_b and UA_c represent the global heat transfer coefficient multiplied by the corresponding heat transfer area in the boiler and head, respectively. M_0, x_0 and $x_{0,cong}$ are the initial total moles, ethanol molar fraction and congeners molar fraction in the boiler just when the first drop of distillate is recovered. The calibration cost function was:

$$J(\theta) = \sum_j^{n_{var}} \sum_{i=1}^{n_{obs}} \left(\frac{\hat{y}_{ij}(u,\theta,t) - y_{ij}(u,t)}{\max(y_{ij})} \right)^2 \tag{4-3}$$

where index j represents the measured variables and index i the samples times. The measured variables were: distilled volume V, head temperature T_c, alcoholic strength GA and relative congener concentration ($N_{cong} = 1 \dots 6$). $\max(y_{ij})$ corresponds to the maximum measured value of variable j during the distillation run. The optimization problem was solved within MATLAB® R2015a with a scatter search metaheuristic code (SSM) (Egea et al., 2007).

The average concentration of the distillate stream leaving the system at the corresponding time interval where the sample was collected is given by:

$$GA_i = \frac{\Delta GA}{\Delta V} = \left(\frac{M_D^e(t_{exp,i}) - M_D^e(t_{exp,i-1})}{V(t_{exp,i}) - V(t_{exp,i-1})} \right) \cdot PM_E \cdot \frac{1}{\rho_e} \cdot 100 \tag{4-4}$$

$$C_{cong,i} = \frac{\Delta C_{cong}}{\Delta V} = \left(\frac{M_{D,cong}(t_{exp,i}) - M_{D,cong}(t_{exp,i-1})}{\left(V(t_{exp,i}) - V(t_{exp,i-1})\right) \cdot (GA_i/100)} \right) \cdot MW_{cong} \cdot 1000 \tag{4-5}$$

where GA_i and $C_{cong,i}$ are the average alcoholic strength and average relative congener concentration in each collected sample, respectively.

4.2.8 Random simulation design

To explore the model reachable space, several simulations were carried out varying input variables (heat input and cut volumes) with uniformly distributed random values.

Specifically, we searched for operating conditions that yield distillates (in the PCA map) like Chilean commercial piscos. Three cases were assessed: (i) random heating power path and fixed head and heart cuts, (ii) fixed heating power path and random head and heart cuts, (iii) random heating power path and random head and heart cuts. The heating power path was discretized in 19 time steps in both the head cut and heart cut. In each case, one hundred simulations were carried out; the heating power path values varied between 250 and 450 W, UA_b and UA_c parameters were assumed like a linear function between the heating power (250W and 450W) and their estimate values (see section 4.3.1), the head volume varied between 75 and 230 mL, and the heart volume varied between 270 and 630 mL. Simulated congener composition in the heart cut (model output) defined the two principal components and these were compared with the commercial distillate in the PCA map.

4.2.9 Multi-objective dynamic optimization

In chemical engineering, multi-objective optimization problems are commonly encountered when several conflicting objectives should be simultaneously satisfied (Bonilla-Petriciolet & Rangaiah, 2013; Sharma & Rangaiah, 2013). Thus, a set of several optimal solutions can be obtained; this is called the Pareto set (Bhaskar et al., 2000). Even though there are many efficient methods to obtain the Pareto set, in our work we used the simple weighting method (Miettinen & Hakanen, 2009). We defined two cost functions: one based on three chemical markers (one for each distillation cut) and another based on PCA decomposition.

4.2.9.1 Multi-objective weighting function based on chemical markers

A multi-objective cost function was defined to get a heart composition that compromise conflicting criteria, i.e., low head compounds, high heart compounds and low tail compounds. Three chemical markers define the distillation cuts: acetaldehyde for head cut, linalool for heart cut and β-phenylethanol for tail cut. Hence, the multi-objective cost function was specified in terms of these chemical markers, i.e., minimize acetaldehyde, maximize linalool and minimize β-phenylethanol:

$$Min\, J_1 = \alpha \cdot \frac{C_{acet}(t_f)}{150} - \beta \frac{C_{lin}(t_f)}{2} + \gamma \frac{C_{\beta-feOH}(t_f)}{20} \qquad (4\text{-}6)$$

$$\alpha + \beta + \gamma = 1$$

$$0 < \alpha < 1$$

$$0 < \beta < 1$$

$$0 < \gamma < 1$$

where, α (positive to minimize acetaldehyde), $-\beta$ (negative to maximize linalool) and γ (positive to minimize β-phenylethanol) are the relative weights of each objective. C_{acet}, C_{lin} and $C_{\beta-feOH}$ are the relative congener concentration in g/hL.a.a. for acetaldehyde, linalool and β-phenylethanol respectively. All objectives were scaled by their maximum values: acetaldehyde maximum concentration in spirits allowed in the Chilean law (Biblioteca del Congreso Nacional de Chile & Ministerio de Agricultura, 2012), linalool mean maximum concentration observed by Matias-Guiu *et al.* (2018) in Muscat wine distillations and β-phenylethanol mean maximum concentration observed by Bordiga *et al.* (2013) in Muscat wines. Six levels for each weight were defined (α, β, γ = [0, 0.2, 0.4, 0.6, 0.8, 1]); all combinations where the sum of the weights was one were tried, resulting in 21 optimization problems. Each of them was run at least twice to ensure we find the global minimum.

4.2.9.2 Multi-objective weighting function based on PCA decomposition

In this case, the aim was to reproduce the chemical profile of different Chilean commercial piscos, using two principal components; hence,

$$Min\, J_2 = \left(PCA_1 - PCA_{1,target}\right)^2 + \left(PCA_2 - PCA_{2,target}\right)^2 \qquad (4\text{-}7)$$

where PCA_1 and PCA_2 are the principal components of the chemical profiles obtained from the simulation of the distillation. $PCA_{1,target}$ and $PCA_{2,target}$ are the principal components of the chemical profile of the target piscos. Five targets (Chilean commercial piscos) were arbitrarily defined: PCh3, PCh4, PCh5, PCh6 and PCh8. According to the exploratory simulations, some of them were within the reachable space of the simulated distillation system and others were unreachable.

4.2.9.3 Multi-objective dynamic optimization formulation

The optimization variables were the heating power, the volume of the head cut and the volume of the heart cut. Additional optimization constraints were: (i) heating power varied between 250 and 450 W, (ii) volume head cut between 40 and 150 mL, (iii) volume heart cut between 200 and 500 mL and finally, (iv) ethanol recovery in the heart cut must be higher than 35%. Like random exploratory simulations (see section 4.2.8), UA_b and UA_c parameters were assumed a linear function with the heating power.

The numerical method applied to solve the optimization problem was the sequential solution (Srinivasan et al., 2003). The heat input was discretized into equally spaced time intervals:

$$u(\Delta t_i) = a_i \qquad (4\text{-}8)$$

where index i represents the n-th time intervals and a_i represents the value of the heat input u in the i-th time interval. Random exploratory simulations were carried out discretizing the heating power path in 19, 9 and 4 time steps in the head and heart cuts.
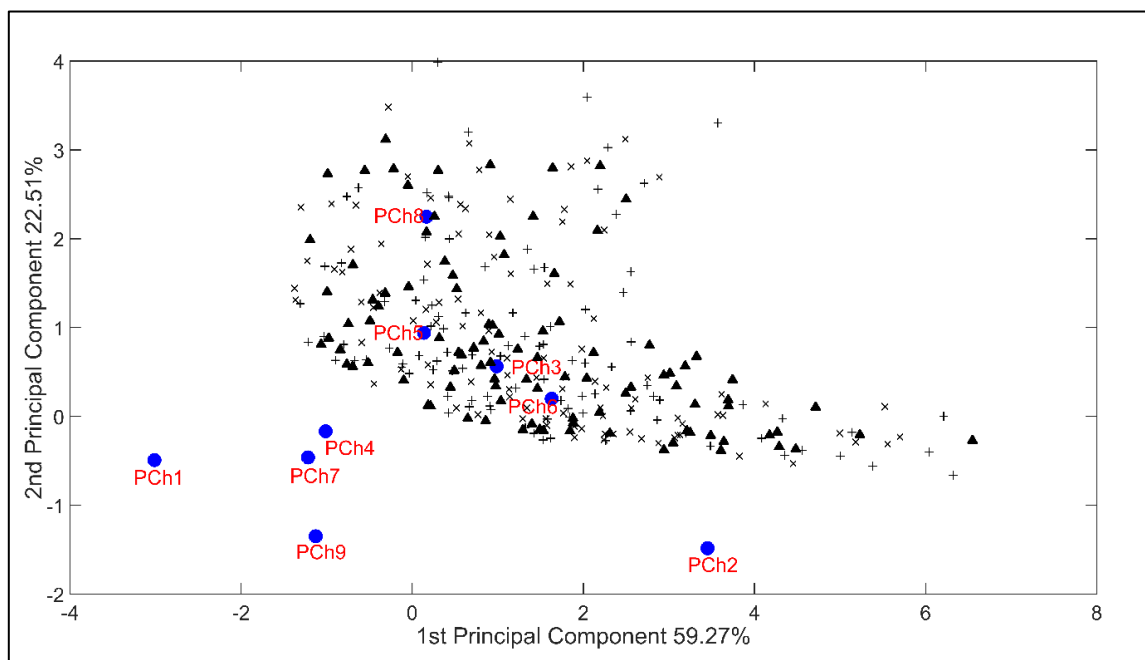
Figure S4-2 indicates that the number of time steps size does not have a significant impact in the aromatic composition of the heart cut. In each simulation case, the results showed similar dispersion and location in the PCA map. Therefore, the head cut was discretized into three

time steps, while the heart cut was discretized into six time steps. The optimization problem was solved within MATLAB® R2015a with a scatter search metaheuristic code (SSM) and the dynamic model of the alembic was solved with MATLAB's solver *ode15s*. The simultaneous approach was not applied since we experienced convergence difficulties with our optimization problem.

4.3 Results

4.3.1 Model calibration

Figure S4-3 and Figure S4-4 show measured values and model outputs of ethanol content, head temperature, distillate volume and congener composition in the distillate of the three replicates of the fast heating rate distillation (450 W). In turn, Figure S4-5 and Figure S4-6 show the fitted variables for the slow heating rate distillation (250 W). The 95% confidence intervals shown in the figures were obtained by simulation, considering the standard deviation in the estimated parameters set ($\theta \pm 2\sigma_\theta$). Table 4-2 shows the fitted parameters for the slow and fast heating power.

Table 4-2. Fitted parameters for distillation strategies.

Parameters	Strategies			
	250W	450W	PCh6	W13
UA_b	0.82 ± 0.04	0.71 ± 0.10	[b]	[b]
UA_c	1.28 ± 0.05	1.73 ± 0.17	[c]	[c]
M_0	93.5 ± 0.3	93.6 ± 0.3	93.3 ± 0.4	93.3 ± 0.2
x_0	0.033 ± 0.0002	0.033 ± 0.0003	0.033 ± 0.0001	0.030 ± 0.0004
$x_{0,cong=1}$	2.37e-5 ± 0.30e-5	2.55e-5 ± 0.17e-5	3.04e-5 ± 0.33e-5	2.45e-5 ± 0.30e-5
$x_{0,cong=2}$	3.18e-5 ± 0.10e-5	3.60e-5 ± 0.096e-5	4.91e-5 ± 0.14e-5	4.33e-5 ± 0.11e-5
$x_{0,cong=3}$	2.95e-6 ± 0.37e-6	3.18e-06 ± 0.17e-6	3.83e-6 ± 0.54e-6	2.92e-6 ± 0.87e-6
$x_{0,cong=4}$	5.78e-8 ± 0.24e-8	6.33e-08 ± 0.38e-8	4.10e-8 ± 0.50e-8	3.41e-8 ± 0.53e-8
$x_{0,cong=5}$	1.33e-6 ± 0.001e-6	1.33e-06 ± 0.01e-6	1.33e-6 ± 0.003e-6	1.32e-6 ± 0.02e-6
$x_{0,cong=6}$	2.43e-6 ± 0.021e-6	2.92e-06 ± 0.12e-6	3.17e-6 ± 0.10e-6	2.30e-6 ± 0.08e-6

[a] Parameters unit: UA_b and UA_c in W/°C, M_0 in mol, x_0 and $x_{0,cong}$ in mol/mol.

[b, c] linear function between UA_b and UA_c values obtained from 250 and 450W respectively.

Both distillation strategies (250 W and 450 W) yielded similar shapes of the evolution curves over time for all compounds. Initial and final values were similar for ethanol, acetaldehyde, ethyl acetate and linalool. Distillations at 450 W evolved faster and were completed in a bit more than 60 minutes. Distillations at 250 W evolved slower and were completed in 160 min. In line with what was observed by Matias-Guiu *et al.* (2018), our experiments and simulations showed higher concentrations of tail compounds in the longer distillations (250 W strategy); 300 vs 180 g/hLa.a. of methanol, 85 vs 25 g/hLa.a. of hexanoic acid and 400 vs 140 g/hLa.a. of β-phenylethanol. Model fitting was in most cases better for the high heating rate distillation than for the low heating rate distillation. Luna *et al.* (2018) had reported similar behavior with the same system but with a simpler mixture, arguing that the higher process time required by the slow distillation made measurements more prone to disturbances. The alcoholic strength and the distilled volume were the best fitted variables in both distillation strategies, as observed by Luna *et al.* (2018).

Head compounds like acetaldehyde and ethyl acetate were predicted well in the head and heart fraction, but in the tail fraction the predictions worsened. Model predictions of acetaldehyde and ethyl acetate were zero in the tail fraction, while measurements showed increasing values. By the end of the distillation, acetaldehyde and ethyl acetate concentrations showed a slower decline than ethanol. Therefore, its relative concentrations are extremely sensitive to ethanol and their measured values in the tail fraction increased. The heart compound linalool was predicted well in all cuts (head, heart and tail) in both fast and slow heating rate distillations. Methanol was predicted well in both strategies in all cuts, especially in the tail cut. Moreover, its predictions were even better than those observed by Luna *et al.* (2018), since in this work we used a better analytical method. Model predictions of hexanoic acid during the heart cut were below the experimental values in both distillations. Finally, in both strategies and all cuts, β-phenylethanol measurements were within the confidence interval of the model predictions.

Congeners such as acetaldehyde, ethyl acetate and methanol were simulated and validated for Charentais alembic distillations of pear wine in Sacher *et al.* (2013) and Sacher *et al.* (2017). These compounds were predicted well and showed the same trend observed in our results. However, β-phenylethanol was not predicted well in their simulations. According to

the simulations of Sacher *et al.* (2017), this compound distilled mainly in the heart fraction, while in our simulations β-phenylethanol distilled mainly in the tail cut. Sacher *et al.* (2013) distilled a pear distillate with 17.9% v/v of ethanol obtained from a previous distillation, whereas our experiments distilled a synthetic wine with 11.4% v/v of ethanol. In addition, initial concentrations of β-phenyethanol in our experiments were 5 times higher than in Sacher *et al.* (2013).

Table 4-2 shows that for both strategies the estimated heat transfer parameter of the boiler was practically the same. The heat transfer parameter of the boiler was less dependent on the heating power in our case, since the heating element is inside the boiler (Luna et al., 2018). In turn, the heat transfer parameter of the head increased with the heating power and was higher than the heat transfer parameter of the boiler. This behavior was also observed by Luna *et al.* (2018) and Sacher *et al.* (2013), arguing that high heating powers induce higher convective air streams, increasing the heat transfer in the head.

4.3.2 Random exploratory conditions

Figure 4-1 shows the results obtained for three simulation cases: (i) random heating power path and fixed cuts, (ii) fixed heating power path and random cuts, (iii) random heating power path and random cuts. These results indicate that cut volumes have a higher influence on the aromatic composition of the distillate (PCA map) than heating power policies. The model could not reproduce some distillates like PCh1, PCh2, PCh4, PCh7 and PCh9. This zone in the PCA map, which is rich in linalool and poor in acetaldehyde, is unreachable with our simulations since:

i) The initial concentration of linalool of our synthetic wine is lower than that of some Muscat wines.

ii) Our model did not consider chemical reactions, in particular the hydrolysis of bounded aromas that occurred during the distillation of Muscat wines (Agosin et al., 2000).

iii) Commercial distillates were produced using plate column stills with higher rectification capacity than Charentais alembics.

iv) Some of these commercial distillates were obtained by double or triple distillation and our simulations considered a single distillation.
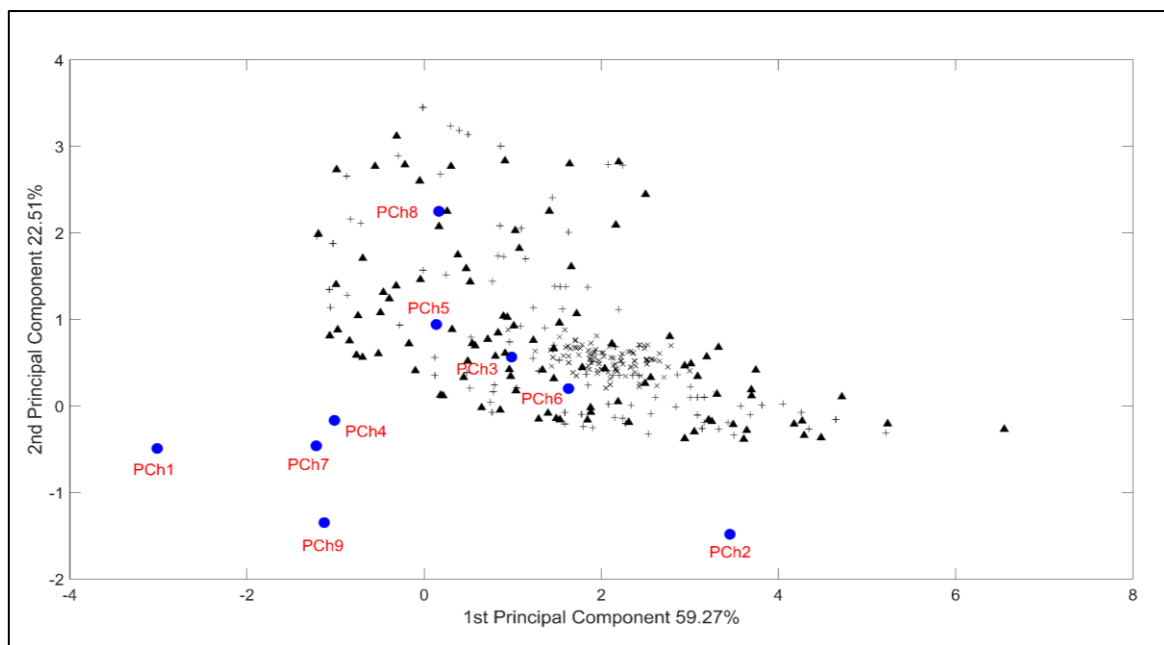
Figure 4-1. PCA map in two principal components: Simulations with random heating power path and random head and heart cuts (▲). Simulations with random heating power path and fixed head and heart cuts (×). Simulations with fixed heating power path and random head and heart cuts (+). Blue points correspond to the commercial piscos.

4.3.3 Multi-objective weighting function based on chemical markers (MO1) and experimental validation

Table 4-3 shows the MO1 optimization results for all weight combinations, including head and heart volumes, ethanol recovery in the heart cut, relative concentrations (g/hLa.a.) of acetaldehyde, linalool and β-phenylethanol as well as PCA_1 and PCA_2 coordinates. During the distillation process, acetaldehyde and linalool are highly volatile and appear in the first fractions of the distillate. Nevertheless, acetaldehyde should be distilled as much as possible in first fraction and linalool should not be lost in the head cut but instead recovered in the heart cut. Our results in Table 4-3 indicate that acetaldehyde concentration (0.70 g/hLa.a.) is minimized when α take on the highest value (run w1); the head and heart cuts were the largest (248.7 and 483.6 mL respectively). Other objectives took on undesirable values; ethanol recovery in the heart fraction (35.2%) was the smallest, linalool concentration was minimum (0.061 g/hL.a.a.) and β-phenylethanol concentration was maximum (43.92 g/hLa.a.). Maximum linalool concentrations (0.930 g/hL.a.a.) were obtained for $\alpha = 0$.

Table 4-3. Results obtained of multi-objective weighting function base on chemical markers in heart cut.

Run	α	β	γ	J_1	Volume head (mL)	Volume heart (mL)	Ethanol recovery (%)	C_{acet}		C_{lin}		$C_{\beta-feOH}$		PCA_1	PCA_2
								g/hLa.a.	OAV[a]	g/hLa.a.	OAV[a]	g/hLa.a.	OAV[a]		
w1	1	0	0	2.170	248.7	483.6	35.2	0.70	0.03	0.061	0.24	43.92	8.78	6.7149	-0.5228
w2	0.8	0.2	0	2.094	249.7	456.9	35.2	0.74	0.03	0.063	0.25	42.41	8.48	6.1376	-0.5987
w7	0.8	0	0.2	0.916	188.7	241.3	40.3	3.51	0.14	0.163	0.65	19.48	3.90	-0.7045	0.3436
w3	0.6	0.4	0	0.788	168.6	241.4	44.4	6.64	0.27	0.232	0.93	17.21	3.44	-1.3241	0.7099
w12	0.6	0	0.4	0.630	129.7	236.0	49.4	14.89	0.60	0.360	1.44	14.23	2.85	-1.9130	1.5723
w8	0.6	0.2	0.2	0.634	131.6	237.8	49.3	15.08	0.60	0.363	1.45	14.29	2.86	-1.8765	1.5895
w9	0.4	0.4	0.2	0.586	101.5	252.9	55.3	27.94	1.12	0.492	1.97	12.91	2.58	-1.5663	2.6575
w16	0.4	0	0.6	0.525	99.3	217.5	50.6	28.21	1.13	0.514	2.05	11.88	2.38	-1.9286	2.7492
w13	0.4	0.2	0.4	0.555	81.6	245.4	57.5	39.85	1.59	0.590	2.36	11.70	2.34	-1.0991	3.5516
w4	0.4	0.6	0	0.545	80.8	239.2	56.4	41.14	1.65	0.605	2.42	11.47	2.29	-1.0835	3.6643
w19	0.2	0	0.8	0.545	57.8	206.8	53.9	71.60	2.86	0.825	3.30	9.60	1.92	0.9272	5.6770
w17	0.2	0.2	0.6	0.556	55.0	206.2	54.1	76.39	3.06	0.852	3.41	9.47	1.89	1.3679	5.9496
w5	0.2	0.8	0	0.601	46.8	205.4	54.7	91.46	3.66	0.930	3.72	9.12	1.82	2.8929	6.7393
w6	0	1	0	0.601	46.8	205.4	54.7	91.46	3.66	0.930	3.72	9.12	1.82	2.8929	6.7393
w10	0.2	0.6	0.2	0.601	46.8	205.4	54.7	91.46	3.66	0.930	3.72	9.12	1.82	2.8929	6.7393
w11	0	0.8	0.2	0.601	46.8	205.4	54.7	91.46	3.66	0.930	3.72	9.12	1.82	2.8929	6.7393
w14	0.2	0.4	0.4	0.601	46.8	205.4	54.7	91.46	3.66	0.930	3.72	9.12	1.82	2.8929	6.7393
w15	0	0.6	0.4	0.601	46.8	205.4	54.7	91.46	3.66	0.930	3.72	9.12	1.82	2.8929	6.7393
w18	0	0.4	0.6	0.601	46.8	205.4	54.7	91.46	3.66	0.930	3.72	9.12	1.82	2.8929	6.7393
w20	0	0.2	0.8	0.601	46.8	205.4	54.7	91.46	3.66	0.930	3.72	9.12	1.82	2.8929	6.7393
w21	0	0	1	0.601	46.8	205.4	54.7	91.46	3.66	0.930	3.72	9.12	1.82	2.8929	6.7393

[a] Odor activity value expressed in units of aroma (u.a.) were calculated by dividing the congeners concentrations in g/hLa.a. of this table by respective odor threshold in Table 4-1.

In these cases, the head and heart volume cuts were the smallest (205.4 and 46.8 mL respectively), ethanol recovery in the heart fraction was the largest (54.7%), acetaldehyde was maximized (91.46 g/hLa.a.) and β-phenylethanol was minimized (9.12 g/hLa.a.). Hence, maximum linalool concentrations in the heart coincide with maximum acetaldehyde concentrations, evidencing a clear trade off that must be solved. In turn, β-phenylethanol is less volatile and appears mainly in the last fraction of the distillate (Figure S4-4 and Figure S4-6) and should not be distilled in the heart fraction. Consequently, to minimize β-phenylethanol in the heart, the head and heart cuts should be the shortest. Therefore, linalool and β-phenylethanol are harmonic objectives, i.e., achieving an improvement in one objective will also lead to an improvement in the other (Weise, 2008). Thus, it is convenient to define the multi-objective cost function with only two objectives (chemical markers): acetaldehyde and linalool or acetaldehyde and β-phenylethanol, i.e., the head marker with the heart marker or the head marker with the tail marker (see Table S4-3).

Matias-Guiu *et al.* (2018) reported the same behavior in a packed column still. Large head volumes favored the extraction of ethanol, head compounds (like acetaldehyde) and linalool in the head-cut, consequently reducing their levels in the heart-cut, while increased tail compounds (like β-phenylethanol) in the heart-cut. They also observed that large heart volumes favored high levels of tail compounds in the heart-cut.

The w13 optimal simulation was chosen to validate the alembic model. Figure S4-7 shows the tracking of the optimal set-point in the head temperature, the evolution of the heating power and the room temperature of these distillations. The measured head temperature had practically the same evolution in all runs despite different evolutions of the environmental temperature. Run 1 showed greater differences when compared to run 2 and 3. Small variations in the manipulated variable efficiently compensated these disturbances, like the alembic distillation system in Luna *et al.* (2018). Figure S4-8 and Figure S4-9 compare simulations with experimental values of the w13 strategy. This strategy was completed in 45 min (including head and heart cuts). Alcoholic strength, head temperature and distillate volume were predicted well. Acetaldehyde, methanol, ethyl acetate, linalool and β-phenylethanol predictions were inside the confidence intervals in the head and heart fractions.

Model predictions of hexanoic acid during the head and heart cuts were below the experimental values. The results of the calibration distillations showed a similar behavior.

4.3.4 Multi-objective weighting function based PCA decomposition (MO2) and experimental validation

Table 4-4 shows the MO2 optimization results, including PCA_1 and PCA_2 optimal coordinates, PCA_1 and PCA_2 target coordinates, as well as the head and heart cut volumes, ethanol recovery and relative concentrations of acetaldehyde, linalool and β-phenylethanol of the heart fraction. Figure 4-2 shows the optimal values of the congeners in the PCA map for each optimization case including both methods: the multi-objective weighting function based on PCA decomposition (see Table 4-4) and the multi-objective weighting function based on chemical markers (see Table 4-3).
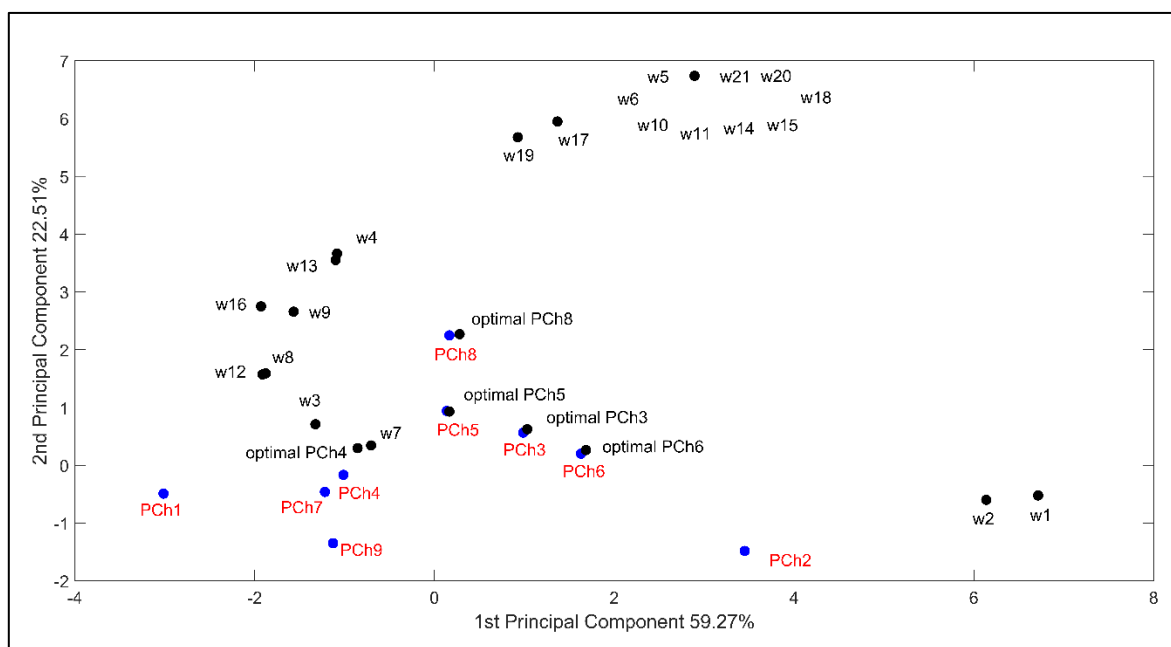
Figure 4-2. PCA map in two principal components: distillate target optimal points by MO2 and weight optimal points by MO1 (black points), and Chilean commercial piscos (blue points).

Table 4-4. Results obtained of multi-objective weighting function base don PCA decomposition.

Target of multi-objective optimization	Simulated											Target	
	Volume head (mL)	Volume heart (mL)	Ethanol recovery (%)	C_{acet}		C_{lin}		$C_{\beta-feOH}$		PCA_1	PCA_2	PCA_1	PCA_2
				g/hLa.a.	OAV[a]	g/hLa.a.	OAV[a]	g/hLa.a.	OAV[a]				
Optimal PCh3	143.2	449.8	58.9	9.66	0.39	0.260	1.04	25.1	5.02	1.0323	0.6233	0.9866	0.5643
Optimal PCh4	200.0	220.8	38.2	3.22	0.13	0.157	0.63	19.1	3.82	-0.8552	0.2964	-1.0124	-0.1676
Optimal PCh5	127.9	408.2	60.3	11.3	0.45	0.284	1.14	21.7	4.34	0.1665	0.9292	0.1375	0.9409
Optimal PCh6	157.3	460.1	55.1	6.53	0.26	0.212	0.85	27.8	5.56	1.6856	0.2637	1.6299	0.1998
Optimal PCh8	95.4	424.8	70.2	27.7	1.11	0.442	1.77	18.8	3.76	0.2802	2.2689	0.1664	2.2484

[a] Odor activity value expressed in units of aroma (u.a.) were calculated by dividing the congeners concentrations in g/hLa.a. of this table by respective odor threshold in Table 4-1

The MO2 strategy achieved good approximations to commercial distillates PCh3, PCh5, PCh6 and PCh8, which were shown previously to be in the reachable space of the alembic´s model (see Figure 4-1). However, the PCh4 distillate was the hardest to reproduce via simulations since this zone of the PCA map is rich in linalool and poor in acetaldehyde. In addition, as discussed above, when linalool is maximized (desirable value) acetaldehyde is also maximized (undesirable value), as they are competing objectives. Thus, our simulation of the PCh4 distillate required a high rectification, yielding a low productivity, with higher ethanol recovery in the head-cut (53.8%) than in the heart-cut (38.2%).

The heating power paths were very different in each evaluated case. Figure 4-3 shows the optimum trajectories of the heating power, the head temperature and the alcoholic strength obtained for optimal cases PCh6 and PCh8. PCh4 strategy yielded the fastest distillation coinciding with the lowest amount of tail compounds (64.4 of methanol, 0.292 of hexanoic acid and 0.443 of β-phenylethanol in g/hLa.a.) as shown in Table S4-2. Conversely, strategy PCh6 yielded the largest heart volume (460.1 mL) and longest distillation, coinciding with a higher amount of tail compounds (82.8 of methanol, 0.774 of hexanoic acid and 1.91 β-phenylethanol in g/hLa.a.) as shown in Table S4-2. In addition, strategy PCh8 yielded the smallest head-cut (95.4 mL), the highest ethanol recovery in the heart-cut (70.2%) and the highest acetaldehyde concentration (25.5 g/hLa.a.), which is 65-80% more than PCh3, PCh5 and PCh6 (Table S4-2).

Finally, the optimal PCh6 strategy was carried out experimentally to validate the alembic model. Figure 4-4 shows how the heating power was adapted to track the optimal set-point despite the room temperature disturbances. This distillation lasted 80 min and was more reproducible than the w13 distillation. Figure 4-5 and Figure 4-6 show that alcohol strength, distillate volume, head temperature and most congeners were well predicted. Only hexanoic acid predictions were biased, like in the calibration experiments (250 W and 450 W strategies); in this case the thermodynamic model used is probably unsuitable.
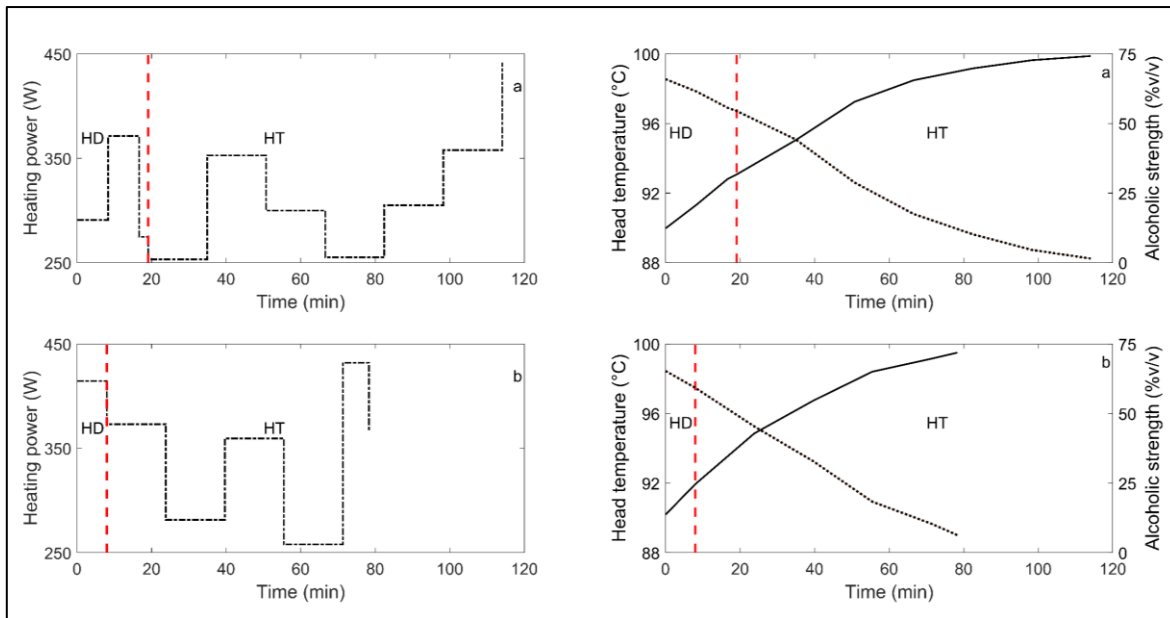
Figure 4-3. Heating power, head temperature and alcoholic strength vs time. PCh6 strategy (a), PCh8 strategy (b), head fraction (HD) and heart fraction (HT). Heating power (−.), head temperature (−) and alcoholic strength (:).
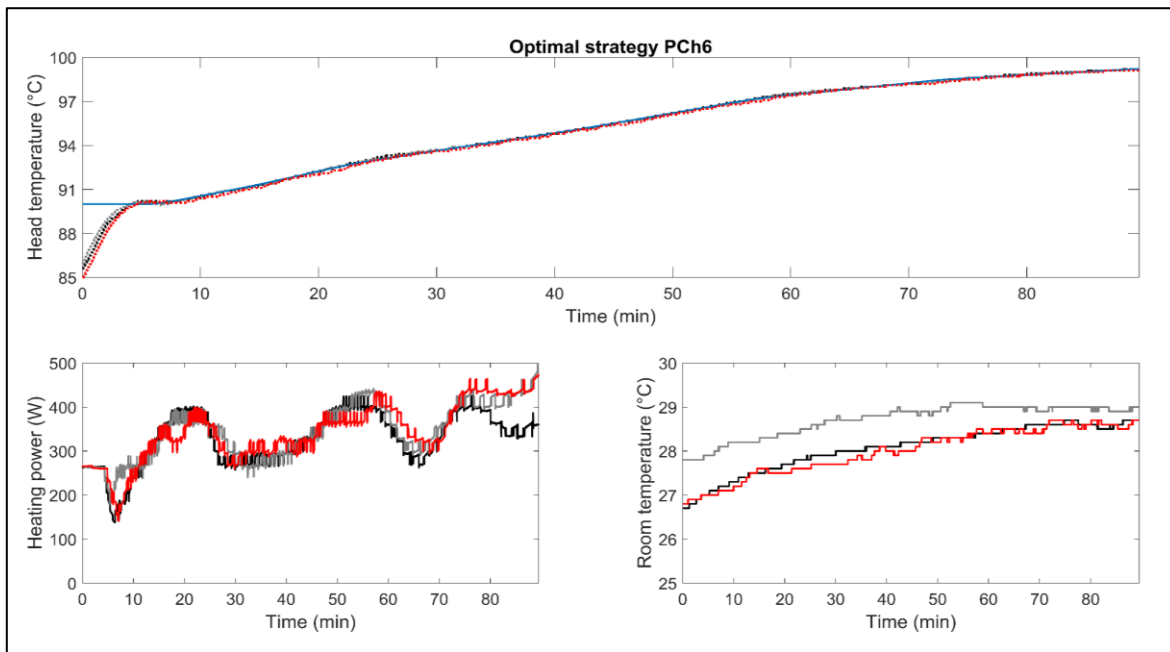
Figure 4-4. Experimental PCh6 optimal strategy in triplicate. Top figure: head temperature set point (sky blue solid line), measured temperatures; run 1 (black dotted lines), run 2 (gray dotted lines) and run 3 (red dotted lines). Bottom Figures: heating power path and room temperature; run 1 (black solid line), run 2 (gray solid line) and run 3 (red solid line).
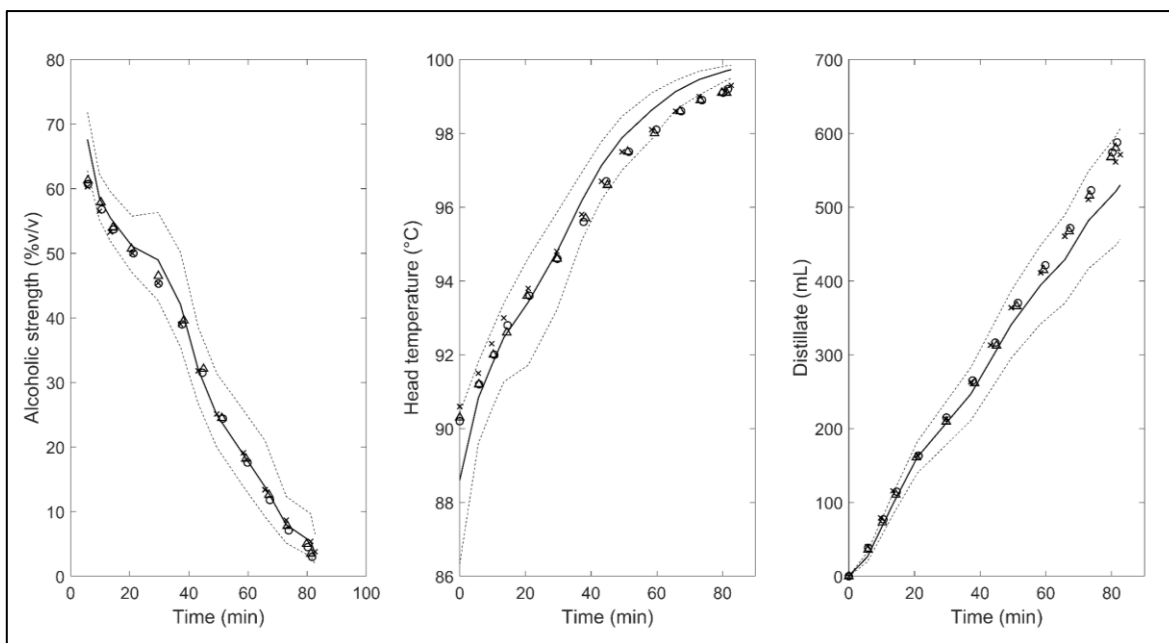
Figure 4-5. Alcoholic strength (%v/v), head temperature and distillate volume vs time for an optimal PCh6 strategy. Experimental data; run 1 (×), run 2 (Δ) and run 3 (○). Simulation (−) and confidence interval (− −).
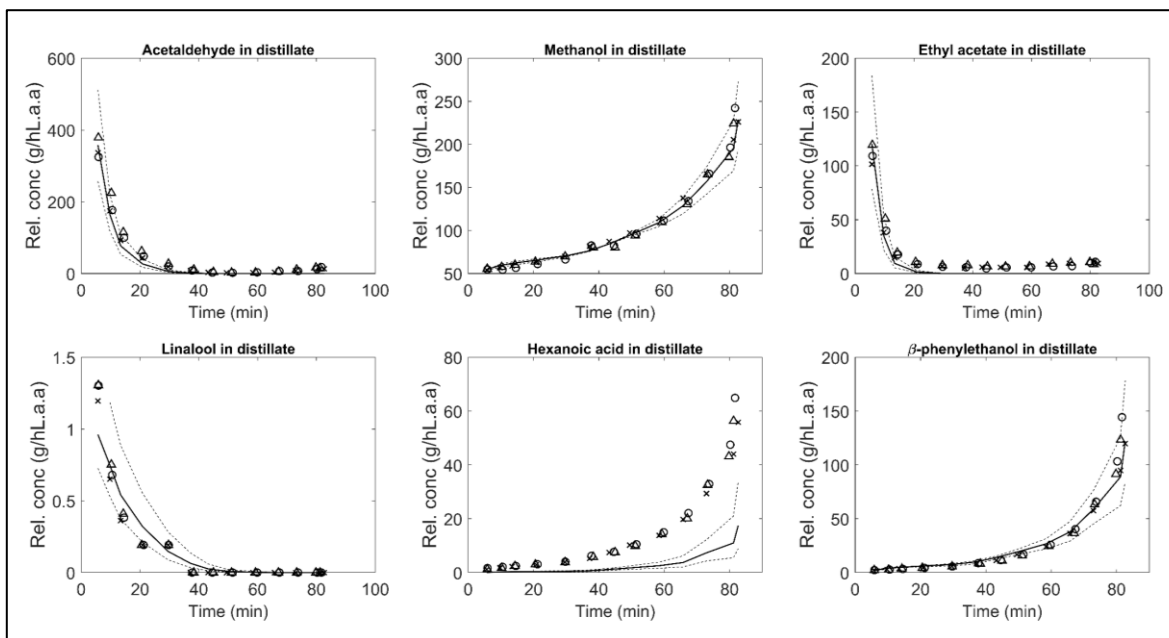
Figure 4-6. Congeners concentrations (g/hL.a.a.) vs time for an optimal PCh6 strategy. Experimental data; run 1 (×), run 2 (Δ) and run 3 (○). Simulation (−) and confidence interval (− −).

4.3.5 Comparison of multi-objective function MO1 and MO2

Figure 4-7 shows the Pareto front (acetaldehyde vs linalool) according to the MO1 results (see section 4.3.3). The upper part of the Pareto front corresponds to optimization runs with β and γ values higher than α. In these distillations, the heating power was kept constant at the lower limit (250 W). The lower part of the Pareto front corresponds to optimization runs with α values higher than β and γ.
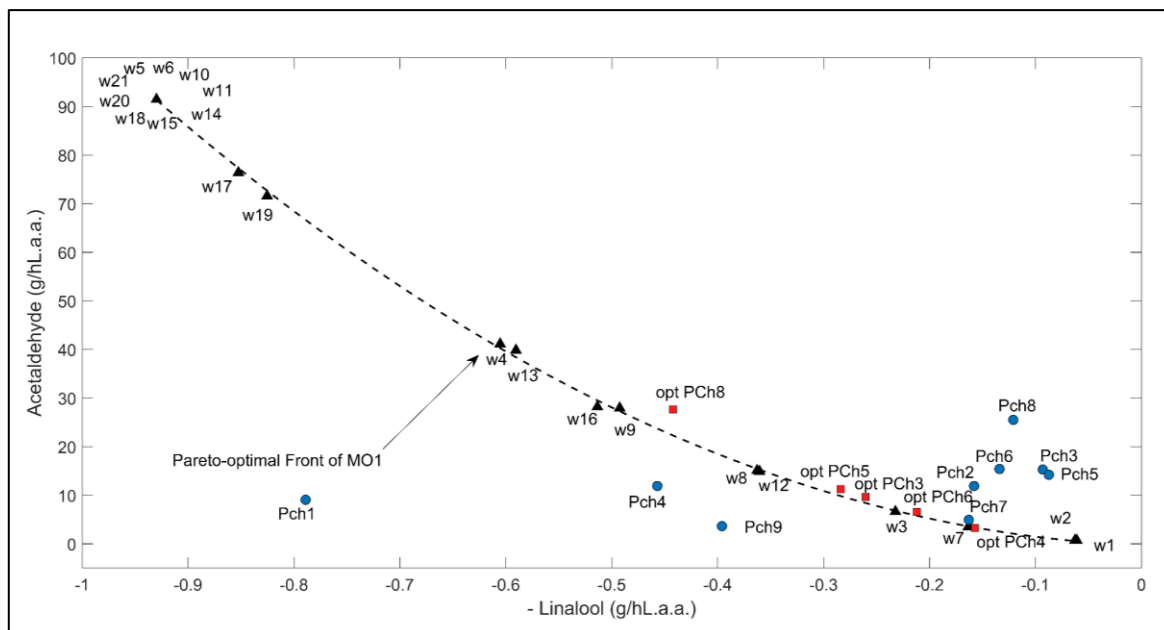
Figure 4-7. Pareto front: relative acetaldehyde concentration vs relative linalool concentration; weight optimal points by MO1 (black triangles), distilled target optimal points by MO2 (red squares) and Chilean commercial distillates (blue circles). Note that the concentrations of linalool are plotted with negative values to preserve the usual shape of Pareto front figures.

Figure 4-7 also includes the MO2 results, showing that many principal component optimization strategies (opt PCh3, opt PCh4, opt PCh5 and opt PCh6) lie close to the lower part of the Pareto front, defined by high values of α. Moreover, many of the commercial piscos analyzed (PCh2, PCh3, PCh5, PCh6, PCh7 and PCh8) lie in this zone. For example, commercial pisco PCh7 lies in the Pareto front and contains practically the same linalool and acetaldehyde concentrations as the w7 optimal solution from MO1 and PCh4 optimal solution of MO2. Contrarily, PCh1, PCh4 and PCh9 commercial piscos lie well below the

Pareto front. These results indicate that many commercial distillates coincided with optimal strategies in the Pareto front, meaning that the skills and years of experience of the pisco distillers were able to reach optimal distilling conditions.

Validation experiments of w13 and PCh6 strategies confirmed that maximizing linalool concentrations implies minimizing β-phenylethanol concentrations (harmonic objectives) and minimizing acetaldehyde concentrations (competitive objectives) in the heart cut. A fast distillation strategy like w13 obtained high concentrations of linalool and head compounds like acetaldehyde and ethyl acetate, and low concentrations of tail compounds such as methanol and β-phenylethanol (see Table S4-3). Conversely, slow distillations like PCh6, yielded low concentrations of acetaldehyde and linalool, and high concentrations of tail compounds (see Table S4-4).

Both validation experiments lie far from the Pareto front, while the corresponding simulations locate exactly in the Pareto front (Figure S4-10). In both experimental cases, more acetaldehyde and less linalool than predicted were obtained, although PCh6 simulations were closer to measured values than w13 predictions. Predictions of the rest of the congeners were also biased, safe for methanol predictions that were quite accurate. Experiments w13 and PCh6 were recalibrated to verify if the model could fit the observations better; calibrated parameters are shown in Table S4-5. UA_b and UA_c parameters showed the most significant differences with those calibrated in section 4.3.1. These new parameters were smaller than those calibrated originally, since environmental temperatures and distillation times were different than those of the calibration experiments. The new simulations (w13 cal and PCh6 cal) lie in the Pareto front close to the original simulations and were not able to fit the measured values better (Figure S4-10). Therefore, a better model relating the heating power and the heat transfer parameters should be developed to improve the predictive ability of the alembic model under varying heating power operation.

MO1 optimizations yielded a wider range of solutions than MO2, although the latter approach was more suitable to attain defined targets. In addition, MO2 contains more information regarding the aromatic composition of the distillates and this procedure can be expanded easily to many more components.

4.4 Conclusions

Two multi-objective functions were applied in the dynamic optimization of batch distillations in alembics. Optimal strategies were found as a function of chemical markers. In Multi-objective weighting functions based on chemical markers (MO1), minimization of head cut markers such as acetaldehyde or ethyl acetate (off flavors) conflict with maximization of heart cut makers such as linalool and with the minimization of tail cut markers such as hexanoic acid or β-phenylethanol. Since the maximization of heart cut makers is harmonic with the minimization of tail cut markers, only two objectives were necessary to define the Pareto front of the MO1 optimization approach. This optimization approach allowed to explore the alembic reachable space better, although simulations were not able to predict well the measured values. Multi-objective optimization based on PCA decomposition (MO2) used all the chemical composition available and allows to attain a defined target easily if that target is reachable by the alembic. Moreover, MO2 simulations were closer to measured values. Some commercial distillates lied closed to the Pareto front; hence, distillers, by skill and experience, were able to produce near optimal distillates.

4.5 Appendix A. Congeners Modeling

This model is complementary to binary model of ethanol-water available in appendix of Luna *et al.* (2018). According to model in Sacher *et al.* (2013), given the pseudo binary assumption, i.e., very low concentrations of the congeners, it is assumed that they do not influence the equilibrium temperature, enthalpy and physical property of the mixture. Each congener is added to the model through the respective mass balance.

Boiler component balance

$$\frac{d(M_B \cdot x_{B,cong})}{dt} = L \cdot x_{L,cong} - V_B \cdot y_{B,cong} \tag{A.4-1}$$

Partial condenser component balance

$$V_B \cdot y_{B,cong} - L \cdot x_{L,cong} - V_D \cdot y_{D,cong} = 0 \tag{A.4-2}$$

Distillate component balance

$$\frac{dM_{cong}}{dt} = y_{D,cong} \cdot V_D \qquad \text{(A.4-3)}$$

Thermodynamic equilibrium relationships of congeners

$$y_{D,cong} = K_{C,cong} \cdot x_{L,cong} \qquad \text{(A.4-4)}$$

$$y_{B,cong} = K_{B,cong} \cdot x_{B,cong} \qquad \text{(A.4-5)}$$

$$x_{L,cong} = \frac{V_B K_{B,cong} x_{B,cong}}{L + V_D K_{C,cong}} \qquad \text{(A.4-6)}$$

Congener equilibrium relationship

The equilibrium constant is calculated by the extended Raoult's law

$$y_{cong} \cdot P = x_{cong} \cdot P_{cong}^{LV} \cdot \gamma_{cong} \qquad \text{(A.4-7)}$$

The partition coefficient is

$$K_{cong} = \frac{y_{cong}}{x_{cong}} = \frac{P_{cong}^{LV} \cdot \gamma_{cong}}{P} \qquad \text{(A.4-8)}$$

The activity coefficient for congeners γ_{cong} were estimated using the UNIFAC contribution groups method. Table 1-2 Shows the UNIFAC groups of six congeners used in this work and their Antoine parameters to calculate the vapor pressure. Given the negligible congener concentrations according to the quasi-binary assumption, the activity coefficient, the vapor pressure and equilibrium temperatures is assumed dependent on the ethanol composition only

$$K_{cong} = \frac{y_{cong}}{x_{cong}} = \frac{P_{cong}^{LV}(x_{eth}) \cdot \gamma_{cong}(x_{eth})}{P} = K_{cong}(x_{eth}) \qquad \text{(A.4-9)}$$

In order to accelerate the CPU time during the integration in the parameter's estimation and dynamic optimization the function is approximated with a 6 order polynomial.

$$K_{cong} = p_{1,cong}x_{eth}^6 + p_{2,cong}x_{eth}^5 + p_{3,cong}x_{eth}^4 + p_{4,cong}x_{eth}^3$$
$$+ p_{5,cong}x_{eth}^2 + p_{6,cong}x_{eth} + p_{7,cong} \qquad \text{(A.4-10)}$$

4.6 Appendix B. Supplementary information
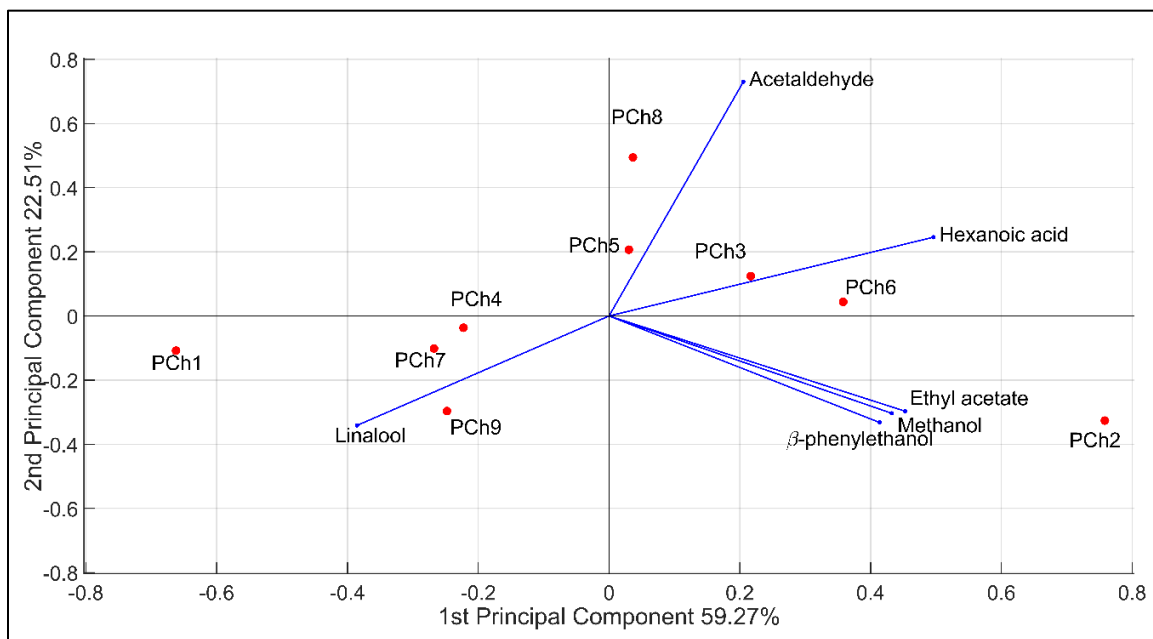
Figure S4-1. Principal component analysis (PCA) applied to data of Chilean commercial piscos.
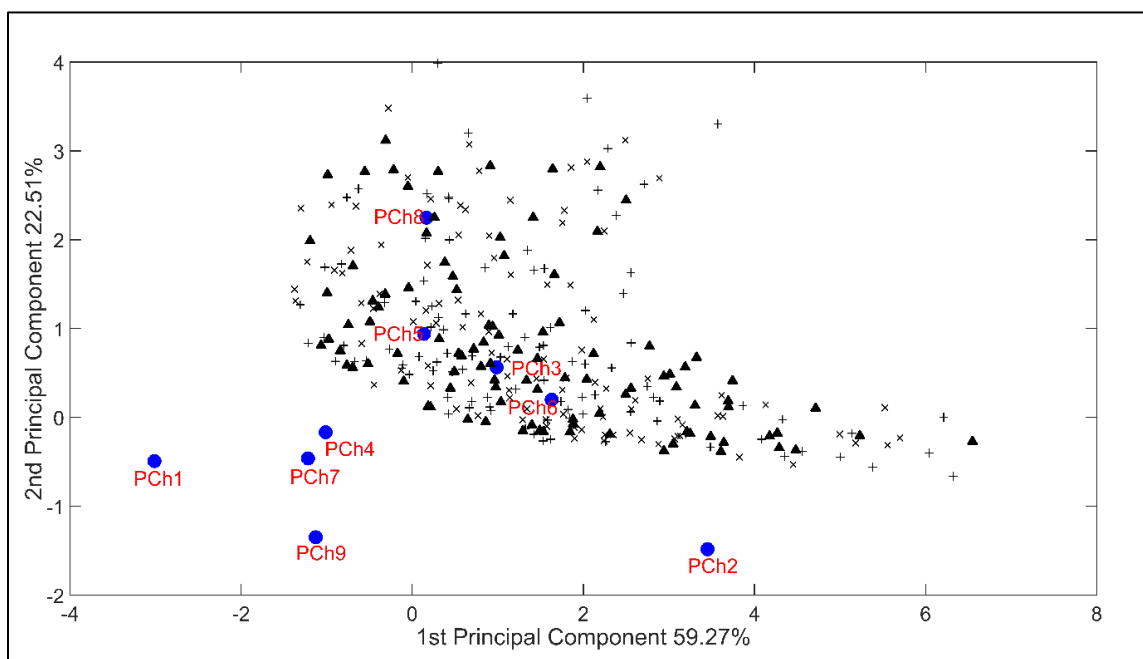
Figure S4-2. PCA map of two principal components: Simulations with 19 time intervals (▲). Simulations with 9 time intervals (×). Simulations with 4 time intervals (+). Blue points correspond to the commercial Chilean piscos.
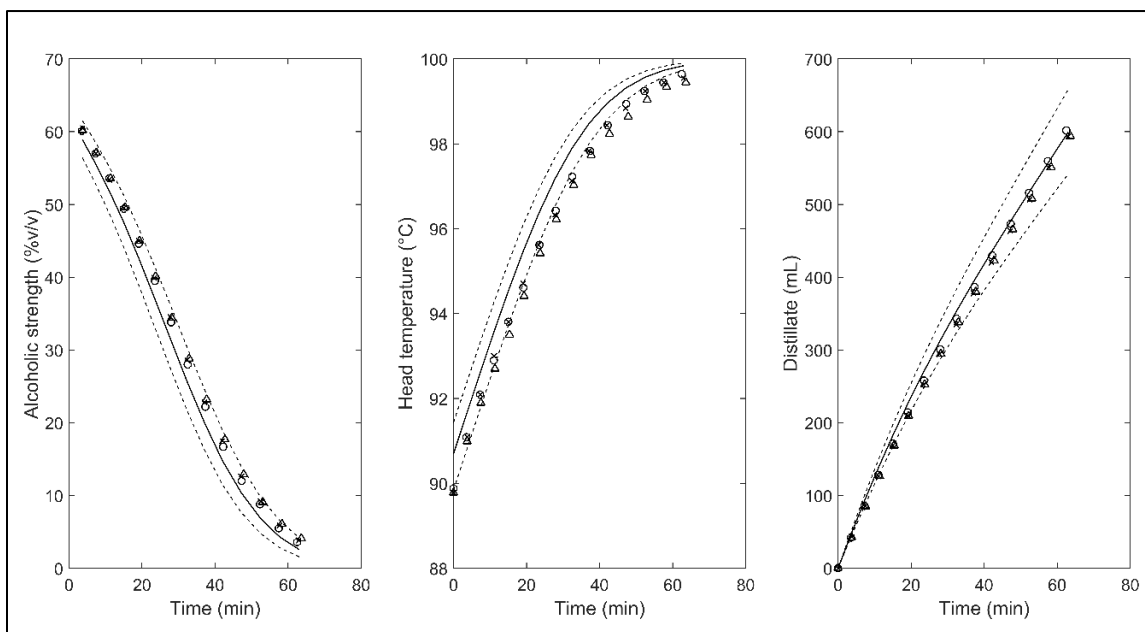
Figure S4-3. Alcoholic strength (%v/v), head temperature and distillate volume vs time for a constant heating power rate of 450W. Experimental data; run 1 (×), run 2 (Δ) and run 3 (○). Simulation (−) and confidence interval (− −).
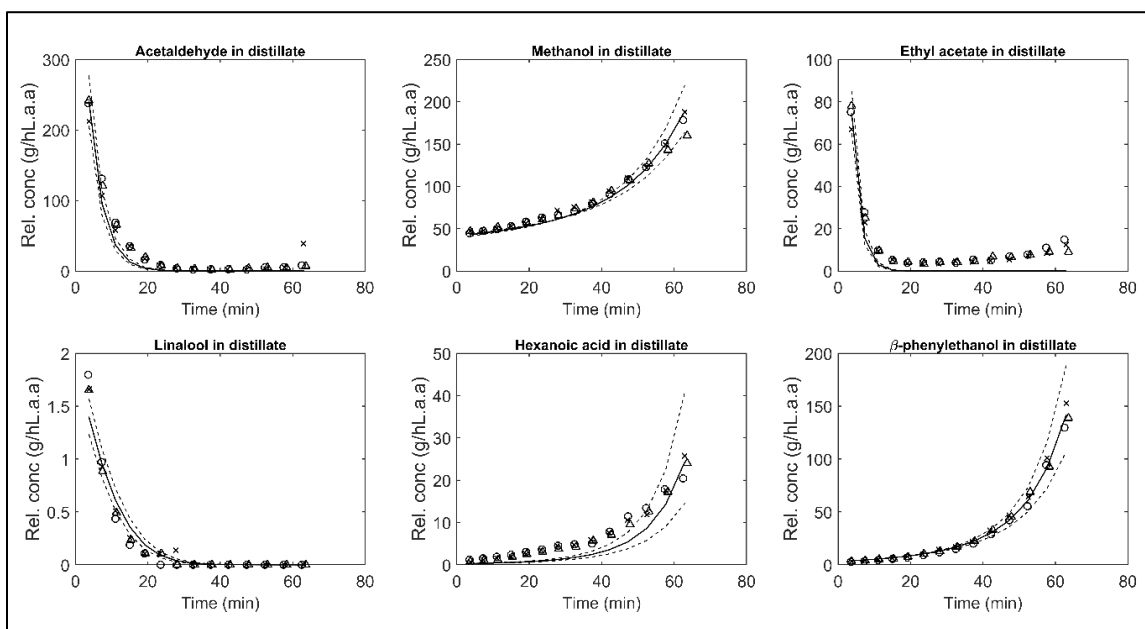
Figure S4-4. Congeners concentrations (g/hL.a.a.) vs time for a constant heating power rate of 450W. Experimental data; run 1 (×), run 2 (Δ) and run 3 (○). Simulation (−) and confidence interval (− −).
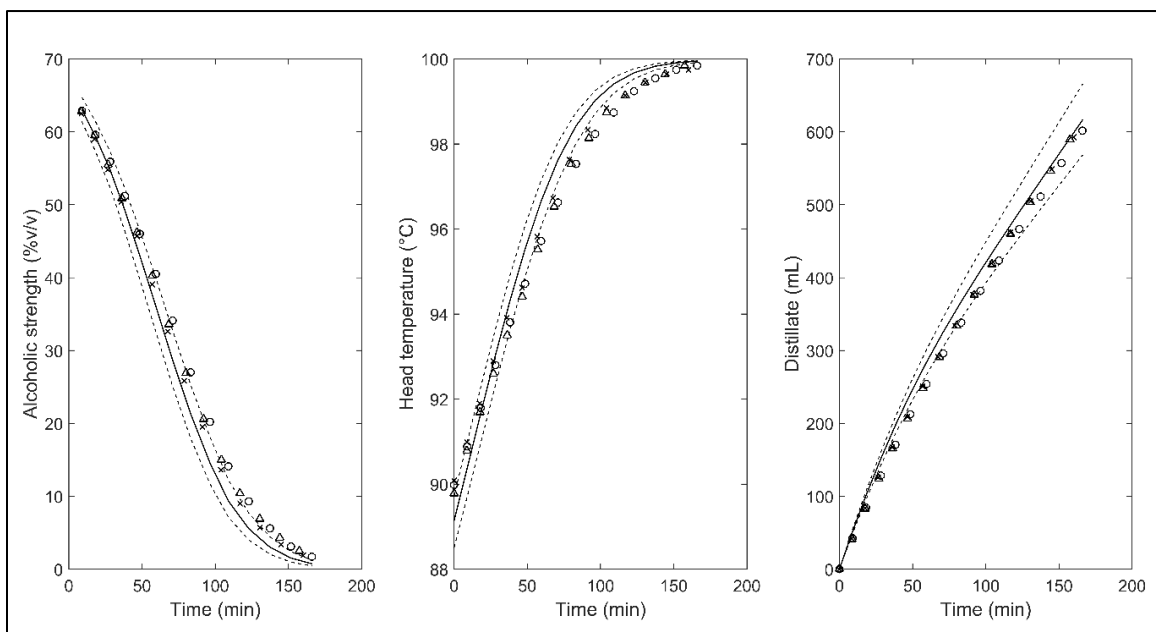
Figure S4-5. Alcoholic strength (%v/v), head temperature and distillate volume vs time for a constant heating power rate of 250W. Experimental data; run 1 (×), run 2 (Δ) and run 3 (○). Simulation (−) and confidence interval (− −).
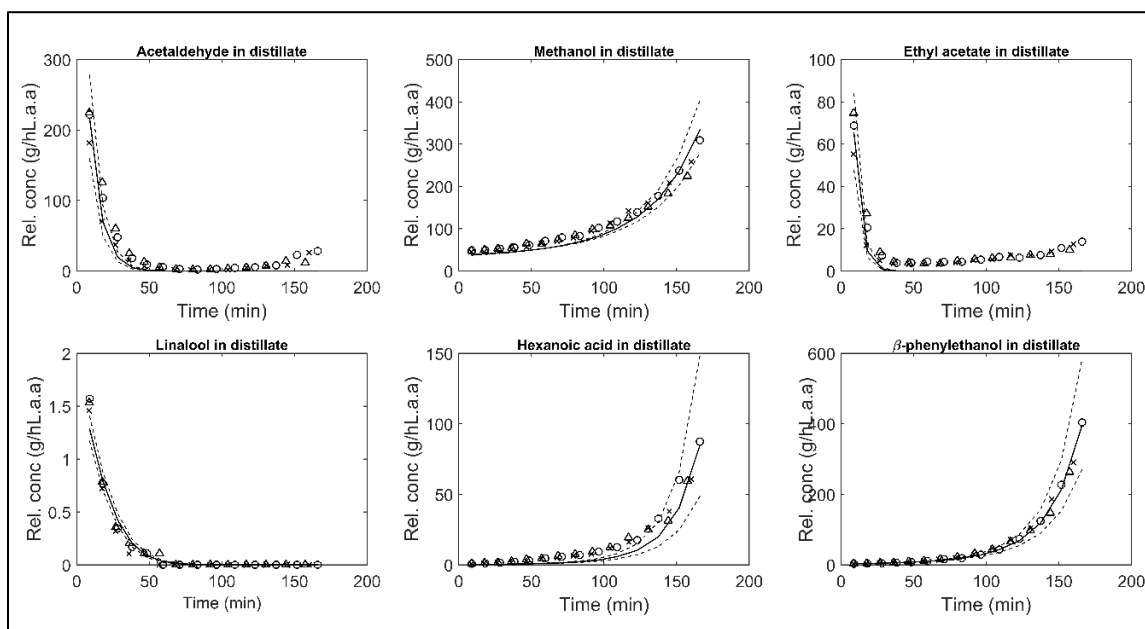
Figure S4-6. Congeners concentrations (g/hL.a.a.) vs time for a constant heating power rate of 250W. Experimental data; run 1 (×), run 2 (Δ) and run 3 (○). Simulation (−) and confidence interval (− −).
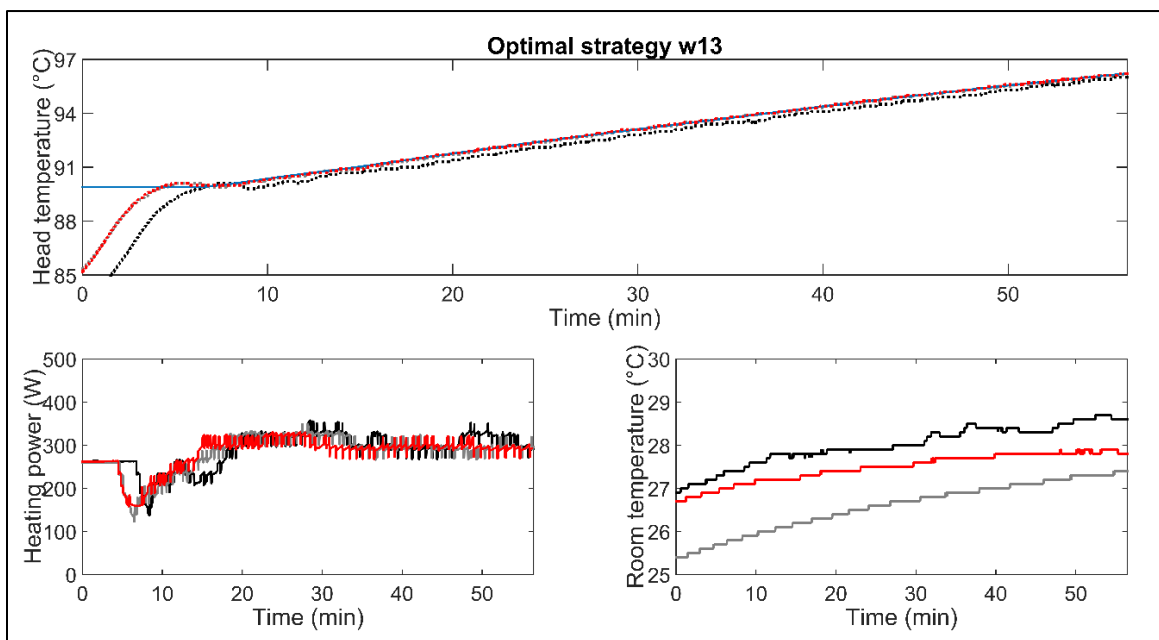
Figure S4-7. Experimental w13 optimal strategy in triplicate. Top figure: head temperature set point (sky blue solid line), measured temperatures; run 1 (black dotted lines), run 2 (gray dotted lines) and run 3 (red dotted lines). Bottom Figures: heating power path and room temperature; run 1 (black solid line), run 2 (gray solid line) and run 3 (red solid line).
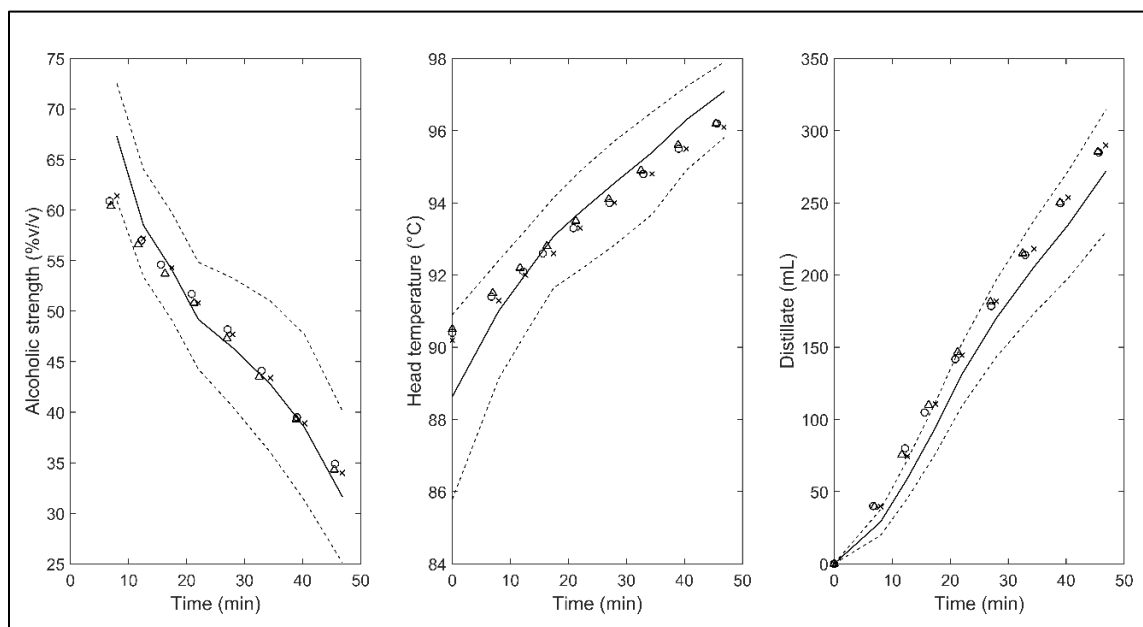
Figure S4-8. Alcoholic strength (% v/v), head temperature and distillate volume vs time for an optimal w13 strategy. Experimental data; run 1 (✕), run 2 (Δ) and run 3 (○). Simulation (−) and confidence interval (− −).
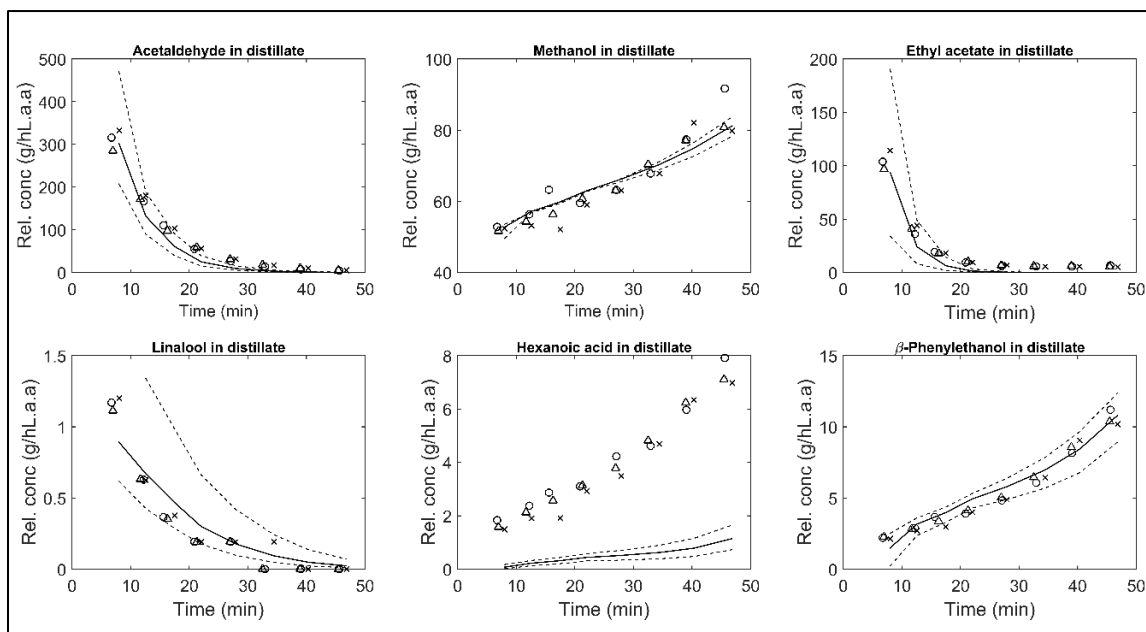
Figure S4-9. Congeners concentrations (g/hL.a.a) vs time for an optimal w13 strategy. Experimental data; run 1 (×), run 2 (Δ) and run 3 (○). Simulation (−) and confidence interval (− −).
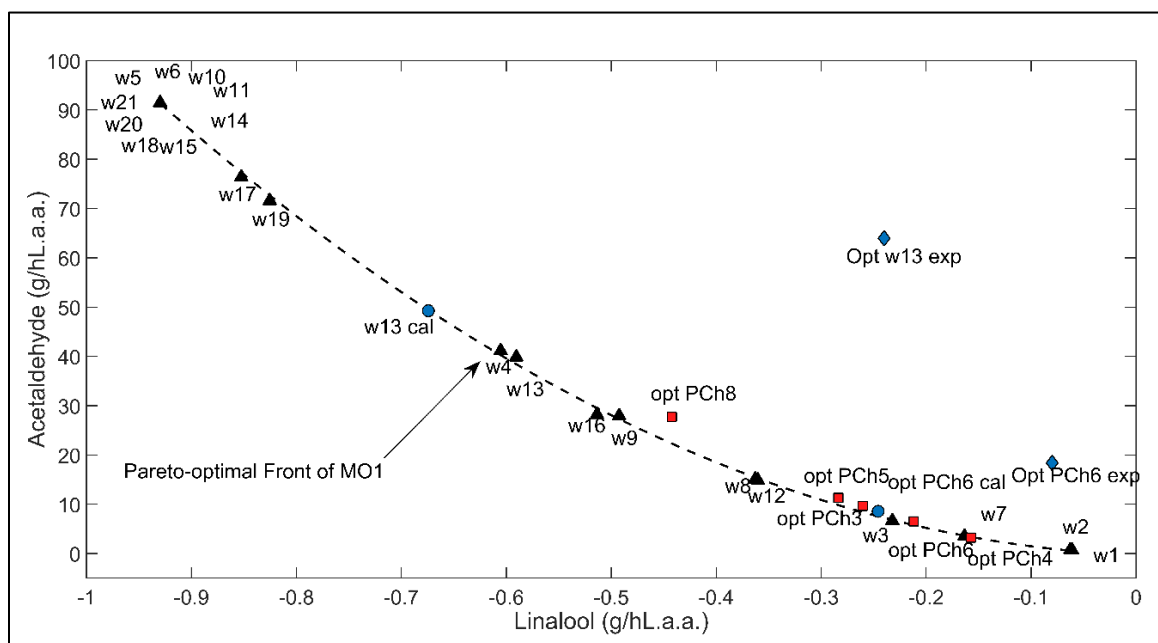
Figure S4-10. Pareto front: relative acetaldehyde concentration vs relative linalool concentration; weight optimal points by MO1 (black triangles), distilled target optimal points by MO2 (red squares), validation experiments (blue diamonds) and model recalibration (blue circles).

Table S4-1. Parameters of calibrated compounds for chemical analysis, ordered according to their chromatographic retention time

Compounds	CAS	Supplier company	Minimum assay (%)	Calculated Kovats retention index
Acetaldehyde	75-07-0	Sigma-Aldrich, Saint Louis, USA	99.5	730
Ethyl acetate	141-78-6	Sigma-Aldrich, Saint Louis, USA	99.0	878
Methanol	67-56-1	PanReac Química, S.A.U. Castellar del Vallès, Spain	99.9	917
2-octanol	123-96-6	Sigma-Aldrich, Saint Louis, USA	97.0	1408
Linalool	78-70-6	Sigma-Aldrich, Saint Louis, USA	97.0	1540
Hexanoic acid	142-62-1	Sigma-Aldrich, Saint Louis, USA	98.0	1905
β-phenylethanol	60-12-8	Sigma-Aldrich, Saint Louis, USA	99.0	1949

Table S4-2. Congeners concentration in Chilean commercial piscos in g/hL.a.a.

Piscos code	Acetaldehyde	Methanol	Ethyl acetate	Linalool	Hexanoic acid	β-phenylethanol
PCh1	9.06	65.1	11.9	0.789	0.0603	0.0958
PCh2	11.9	83.0	19.3	0.158	0.890	15.0
PCh3	15.3	74.8	16.2	0.0931	0.686	1.77
PCh4	11.9	64.4	16.3	0.457	0.292	0.443
PCh5	14.2	67.0	14.7	0.0874	0.648	1.94
PCh6	15.4	82.8	16.6	0.134	0.774	1.91
PCh7	4.93	65.1	15.0	0.163	0.165	0.392
PCh8	25.5	64.8	14.6	0.121	0.590	1.36
PCh9	3.64	71.5	15.8	0.396	0.136	0.450

Table S4-3. Congeners concentration of MO1.

Run	Acetaldehyde	Methanol	Ethyl acetate	Linalool	Hexanoic acid	β-phenylethanol
w1	0.70	103.3	0.0050	0.061	3.48	43.92
w2	0.74	102.8	0.0054	0.063	3.22	42.41
w7	3.51	80.35	0.084	0.163	1.04	19.48
w3	6.64	77.39	0.264	0.232	0.867	17.21
w12	14.89	72.86	1.08	0.360	0.677	14.23
w8	15.08	72.92	1.10	0.363	0.690	14.29
w9	27.94	70.63	3.25	0.492	0.613	12.91
w16	28.21	69.08	3.11	0.514	0.534	11.88
w13	39.85	68.74	5.91	0.590	0.525	11.70
w13 exp	63.96	64.92	14.61	0.24	3.96	5.38
w4	41.14	68.35	6.15	0.605	0.517	11.47
w19	71.60	65.36	14.59	0.825	0.404	9.60
w17	76.39	65.12	16.21	0.852	0.397	9.47
w5	91.46	64.52	21.78	0.930	0.380	9.12
w6	91.46	64.52	21.78	0.930	0.380	9.12
w10	91.46	64.52	21.78	0.930	0.380	9.12
w11	91.46	64.52	21.78	0.930	0.380	9.12
w14	91.46	64.52	21.78	0.930	0.380	9.12
w15	91.46	64.52	21.78	0.930	0.380	9.12
w18	91.46	64.52	21.78	0.930	0.380	9.12
w20	91.46	64.52	21.78	0.930	0.380	9.12
w21	91.46	64.52	21.78	0.930	0.380	9.12

Table S4-4. Congeners concentration of MO2.

Target	Acetaldehyde	Methanol	Ethyl acetate	Linalool	Hexanoic acid	β-phenylethanol
Optimal PCh3	9.67	85.35	0.59	0.260	1.54	25.1
Optimal PCh4	3.22	80.34	0.071	0.157	0.974	19.1
Optimal PCh5	11.3	81.59	0.78	0.284	1.29	21.7
Optimal PCh6	6.53	88.03	0.30	0.212	1.77	27.8
Opt PCh6 exp	18.38	87.81	7.16	0.08	8.88	15.21
Optimal PCh8	27.7	78.14	3.72	0.442	1.06	18.8

Table S4-5. Fitted parameters for optimal strategies

Parameters[a]	Optimal Strategies	
	PCh6	w13
UA_b	0.283 ± 0.006	0.422 ± 0.065
UA_c	1.13 ± 0.03	1.04 ± 0.06
M_0	93.32 ± 0.18	93.50 ± 0.08
x_0	0.0335 ± 0.0009	0.0335 ± 0.0002
$x_{0,cong=1}$	$3.49\text{e-}5 \pm 0.05\text{e-}5$	$3.54\text{e-}5 \pm 0.27\text{e-}5$
$x_{0,cong=2}$	$3.97\text{e-}5 \pm 0.03\text{e-}5$	$4.57\text{e-}5 \pm 0.4\text{e-}5$
$x_{0,cong=3}$	$4.75\text{e-}6 \pm 0.67\text{e-}6$	$4.63\text{e-}6 \pm 0.58\text{e-}6$
$x_{0,cong=4}$	$3.89\text{e-}8 \pm 0.16\text{e-}8$	$3.99\text{e-}8 \pm 0.29\text{e-}8$
$x_{0,cong=5}$	$1.31\text{e-}6 \pm 0.04\text{e-}6$	$1.31\text{e-}6 \pm 0.03\text{e-}6$
$x_{0,cong=6}$	$1.59\text{e-}6 \pm 0.04\text{e-}6$	$2.01\text{e-}6 \pm 0.08\text{e-}6$

[a] Parameters unit: UA_b and UA_c in W/°C, M_0 in mol, x_0 and $x_{0,cong}$ in mol/mol.

4.7 Appendix C. Model code

```matlab
function alembic_simulation
% This function contain the routine for simulating an experimental Charentais alembic.
% The model includes ethanol-water plus six congeners.
% This model is useful for any fruit distillate.
% Each congener can be added to the model through the respective mass balance.
% In this model, the equilibrium relationship was calculated using UNIFAC contribution
% group for each congener.
% Author: Ricardo Luna Hernández
% Previous publication with this model:
% Luna, R., López, F., Pérez-Correa, J.R (2018).
% Minimizing methanol content in experimental charentais alembic distillation.
% Journal of Industrial and Engineering Chemistry, 57, 160-170.
% link: https://www.sciencedirect.com/science/article/pii/S1226086X17304379
clear; clc; close all;
% =============== CONGENER LIST AND INFORMATION ==========================
% Head compounds
    % Acetaldehyde
    % Methanol
    % Ethyl Acetate
% Terpenic compounds (heart compound)
    % Linalool
% Tail compounds
    % Hexanoic acid
    % b-phenethyl alcohol
% =======================================================================
% congeners name
congener_list = {'Acetaldehyde','Methanol','Ethyl acetate',...
    'Linalool','Hexanoic acid','Phenethyl alcohol'}';
% congeners molar weigth (g/mol)
congener_PM = [44.0526 32.0419 88.1051 154.2493 116.1583 122.1644]';
% number of congeners
Ncong = length(congener_list);
% ========= INITIAL CONDITIONS: CONCENTRATION IN MUSCAT WINE ============
Mb_ini      = 94.9533;          % Molar hold-up in bottom (mol)
xB_ini      = 0.0379;           % Ethanol molar fraction in bottom (mol/mol)
Vd_ini      = 0;                % Distillate volume (mL)
Etdes_ini   = 0;                % Ethanol moles in distillate (mol)
% Congeners molar fraction in bottom (mol/mol)
xB_cong_ini = [7.15699480813622e-05;5.38735319152059e-05; ...
    1.55021174372479e-05;1.26766600263018e-07; ...
    1.33861074704985e-06;5.00325445648047e-06]';
Md_cong_ini  = zeros(1,Ncong); % Congeners moles in distillate (mol)
% initial condition vector
x0    = [Mb_ini xB_ini Vd_ini Etdes_ini xB_cong_ini Md_cong_ini];
% initial concentration in wine
x0_wine = x0;
% ================== SIMULATION CONFIGURATION ===========================
% ===================== ODE CONFIGURATION ==============================
% flag_cut
% 1: Normal integration with ODE function (without ODE event).
```

```matlab
% 2: Integration with ODE event to make the head and heart cuts.
flag_cut    = 1;
% ODE options, tolerances of integration
odeoptions=odeset('Reltol',1e-9,'Abstol',1e-9);
% ============= UA parameter configuration =============================
% flag_UA
% 1: linear fuction of heating power
% 2: linear fuction of heating power + 2*sigma
% 3: linear fuction of heating power - 2*sigma
% 4: contant parameters p = [UAb UAc]. This option is usefull to parammeter
% estimation
flag_UA     = 1;
p = [0.82 0.71];
% ========================= MODEL INPUTS =============================
% inputs to simulation without cuts (flag_cut = 1)
if  flag_cut ==1
    n = 15;                                    % Number of time step(n-1)
    t_end = 120;                               % Time of distillation (min)
    tspan = linspace(0,t_end,n)'*60;           % Integration time (s)
    Qcal  = ones(length(tspan),1)*300;         % Heating power (W)
    T_env     = ones(length(tspan),1)*(30+273.15);  % Room temperature (K)
    u     = [tspan,Qcal,T_env];                % input vector
    V_head = 100;
    V_heart = 400;
% inputs to simulation with cuts, ode event (flag_cut = 2)
elseif flag_cut ==2
    % head cut simulation
    n_head     = 4;                            % Number of time step(n-1)
    V_head     = 100;                          % Volume head (mL)
    t_head     = 25;                           % Time of head cut (min)
    tspan1     = linspace(0,t_head,n_head)'*60;  % Integration time (s)
    Qcal_head  = ones(length(tspan1),1)*300;   % Heating power (W)
    T_env1     = ones(length(tspan1),1)*(30+273.15); % Room temperature (K)
    u_head     = [tspan1,Qcal_head,T_env1];    % Input vector
    % heart cut simulation
    n_heart    = 7;                            % number of time step(n-1)
    V_heart    = 400;                          % Volume heart (mL)
    t_heart    = 120;                          % Time of heart cut (min)
    tspan2     = linspace(0,t_heart,n_heart)'*60;  % Integration time (s)
    Qcal_heart = ones(length(tspan2),1)*400;   % Heating power (W)
    T_env2     = ones(length(tspan2),1)*(30+273.15); % Room temperature (K)
    u_heart    = [tspan2,Qcal_heart,T_env2];   % Input vector
end
% simulation without cuts
% ======================= INTEGRATION =============================
if flag_cut == 1
    [t,x,TB,TC,F,GAi,GAd,GAd_frac,rec,V,C_cong,C_cong_frac,C_rcong, ...
        C_rcong_frac,rec_cong]= alembic_outputs(Ncong,congener_PM,x0,...
        x0_wine,u,p,odeoptions,flag_UA,flag_cut,V_head,V_heart,'none');
    % simulation with cuts, ode event
elseif flag_cut ==2
    % ======================= HEAD INTEGRATION =============================
    [time_head,x_head,TB_head,TC_head,F_head,GAi_head,GAd_head, ...
        GAd_head_frac,rec_head,V_head,C_cong_head,C_cong_head_frac, ...
```

```matlab
            C_rcong_head,C_rcong_head_frac,rec_cong_head]= ...
            alembic_outputs(Ncong,congener_PM,x0,...
            x0_wine,u_head,p,odeoptions,flag_UA,flag_cut,...
            V_head,V_heart,'head');
        % concatenation the Qcal vector with the time vector, when the simulation
        % was stopped before the time of simulation to make the cut.
        if length(time_head)==(length(tspan1)-1)
            Qcal_head = Qcal_head(1:end-1);
            Qcal_heart(1) = Qcal_head(end);
        elseif length(time_head)==(length(tspan1)-2)
            Qcal_head = Qcal_head(1:end-2);
            Qcal_heart(1) = Qcal_head(end);
        elseif length(time_head)==(length(tspan1)-3)
            Qcal_head = Qcal_head(1:end-3);
            Qcal_heart(1) = Qcal_head(end);
        end
        % initial concentration in heart cut
        x0_heart = x_head(end,:);
        x0_heart([3,4,11,12,13,14,15,16])=0;
        % ========================= HEART INTEGRATION =========================
        [time_heart,x_heart,TB_heart,TC_heart,F_heart,GAi_heart,GAd_heart, ...
            GAd_heart_frac,rec_heart,V_heart,C_cong_heart,C_cong_heart_frac, ...
            C_rcong_heart,C_rcong_heart_frac,rec_cong_heart]= ...
            alembic_outputs(Ncong,congener_PM,x0_heart,...
            x0_wine,u_heart,p,odeoptions,flag_UA,flag_cut,V_head,V_heart,'heart');
        % concatenation the Qcal vector with the time vector, when the simulation
        % was stopped before the time of simulation to make the cut.
        if length(time_heart) == (length(tspan2)-1)
            Qcal_heart = Qcal_heart(1:end-1);
        elseif length(time_heart) == (length(tspan2)-2)
            Qcal_heart = Qcal_heart(1:end-2);
        elseif length(time_heart) == (length(tspan2)-3)
            Qcal_heart = Qcal_heart(1:end-3);
        end
        %  ============= concatenate vector of head and heart cuts =============
        time_process=[time_head;time_heart(2:end)+time_head(end)]/60; % time (min)
        Qcal_process = [Qcal_head;Qcal_heart(2:end)]; % heating power (w)
        TC  = [TC_head;TC_heart(2:end)]-273.15; % head temeprature (°C)
        GAi = [GAi_head;GAi_heart(2:end)]; % instantaneous alcoholic strength
    end
% ==================== FIGURES AND RESULTS ============================
% Results for flag_cut = 1
if flag_cut == 1
    % ========================= FIGURE 1 =================================
    figure()
    for i =1:Ncong
        subplot(2,3,i)
        plot(t(2:end)/60,C_rcong_frac(:,i),'-sk')
        hold on
        plot(t/60,C_rcong(:,i),'-r')
        xlabel('Time (min)','FontSize',14)
        ylabel('Rel. conc (g/hL.a.a)','FontSize',14)
        title([char(congener_list(i)),' in distillate'],'FontSize',12)
        set(gca,'FontSize',11);
```

```matlab
        legend('accumulated in samples collected','accumulated in one sample')
    end
    % ======================== FIGURE 2 ===============================
    figure()
    subplot(1,3,1)
    plot(t(2:end)/60,GAd_frac,'-sk')
    hold on
    plot(t/60,GAd,'-r')
    hold off
    xlabel('Time (min)','FontSize',14)
    ylabel('Alcoholic strength (%v/v)','FontSize',14)
    set(gca,'FontSize',11);
    legend('accumulated in samples collected','accumulated in one sample')
    subplot(1,3,2)
    plot(t/60,TC-273.15,'-k')
    xlabel('Time (min)','FontSize',14);
    ylabel('Head temperature (°C)','FontSize',14)
    set(gca,'FontSize',11);
    subplot(1,3,3)
    plot(t/60,x(:,3),'-k')
    xlabel('Time (min)','FontSize',14);
    ylabel('Distillate (mL)','FontSize',14)
    set(gca,'FontSize',11);
elseif flag_cut == 2
    % ======================== FIGURE 3 ===============================
    subplot(1,2,1)
    stairs(time_process,Qcal_process,'-.k','LineWidth',1.5)
    hold on
    plot([time_head(end)/60 time_head(end)/60],[250 450],'--r','LineWidth',2.0)
    hold off
    xlabel('Time (min)','FontSize',16)
    ylabel('Heating power (W)','FontSize',16)
    set(gca,'FontSize',14,'YTick',linspace(250,450,3));
    xlim([0 time_process(end)])
    ylim([250 450])
    subplot(1,2,2)
    [hAx,hLine1,hLine2]=plotyy(time_process,TC,time_process,GAi);
    hAx(1).YColor = 'k';
    hAx(2).YColor = 'k';
    ylabel(hAx(1),'Head temperature (°C)','FontSize',16) % left y-axis
    ylabel(hAx(2),'Alcoholic strength (%v/v)','FontSize',16) % right y-axis
    hLine1.LineStyle = '-';
    hLine2.LineStyle = ':';
    line(time_process,TC,'Parent',hAx(1),'LineWidth',1.5,'LineStyle', ...
        '-','Color','k','Marker','none')
    line(time_process,GAi,'Parent',hAx(2),'LineWidth',2.0,'LineStyle', ...
        ':','Color','k','Marker','none')
    xlabel('Time (min)','FontSize',16)
    hold on
    plot([time_head(end)/60 time_head(end)/60],[88 100],'--r','LineWidth',2.0)
    hold off
    set(hAx(1),'Xlim',[0 time_process(end)]);
    set(hAx(1),'Ylim',[88 100]);
    set(hAx(1),'FontSize',14)
```

```
        set(hAx(2),'Xlim',[0 time_process(end)]);
        set(hAx(2),'Ylim',[0 75]);
        set(hAx(2),'FontSize',14)
        set(hAx(1),'YTick',linspace(88,100,4));
        set(hAx(2),'YTick',linspace(0,75,4));
end
%=========================================================================
function [t,x,TB,TC,F,GAi,GAd,GAd_frac,rec,V,C_cong,C_cong_frac, ...
        C_rcong,C_rcong_frac,rec_cong] = alembic_outputs ...
        (Ncong,congener_PM,x0,x0_wine,u,p,odeoptions,flag_UA,flag_cut, ...
        V_head,V_heart,cut)
% This function solve the model by numeric integration and give the all the
% results. The ODE function can be excute by two configurations;
% Normal integration with ODE function (wihout ODE event). flag_cut = 1
% Integration with ODE event to make the head and heart cuts. flag_cut = 2
% Then, it is call @congener_conc function to calculate the concentrations
% of all components; alcoholic strength (GAd) and congeneres (C_cong or C_rcong).
% In addition, @online_outputs function obtaining the boiler (TB) and
% head temperatures (TC),distillate flow (F) rate and instantaneous
% alcoholic strenght (GAi).
% Inputs:
% Ncong: number of congeners
% congener_PM: congeners molar weigth
% x0: initial concentration in head or head fraction
% x0_wine: initial concentration in wine
% u: input vector
% p: parameters vector [UAb UAc]
% odeoptions: options for odefunction
% flag_UA: UA parameter configuration
% flag_cut: ODE configuration with (2) or without (1) ode event.
% V_head: volume head
% V_heart: volume heart
% cut: string with the words 'head' or 'heart' to define the distillation
% fraction in the simulation. This option is on when flag_cut is 2
% (integration with ODE event).
% Outputs:
% t:               Integrate time vector (s)
% x:               Integrated vector from ODE function
% TB:              Boiler Temperature (K)
% TC:              Head Temperature (K)
% F:               Distillate flow rate (mL/min)
% GAi:             Instantaneous alcoholic strength (%v/v)
% GAd:             Alcoholic strength accumulated (%v/v)
% GAd_frac         Alcoholic strength in the samples collected
% rec:             Ethanol recovery (%)
% V:               Distillate volume (mL)
% C_cong:          Absolute congener concentration (mg/L)
% C_cong_frac:     Absolute congener concentration in the samples collected
% C_rcong:         Relative congener concentration (g/hL.a.a.)
% C_rcong_frac:    Relative congener concentration in the samples collected
% rec_cong:        Congener recovy (%)
% Ouputs

% inputs variable declaration
```

```matlab
tspan = u(:,1);
Qcal  = u(:,2);
Tamb  = u(:,3);
% ======= selection of ODE event according the head or heart simulation ===
if strcmp(cut,'head')
    % ODE event to stop the simulation in head cut
    odeoptions.Events = @volume_head;
elseif strcmp(cut,'heart')
    % ODE event to stop the simulation in heart cut
    odeoptions.Events = @volume_heart;
elseif strcmp(cut,'none')
end
% =============== Normal integration with ODE function =================
if flag_cut == 1
    [t,x]=ode15s(@alembic_model,tspan,x0,odeoptions,u,p,flag_UA,Ncong,V_head,V_heart);
% ======= Integration with ODE event to make the head and heart cuts======
elseif flag_cut == 2

[t,x,TE,YE,IE]=ode15s(@alembic_model,tspan,x0,odeoptions,u,p,flag_UA,Ncong,V_head,V_heart);
end
% calculations of alcoholic strength and congeners concentration
[GAd, rec,C_cong,C_rcong,rec_cong,GAd_frac,C_cong_frac,C_rcong_frac] ...
    = congener_conc(x,x0_wine,congener_PM,Ncong);
xB = x(:,2); % xB declaration
V=x(:,3); % distillate volume declaration
% Obtaining of variables TB, TC, GAi, F
[TB, TC, GAi, F] = online_outputs(xB,u,p,flag_UA);
%=========================================================================
function dxdt = alembic_model(t,x,u,p,flag_UA,Ncong,V_head,V_heart)

% This function correspond to Charentais alembic model for ethanol-water
% mixture plus congeners
% Inputs:
% t: Integration time
% x: State variables (4 for ethanol-water + 2 per congener)
% u: Input vector
% p: parameters vector p = [UAb UAc]
% Ouputs:
% dxdt: state variables integrated

% state variables declaration
Mb=x(1);                      % Molar hold-up in bottom (mol)
xB=x(2);                      % Ethanol molar fraction in bottom (mol/mol)
Vd=x(3);                      % Distillate volume (mL)
Et_d=x(4);                    % Ethanol moles in distillate (mol)
xB_cong=x(4+1:4+Ncong);       % Congeners molar fraction in bottom (mol/mol)
Md_cong=x(4+Ncong+1:end);     % Congeners moles in distillate (mol)
% inputs variable declaration
tspan  = u(:,1);              % integration time
Qcal_t = u(:,2);              % heating power (W)
Tamb_t = u(:,3);              % room temperature (K)
% ==== execute each heating power element in their correspond time step ===
e=1;
cond=true;
```

```matlab
while cond
    if (t >= tspan(e)) && (t <= tspan(e+1))
        cond = false;
        Qcal = Qcal_t(e);
        Tamb = Tamb_t(e);
    else
        cond=true;
        e=1+e;
    end
end
% ============= linear fuction of heating power ========================
if flag_UA == 1;
    % Global coefficient and area of heat transfer:
    % Boiler zone
    UAb  = ((0.711-0.821)/(450-250))*(Qcal-250)+0.821;
    % head of alembic zone
    UAc  = ((1.730-1.277)/(450-250))*(Qcal-250)+1.277;
% =========  linear function + 2*sigma (95% confidence interval) =======
elseif flag_UA == 2;
    % Boiler zone
    UAb  = (((0.711-0.821)/(450-250))*(Qcal-250)+0.821)+2*0.098;
    % head of alembic zone
    UAc  = (((1.730-1.277)/(450-250))*(Qcal-250)+1.277)+2*0.167;
% =========  linear function - 2*sigma (95% confidence interval) =======
elseif flag_UA == 3;
    % Boiler zone
    UAb  = (((0.711-0.821)/(450-250))*(Qcal-250)+0.821)-2*0.098;
    % head of alembic zone
    UAc  = (((1.730-1.277)/(450-250))*(Qcal-250)+1.277)-2*0.167;
% ===================== constant parameters ============================
elseif flag_UA == 4;
    % Boiler zone
    UAb = p(1);
    % head of alembic zone
    UAc = p(2);
end
% ======= THERMODYNAMIC EQUILIBRIUM ETHANOL-WATER IN THE BOILER ==========
% All calculations of equilibrium are through empirical correlations
% from Sacher et al. (2013). These equations are polynomic functions
% that depend on the ethanol molar fraction (xB,xL).

% Ethanol molar fraction in the vapor flow from the bottom
yb = -59.6868501+-89.4037240*xB+-39.8552042*xB.^1.5...      % (Eq. A.9)
    +81.47664393*exp(xB)-21.7897938*exp(-xB);
% Boiler temperature
if xB <=0.1661                                    % (Eq. A.10)
    Tb=273.15+(-0.02214517+-0.05785120*xB.^1.5+0.032146591*exp(xB)).^-1;
else
    Tb =273.15+278.3854921+-141.465178*xB+49.67113604.*xB.*log(xB)...
        +9.159930587*xB.^3+-184.225674*exp(-xB);
end
% Molar specific enthalpy in the bottom
hb = (55.678*xB+75.425)*Tb-15208.44*xB-20602.34;
% Molar specific enthalpy in the vapor flow
```

```matlab
Hb =   36172.03-2919.83*yb+(31.461-11.976*yb)*Tb...
          +(4.063*10^-4+0.0734*yb)*Tb^2;
% Partial derivative delta(hb)/delta(xb)=f(Tb(xb))
deltahbdeltaxb = 55.678*Tb-15208.44;
% Partial derivative delta(hb)delta(Tb)=f(xb)
deltahbdeltaTb = 55.678*xB+75.425;
% Temperature derivate respecto to ethanol concentration (xB)
if xB<=0.1661
    dTbdxB=-(1.5*-0.05785120*xB.^0.5+0.032146591*exp(xB))./ ...
        (-0.02214517+-0.05785120*xB.^1.5+0.032146591*exp(xB)).^2;
else
    dTbdxB=-141.465178+49.67113604.*log(xB)+49.67113604+ ...
        3*9.159930587*xB.^2+184.225674*exp(-xB);
end
% total derivate dhb/dxb
dhbdxb=deltahbdeltaxb+deltahbdeltaTb*dTbdxB;
% ===== IMPLICIT EQUATION - ENEGERY BALANCE IN THE BOTTOM (Eq.A.23) =======
xLstart=1.1*xB; % initial iteration value of xL
par=[xB Qcal UAb UAc Tamb yb hb Hb dhbdxb];
options=optimset('Display','off');
% solve implicit equation with fsolve to calculate xL
[xL,fval,exitflag]=fsolve(@(x) xLsolve(x,par),xLstart,options);
% ======= THERMODYNAMIC EQUILIBRIUM ETHANOL-WATER IN THE HEAD ZONE ========
% Empirical correlations are evaluate in xL
% Head temperature
if xL <=0.1661                                     %TL=f(xL) (K)
    TL=273.15+(-0.02214517+-0.05785120*xL.^1.5+0.032146591*exp(xL)).^-1;
 else
    TL =273.15+278.3854921+-141.465178*xL+49.67113604.*xL.*log(xL)...
        +9.159930587*xL.^3+-184.225674*exp(-xL);
end
% Ethanol molar fraction in the distillate flow
yd = -59.6868501+-89.4037240*xL+-39.8552042*xL.^1.5...
    +81.47664393*exp(xL)-21.7897938*exp(-xL);
% Molar specific enthalpy in the liquid reflux
hL = (55.678*xL+75.425)*TL-15208.44*xL-20602.34;
% Molar specific enthalpy in the distillate flow
Hd = 36172.03-2919.83*yd+(31.461-11.976*yd)*TL...
        +(4.063*10^-4+0.0734*yd)*TL^2;
% ============ Mass balances in the head (partial condenser) =============
% Vapor flow from the bottom
Vb= UAc*(TL-Tamb) / ( (Hb-Hd)+(yb-yd)/(xL-yd)*(Hd-hL) );
% Liquid natural reflux flow
L =-UAc*(TL-Tamb) / ( (hL-Hd)+(xL-yd)/(yb-yd)*(Hd-Hb) );
% Distilllate flow
Vd = Vb-L;
% =========== EMPIRICAL CORRELACIÓN DENSITY (NEURBURG 1994) ==============
MW1=46.07;                   % Weight molar Etanol
MW2=18.0153;                 % Weigth molar water
Mwp=MW1*yd+(1-yd)*MW2;   % Weigth molar mixture
rhow=1;                      % g/mL density water pure
% apparent molal volume of liquid mixtures [m3/kmol] (Eq. A.16)
phi=5.1214e-2+...
    6.549e-3*yd+7.406e-5*(TL-273.15);
```

```matlab
% Mixture density (Eq. A.16)
rhop=MWp/(phi*1000*yd+(1-yd)*(MW2/rhow));
% Distillate flow rate (mL/s)
F=Vd*MWp*(1/rhop);
% ===================== ODES ETHANOL-WATER ============================
dxdt=zeros(6,1);
% Total mass balance in the boiler
dxdt(1) = L-Vb;
% Ethanol mass balance in the boiler
dxdt(2) = 1/Mb*(L*(xL-xB)-Vb*(yb-xB));
% Toal mass balances in the distillate (distillate volume)
dxdt(3) = F;
% Ethanol mas balance in the distillate (ethanol moles)
dxdt(4) = Vd*yd;
% ===================== CONGENER CALCULATIONS =============================
Kcong_b     =   zeros(Ncong,1);
Kcong_c     =   zeros(Ncong,1);
yb_cong     =   zeros(Ncong,1);
xL_cong     =   zeros(Ncong,1);
yd_cong     =   zeros(Ncong,1);

for i=1:Ncong
%  parameters polynomial approximation for each congener (eq A.9)
PolKcong = zeros(Ncong,7);
% Acetaldehyde
PolKcong(1,1:7)=[2132.48647470687 -7325.32158274884 9975.65026598049 ...
    -6877.34768142094 2557.05908782731 -514.677851684226 59.8488158884235];
% Methanol
PolKcong(2,1:7)=[344.843341522534 -1174.41754890585 1583.17398976036 ...
    -1073.73582253337 388.389261160545 -73.6515297026980 7.47712492793083];
% Ethyl acetate
PolKcong(3,1:7)=[6708.80545814955 -22825.1298638850 30638.8774877421 ...
    -20622.5403332238 7323.26442993318 -1326.16274539085 108.370963453395];
% Linalool
PolKcong(4,1:7)=[5903.54406919218 -19642.5313045736 25537.6690914762 ...
    -16362.2715807274 5343.77291171908 -823.424096778676 45.8635924063960];
% Hexanoic acid
PolKcong(5,1:7)=[79.3503646604582 -265.323418070129 347.411506679424 ...
    -225.065622269698 74.9248170603414 -11.9950927956312 0.736427102093912];
% Phenethyl alcohol
PolKcong(6,1:7)=[349.984114473148 -1168.19810837707 1525.76323298408 ...
    -984.481408366268 325.376073822477 -51.3026635899384 3.01613099316598];
% Partition coefficient in bottom
Kcong_b(i,1)=PolKcong(i,1)*xB^6+PolKcong(i,2)*xB^5+PolKcong(i,3)*xB^4+ ...
    PolKcong(i,4)*xB^3+PolKcong(i,5)*xB^2+PolKcong(i,6)*xB^1+PolKcong(i,7);
% Partition coefficient in head
Kcong_c(i,1)=PolKcong(i,1)*xL^6+PolKcong(i,2)*xL^5+PolKcong(i,3)*xL^4+ ...
    PolKcong(i,4)*xL^3+PolKcong(i,5)*xL^2+PolKcong(i,6)*xB^1+PolKcong(i,7);
% Thermodynamic equilibrium L-V relationships of congeners in bottom
yb_cong(i,1)=Kcong_b(i,1).*xB_cong(i);
% Congener molar fraction in the liquid reflux
xL_cong(i,1)=(Vb*yb_cong(i,1))./(L+Vd*Kcong_c(i,1));
% Thermodynamic equilibrium L-V relationship of congeners in head
yd_cong(i,1)=xL_cong(i,1).*Kcong_c(i,1);
```

```matlab
% ======================= ODES CONGENERS ===============================
% Congener component balance in the boiler
dxdt(4+i)= 1/Mb*(L*(xL_cong(i,1)-xB_cong(i))-Vb*(yb_cong(i,1)-xB_cong(i)));
% Congener component balance in the distillate
dxdt(4+Ncong+i)= Vd*yd_cong(i);
end
%=====================================================================
function [value,isterminal,direction] = ...
    volume_head(t,x,u,p,flag_UA,Ncong,V_head,V_heart)
% This function correspond to ODE event. The function determine the time
% to stop the simulation when comply a specific event.
% The event is stop the simulation when the distillate volume of simulation
% is equal to head volume.
value = x(3)-V_head;
isterminal = 1;
direction  = 0;
%=====================================================================
function [value,isterminal,direction] =  ...
    volume_heart(t,x,u,p,flag_UA,Ncong,V_head,V_heart)
% This function correspond to ODE event. The function determine the time
% to stop the simulation when comply a specific event.
% The event is stop the simulation when the distillate volume of simulation
% is equal to heart volume.
value = x(3)-V_heart;
isterminal = 1;
direction  = 0;
%=====================================================================
function [GAd,rec,C_cong,C_rcong,rec_cong,GAd_frac,C_cong_frac, ...
    C_rcong_frac] = congener_conc(x,x0_wine,MW,Ncong)
% This function calculate the alcoholic strength, ethanol recovery,
% absolute congener concentration, relative congener concentration
% accumulated in the distillate. In addition, are calculate the alcoholic
% strength, absolute and relative congener concentration where were
% collected the samples or fractions, i.e, the accumulated in the each step
% of integration time.
% Inputs
% x:             Integrated vector from ODE function
% x0_wine:       Initial concentations in wine
% MW:            congeners molar weigth (g/mol)
% Ncong:         Number of congeners
% Ouputs
% GAd:           Alcoholic strength accumulated (%v/v)
% rec:           Ethanol recovery (%)
% C_cong:        Absolute congener concentration (mg/L)
% C_rcong:       Relative congener concentration (g/hL.a.a.)
% rec_cong:      Congener recoveries (%)
% GAd_frac:      Alcoholic strength in the samples collected
% C_cong_frac:   Absolute congener concentration in the samples collected
% C_rcong_frac:  Relative congener concentration in the samples collected

% Variables declaration
Mb      = x(:,1);                     % Molar hold-up in bottom (mol)
xb      = x(:,2);                     % Ethanol molar fraction in bottom (mol/mol)
V       = x(:,3);                     % Distillate volume (mL)
```

```
Md       = x(:,4);                     % Ethanol moles in distillate (mol)
xb_cong = x(:,4+1:4+Ncong);            % Congeners molar fraction in bottom (mol/mol)
Md_cong = x(:,4+Ncong+1:end);          % Congeners moles in distillate (mol)
Mb_wine      = x0_wine(1);             % Initial moles in bottom
xb_wine      = x0_wine(2);             % Initial ethanol molar fration in bottom
xb_cong_wine = x0_wine(4+1:4+Ncong);   % Initial congeners molar fraction in bottom
GAd = Md.*46.07.*(1/0.7893).*100./V;   % Alcoholic strenght (%v/v)
rec = (Md*100)./(Mb_wine*xb_wine);     % Ethanol recovery (%)
[nrow,ncolumn] = size(Md_cong);        % variables dimension
C_cong       = zeros(nrow,ncolumn);    % Absolute congeners concentration (mg/L)
C_rcong      = zeros(nrow,ncolumn);    % Relative congeners concentration (g/hL.a.a.)
rec_cong     = zeros(nrow,ncolumn);    % Congener recoveries (%)
GAd_frac     = zeros(nrow-1,1);        % Alcoholic strength in the samples
C_cong_frac  = zeros(nrow-1,ncolumn);  % Absolute congener concentration in the samples
C_rcong_frac = zeros(nrow-1,ncolumn);  % Relative congener concentration in the samples

for j=2:length(Md)
    GAd_frac(j-1)    = (Md(j)-Md(j-1))*46.07*(1/0.7893)*100/(V(j)-V(j-1));
    for i=1:ncolumn
        C_cong(:,i)   = (Md_cong(:,i)*MW(i)*1000)./(V/1000);
        C_rcong(:,i)  = (Md_cong(:,i)*MW(i)*1000*100)./(V.*(GAd/100));
        rec_cong(:,i) = (Md_cong(:,i)*100)./(Mb_wine*xb_cong_wine(i));
        C_cong_frac (j-1,i)   = ((Md_cong(j,i)-Md_cong(j-1,i))*MW(i)*1000)./ ...
            ((V(j)-V(j-1))/1000);
        C_rcong_frac(j-1,i)   = ((Md_cong(j,i)-Md_cong(j-1,i))*MW(i)*1000*100)./ ...
            ((V(j)-V(j-1)).*(GAd_frac(j-1)/100));
    end
end
%=========================================================================
function [Tb TL yd F]=evalfun(xB,u,p,flag_UA)
% This function eval the xB integrated obtained from Ode function.
% The aim is obtaining the temperatures data, instantaneous ethanol moles
% in the distillate and distillate flow rate.
% Inputs:
% xB:          Integrated vector of xB (x(:,2))
% u:           Input vector
% p:           Parameter vector p = [UAb UAc]
% Outputs:
% Tb:          Boiler temperature (K).
% TL:          Head temperature (K).
% yd:          Ethanol molar fration in the vapor that become in distillate

% Input variales declaration
tspan = u(1); % Time
Qcal  = u(2); % Heatig power
Tamb  = u(3); % Room temperature
% ============== linear fuction of heating power ========================
if flag_UA == 1;
    % Global coefficient and area of heat transfer:
    % Boiler zone
    UAb  = ((0.711-0.821)/(450-250))*(Qcal-250)+0.821;
    % head of alembic zone
    UAc  = ((1.730-1.277)/(450-250))*(Qcal-250)+1.277;
% =========  linear function + 2*sigma (95% confidence interval) =======
```

```matlab
elseif flag_UA == 2;
    % Boiler zone
    UAb  = (((0.711-0.821)/(450-250))*(Qcal-250)+0.821)+2*0.098;
    % head of alembic zone
    UAc  = (((1.730-1.277)/(450-250))*(Qcal-250)+1.277)+2*0.167;
% =========  linear function - 2*sigma (95% confidence interval) =======
elseif flag_UA == 3;
    % Boiler zone
    UAb  = (((0.711-0.821)/(450-250))*(Qcal-250)+0.821)-2*0.098;
    % head of alembic zone
    UAc  = (((1.730-1.277)/(450-250))*(Qcal-250)+1.277)-2*0.167;
% ===================== constant parameters ============================
elseif flag_UA == 4;
    % Boiler zone
    UAb = p(1);
    % head of alembic zone
    UAc = p(2);
end
% ======= THERMODYNAMIC EQUILIBRIUM ETHANOL-WATER IN THE BOILER ===========
% All calculations of equilibrium are through empirical correlations
% from Sacher et al. (2013). These equations are polynomic functions
% that depend on the ethanol molar fraction (xB,xL).

% Ethanol molar fraction in the vapor flow from the bottom
yb = -59.6868501+-89.4037240*xB+-39.8552042*xB.^1.5...      % (Eq. A.9)
    +81.47664393*exp(xB)-21.7897938*exp(-xB);
% Boiler temperature
if xB <=0.1661                                             % (Eq. A.10)
    Tb=273.15+(-0.02214517+-0.05785120*xB.^1.5+0.032146591*exp(xB)).^-1;
else
    Tb =273.15+278.3854921+-141.465178*xB+49.67113604.*xB.*log(xB)...
        +9.159930587*xB.^3+-184.225674*exp(-xB);
end
% Molar specific enthalpy in the bottom
hb = (55.678*xB+75.425)*Tb-15208.44*xB-20602.34;
% Molar specific enthalpy in the vapor flow
Hb =  36172.03-2919.83*yb+(31.461-11.976*yb)*Tb...
        +(4.063*10^-4+0.0734*yb)*Tb^2;
% Partial derivative delta(hb)/delta(xb)=f(Tb(xb))
deltahbdeltaxb = 55.678*Tb-15208.44;
% Partial derivative delta(hb)delta(Tb)=f(xb)
deltahbdeltaTb = 55.678*xB+75.425;
% Temperature derivate respecto to ethanol concentration (xB)
if xB<=0.1661
    dTbdxB=-(1.5*-0.05785120*xB.^0.5+0.032146591*exp(xB))./ ...
        (-0.02214517+-0.05785120*xB.^1.5+0.032146591*exp(xB)).^2;
else
    dTbdxB=-141.465178+49.67113604.*log(xB)+49.67113604+ ...
        3*9.159930587*xB.^2+184.225674*exp(-xB);
end
% total derivate dhb/dxb
dhbdxb=deltahbdeltaxb+deltahbdeltaTb*dTbdxB;
% ===== IMPLICIT EQUATION - ENEGERY BALANCE IN THE BOTTOM (Eq.A.23) =======
xLstart=1.1*xB; % initial iteration value of xL
```

```matlab
par=[xB Qcal UAb UAc Tamb yb hb Hb dhbdxb];
options=optimset('Display','off');
% solve implicit equation with fsolve to calculate xL
[xL,fval,exitflag]=fsolve(@(x) xLsolve(x,par),xLstart,options);
% ======= THERMODYNAMIC EQUILIBRIUM ETHANOL-WATER IN THE HEAD ZONE ========
% Empirical correlations are evaluate in xL
% Head temperature
if xL <=0.1661                                       %TL=f(xL) (K)
    TL=273.15+(-0.02214517+-0.05785120*xL.^1.5+0.032146591*exp(xL)).^-1;
 else
    TL =273.15+278.3854921+-141.465178*xL+49.67113604.*xL.*log(xL)...
        +9.159930587*xL.^3+-184.225674*exp(-xL);
end
% Ethanol molar fraction in the distillate flow
yd = -59.6868501+-89.4037240*xL+-39.8552042*xL.^1.5...
    +81.47664393*exp(xL)-21.7897938*exp(-xL);
% Molar specific enthalpy in the liquid reflux
hL = (55.678*xL+75.425)*TL-15208.44*xL-20602.34;
% Molar specific enthalpy in the distillate flow
Hd = 36172.03-2919.83*yd+(31.461-11.976*yd)*TL...
        +(4.063*10^-4+0.0734*yd)*TL^2;
% ============ Mass balances in the head (partial condenser) =============
% Vapor flow from the bottom
Vb= UAc*(TL-Tamb) / ( (Hb-Hd)+(yb-yd)/(xL-yd)*(Hd-hL) );
% Liquid natural reflux flow
L =-UAc*(TL-Tamb) / ( (hL-Hd)+(xL-yd)/(yb-yd)*(Hd-Hb) );
% Distilllate flow
Vd = Vb-L;
% =========== EMPIRICAL CORRELACIÓN DENSITY (NEURBURG 1994) ===============
MW1=46.07;                  % Weight molar Etanol
MW2=18.0153;                % Weigth molar water
Mwp=MW1*yd+(1-yd)*MW2;      % Weigth molar mixture
rhow=1;                     % g/mL density water pure
% apparent molal volume of liquid mixtures [m3/kmol] (Eq. A.16)
phi=5.1214e-2+...
    6.549e-3*yd+7.406e-5*(TL-273.15);
% Mixture density (Eq. A.16)
rhop=Mwp/(phi*1000*yd+(1-yd)*(MW2/rhow));
% Distillate flow rate (mL/s)
F=Vd*Mwp*(1/rhop);
%========================================================================
function [TB, TC, GAi, F] = online_outputs(xB,u,p,flag_UA)
% This function concatenate the equilibrium temperatures, instantaneous
% alcoholic strength and distillate flow rate. This variables correspond
% to on-line measures variables in the experiments.
% inputs:
% xB:           Integrated vector of xB (x(:,2))
% u:            Input vector
% p:            Parameter vector p = [UAb UAc]
% flag_UA:      UA parameter configuration
% outputs:
% TB:           Boiler temperature (K).
% TC:           Head temperature (K).
% GAi:          Instantaneous alcoholic strength
```

```matlab
% F:          Distillate flow rate (mL/min)

% Input variales declaration
tspan = u(:,1);
Qcal  = u(:,2);
Tamb  = u(:,3);
% vector creation
TB  = zeros(length(xB),1); % Boiler temperature (K)
TC  = zeros(length(xB),1); % Head temperature (K)
yD  = zeros(length(xB),1); % Ethanol molar fraction in the vapor (mol/mol)
F   = zeros(length(xB),1); % Distillate flow rate (mL/s)
% =========== EVALUATION OF EVALFUN FOR EACH ELEMENT OF xB ===============
for i=1:length(xB)
    xb=xB(i);
    ui = [tspan(i) Qcal(i) Tamb(i)];
    [Tb, TL, yd, f] = evalfun(xb,ui,p,flag_UA);
    TB(i) = Tb;
    TC(i) = TL;
    yD(i) = yd;
    F(i)  = f*60; % here, distillate flow rate is multiplicate for 60 to obtain mL/min
end
% This polynomial function relationship the head temperature equilibrium
% with the alcoholic strength of distillate.
P=[-38.950116015168470 2.310609445800233e+02 -5.482530421230588e+02 ...
    7.048795688586179e+02 -5.700321285089950e+02 3.213122048471700e+02 ...
    0.001131244289002];
GAi = polyval(P,yD); % instantaneous alcoholic strength
%========================================================================
function f=xLsolve(xL,par)
% This function contains the routine that calculate xL by nonlinear equation
% solver (fsolve).
% Inputs:
% xL: variable of iteration with fsolve
% par: vector parameters that contain variables that are calculate previous
% to enter to this function.
% Outputs:
% f: correspond to value of implicit equation (A.23)

% Variable declaration
xB      = par(1);
Qcal    = par(2);
UAb     = par(3);
UAC     = par(4);
Tamb    = par(5);
yb      = par(6);
hb      = par(7);
Hb      = par(8);
dhbdxb  = par(9);
% Boiler temperature
if xB <=0.1661
    Tb=273.15+(-0.02214517+-0.05785120*xB.^1.5+0.032146591*exp(xB)).^-1;
 else
    Tb =273.15+278.3854921+-141.465178*xB+49.67113604.*xB.*log(xB)...
        +9.159930587*xB.^3+-184.225674*exp(-xB);
```

```
end
% Head temperature
if xL <=0.1661
    TL=273.15+(-0.02214517+-0.05785120*xL.^1.5+0.032146591*exp(xL)).^-1;
 else
    TL =273.15+278.3854921+-141.465178*xL+49.67113604.*xL.*log(xL)...
        +9.159930587*xL.^3+-184.225674*exp(-xL);
end
% Ethanol molar fraction in the distillate flow
yd = -59.6868501+-89.4037240*xL+-39.8552042*xL.^1.5...
    +81.47664393*exp(xL)-21.7897938*exp(-xL);
% Molar specific enthalpy in the liquid reflux
hL = (55.678*xL+75.425)*TL-15208.44*xL-20602.34;
% Molar specific enthalpy in the distillate flow
Hd = 36172.03-2919.83*yd+(31.461-11.976*yd)*TL...
        +(4.063*10^-4+0.0734*yd)*TL^2;
% Vapor flow from the bottom
Vb= UAc*(TL-Tamb)/((Hb-Hd)+(yb-yd)/(xL-yd)*(Hd-hL));
% Liquid natural reflux flow
L =-UAc*(TL-Tamb)/((hL-Hd)+(xL-yd)/(yb-yd)*(Hd-Hb));
% Implicit equation that depend on xL, F(xL)=0.
f=-(L*(xL-xB)-Vb*(yb-xB))*(dhbdxb)+L*(hL-hb)-Vb*(Hb-hb)+(Qcal-UAb*(Tb-Tamb));
```

4.8 Acknowledgements

CONCLUSIONS

In the present work was proposed a model-based design to obtain distillates rich in fruit and floral aromas and low in off-flavors and toxic compounds in batch distillation using Charentais copper alembic.

In chapter II, was developed a robust automatic control strategy through a phenomenological model of Charentias copper alembic distillation. Control algorithms such as PI, PID, IMC and FOPID were tried in several disturbances scenarios during the distillation process like variations in the room temperature and noises in the manipulated variable. FOPID controller achieved better control efforts when increased the disturbances. This controller demonstrated be a good alternative as compared traditional controllers since was tried in a nonlinear and non-steady process like batch distillation using suitable simple ruled-based tuning techniques.

In Chapter III, we focus on using modern engineering tools to consistently produce spirits with low methanol content in Charentais alembics. The method involved developing, simulation and calibration of a dynamic model. Then, a multi-objective function was formulated and solved the dynamic optimization problem. Optimization yielded a variable temperature in the partial condenser, which was tracked by an experimental automatic control system that manipulated the heat addition in the boiler. Here, the optimal operation obtained distillates with 12% less methanol than standard distillates, with a moderate reduction (2.4%) in the ethanol recovery. This means that much better distillates spirits can be obtained by applying model-based engineering tools than those achieved by trial and error experimentation or intuitively.

In Chapter IV, we focus on model-based methodology to produce recipes for Muscat wine distillations in Charentais alembics. The recipes were obtained by dynamic multi-objective optimization of a multi-component phenomenological model (DAES). Two multi-objective functions were developed considering chemical markers that define the aromatic characteristic of the distillates. The first function included three chemical markers characteristic of each distillation cut (head, heart and tail). The second considered a Principal Component analysis (PCA) applied to the chemical profile of Chilean commercial distillates.

The optimal recipes were experimentally validated in an automatized Charentais alembic using a synthetic Muscat wine consisting of ethanol, water plus six congeners. The experimental results indicated that using model-based optimization techniques, it is possible to obtain spirits with a chemical composition like Chilean commercial distillates. In addition, the chemical composition of many commercial distillates lied close to a Pareto front defining a compromise between linalool, a characteristic Muscat floral aroma, and acetaldehyde, a head contaminant marker.

FUTURE PERSPECTIVES

The results of this project will allow to design distillation recipes for Charentais stills to produce any spirit with enhanced specific aromatic characteristic and with minimum levels of toxic compounds and aromatic defects. Even though our results were obtained in a lab-scale alembic, the methodology can be easily extended at industrial scale since the system implementation is relatively simple and low cost. The application of this methodology could generate a robust technological package that can solve and help to distillers in the industry by engineering tools used in the present work. Thus, it will possible design distillation recipes in an optimal way, employing less experimental effort, cost and time.

This study will be of interest to researches and practitioners working in the distillation of complex mixtures such as spirits, essential oils and the like. In addition, this approach will be interest and can be extended in the field of optimal design of food products using the multi-objective optimization techniques and analysis multi-variable methods.

REFERENCES

A. Waechter, a, & Biegler, L. T. (2006). *On the Implementation of a Primal-Dual Interior Point Filter Line Search Algorithm for Large-Scale Nonlinear Programming*. *Mathematical Programming* (Vol. 106).

Agosin, E., Belancic, A., Ibacache, A., Baumes, R., Bordeu, E., Crawford, A., & Bayonove, C. (2000). Aromatic potential of certain Muscat grape varieties important for Pisco production in Chile. *American Journal of Enology and Viticulture*, *51*(4), 404–408.

Aguiar, R. A., Franco, I. C., Leonardi, F., & Lima, F. (2018). Fractional PID Controller Applied to a Chemical Plant with Level and pH Control. *Chemical Product and Process Modeling*, *0*(0), 1–12.

Aguila-Camacho, N., & Duarte-Mermoud, M. A. (2013). Fractional adaptive control for an automatic voltage regulator. *ISA Transactions*, *52*(6), 807–815.

Aguila-Camacho, N., Le Roux, J. D., Duarte-Mermoud, M. A., & Orchard, M. E. (2017). Control of a grinding mill circuit using fractional order controllers. *Journal of Process Control*, *53*, 80–94.

Ang, K. H., Chong, G. C. Y., & Li, Y. (2007). PID Control System Analysis , Design , and Technology, *13*(November), 559–576.

APMonitor. (2018). APOPT Solver. Retrieved November 20, 2018, from https://github.com/APMonitor/apopt

Arrieta-Garay, Y., Blanco, P., López-Vázquez, C., Rodríguez-Bencomo, J. J., Pérez-Correa, J. R., López, F., & Orriols, I. (2014). Effects of distillation system and yeast strain on the aroma profile of Albariño (Vitis vinifera L.) grape pomace spirits. *Journal of Agricultural and Food Chemistry*, *62*, 10552–10560.

Arrieta-Garay, Y., García-Llobodanin, L., Pérez-Correa, J. R., López-Vázquez, C., Orriols, I., & López, F. (2013). Aromatically enhanced pear distillates from blanquilla and conference varieties using a packed column. *Journal of Agricultural and Food Chemistry*, *61*, 4936–4942.

Arrieta-Garay, Y., López-Vázquez, C., Blanco, P., Pérez-Correa, J. R., Orriols, I., & López, F. (2014). Kiwi spirits with stronger floral and fruity characters were obtained with a packed column distillation system. *Journal of the Institute of Brewing*, *120*, 111–118.

Åström, K. J., & Hägglund, T. (2006). *Advanced PID Control*. ISA-The Instrumentation, Systems, and Automation Society.

Barton, P. I., Allgor, R. J., Feehery, W. F., & Galán, S. (1998). Dynamic Optimization in a Discontinuous World. *Industrial & Engineering Chemistry Research*, *37*(97), 966–981. https://doi.org/10.1021/ie970738y

Beal, L., Hill, D., Martin, R., & Hedengren, J. (2018). GEKKO Optimization Suite. *Processes*, *6*(8), 106.

Bennett, S. (1996). A brief history of automatic control. *IEEE Control Systems*, *16*(3), 17–25.

Bhaskar, V., Gupta, S. K., & Ray, A. K. (2000). Applications of Multiobjective Optimization in Chemical Engineering. *Reviews in Chemical Engineering*, *16*, 1–54.

Biblioteca del Congreso Nacional de Chile, & Ministerio de Agricultura. (2012). Biblioteca del Congreso Nacional de Chile - www.leychile.cl - documento generado el 24-Nov-2012. *Reglamenta Ley N° 18.455 Que Fija Normas Sobre Producción, Elaboración y Comercialización de Alcoholes Etilicos, Bebidas Alcohólicas y Vinages*.

Biegler, L. T. (2007). An overview of simultaneous strategies for dynamic optimization. *Chemical Engineering and Processing: Process Intensification*, *46*(June 2006), 1043–1053.

Biegler, L. T. (2010). *Nonlinear Programming Concepts, Algorithms, and Applications to Chemical Processes*. (T. Liebling, Ed.). Pittsburgh, Pennsylvania.

Biegler, L. T., Cervantes, A. M., & Wächter, A. (2002). Advances in simultaneous strategies for dynamic process optimization. *Chemical Engineering Science*, *57*, 575–593.

Bisschop, J., & Meeraus, A. (1982). On the development of a general algebraic modeling system in a strategic planning environment. In J.-L. Goffin & J.-M. Rousseau (Eds.), *Applications* (pp. 1–29). Berlin, Heidelberg: Springer Berlin Heidelberg.

Bonilla-Petriciolet, A., & Rangaiah, G. P. (2013). Introduction. In *Multi-Objective Optimization in Chemical Engineering* (pp. 1–16). Wiley-Blackwell.

Bonsfills, a., & Puigjaner, L. (2004). Batch distillation: Simulation and experimental validation. *Chemical Engineering and Processing: Process Intensification*, *43*, 1239–1252.

Bordeu, E., Agosín, E., & Casaubon, G. (2012). 16 - Pisco: production, flavor chemistry, sensory analysis and product development. In J. Piggott (Ed.), *Alcoholic Beverages* (pp. 331–347). Woodhead Publishing.

Bordeu, E., Formas, G., & Agosin, E. (2004). Proposal for a standardized set of sensory terms for pisco, a young muscat wine distillate. *American Journal of Enology and Viticulture*, *55*(1), 104–107.

Bordiga, M., Rinaldi, M., Locatelli, M., Piana, G., Travaglia, F., Coïsson, J. D., & Arlorio, M. (2013). Characterization of Muscat wines aroma evolution using comprehensive gas chromatography followed by a post-analytic approach to 2D contour plots comparison. *Food Chemistry*, *140*(1–2), 57–67.

Brosilow, C., & Joseph, B. (2002). *Techniques of Model-Based Control*. Prentice Hall.

Byers, J. A. (1997). Vapor pressure of Volatile Chemicals. Retrieved September 5, 2018, from http://www.chemical-ecology.net/java/jav-vp.htm

Cacho, J., Moncayo, L., Palma, J. C., Ferreira, V., & Culleré, L. (2012). Characterization of the aromatic profile of the Italia variety of Peruvian pisco by gas chromatography-olfactometry and gas chromatography coupled with flame ionization and mass spectrometry detection systems. *Food Research International*, *49*(1), 117–125.

Camacho, E. F., & Alba, C. B. (2013). *Model Predictive Control*. Springer London.

Carvallo, J., Labbe, M., Pérez-Correa, J. R., Zaror, C., & Wisniak, J. (2011). Modelling methanol recovery in wine distillation stills with packing columns. *Food Control*, *22*(8), 1322–1332.

Christoph, N., & Bauer-Christoph, C. (2007). Flavour of Spirit Drinks: Raw Materials, Fermentation, Distillation, and Ageing. In R. G. Berger (Ed.), *Flavours and Fragrances: Chemistry, Bioprocessing and Sustainability* (pp. 219–239). Berlin, Heidelberg: Springer Berlin Heidelberg.

Claus, M. J., & Berglund, K. a. (2005). Fruit brandy production by batch column distillation with reflux. *Journal of Food Process Engineering*, *28*, 53–67.

Clutton, D. W., & Evans, M. B. (1978). The flavour constituents of gin. *Journal of Chromatography A*, *167*(C), 409–419.

Da Porto, C., & Decorti, D. (2008). Effect of cooling conditions on separation of volatile compounds in grappa using tray and packed columns without reflux. *International Journal of Food Science and Technology*, *43*, 638–643.

De Lucca, F., Munizaga-Miranda, R., Jopia-Castillo, D., Gelmi, C. a., & Pérez-Correa, J. R. (2013). Operation Strategies to Minimize Methanol Recovery in Batch Distillation of Hydroalcoholic Mixtures. *International Journal of Food Engineering*, *9*(3), 259–265.

Delfini, C., Cocito, C., Bonino, M., Schellino, R., Gaia, P., & Baiocchi, C. (2001). Definitive evidence for the actual contribution of yeast in the transformation of neutral precursors of grape aromas. *Journal of Agricultural and Food Chemistry*, *49*(11), 5397–5408.

Diwekar, U. (1995). *Batch Distillation: Simulation, Optimal Design, And Control*. Taylor & Francis.

Egea, J. a., Rodríguez-Fernández, M., Banga, J. R., & Martí, R. (2007). Scatter search for chemical and bio-process optimization. *Journal of Global Optimization*, *37*, 481–503.

Elgue, S., Prat, L., Cabassud, M., Lann, J. M. Le, & Cézerac, J. (2004). Dynamic models for start-up operations of batch distillation columns with experimental validation. *Computers and Chemical Engineering*, *28*, 2735–2747.

Faúndez, C. A., Quiero, F. A., & Valderrama, J. O. (2010). Phase equilibrium modeling in ethanol + congener mixtures using an artificial neural network. *Fluid Phase Equilibria*, *292*(1–2), 29–35.

Faúndez, C. A., Quiero, F. A., & Valderrama, J. O. (2011). Correlation and prediction of VLE of water+congener mixtures found in alcoholic beverages using an artificial neural network. *Chemical Engineering Communications*, *198*(1), 102–119.

Fernandez-Fernandez, M., Lefranc, G., Luna, R., & Perez-Correa, J. R. (2016). Comparison of PID-IMC and Hill Control applied to heating power of a fruit-derived alcohol production alembic. In *CHILECON 2015 - 2015 IEEE Chilean Conference on Electrical, Electronics Engineering, Information and Communication Technologies, Proceedings of IEEE Chilecon 2015*.

Ferreira, V., López, R., Escudero, A., & Cacho, J. F. (1998). Quantitative determination of trace and ultratrace flavour active compounds in red wines through gas chromatographic-ion trap mass spectrometric analysis of microextracts. *Journal of Chromatography A*, *806*(2), 349–354.

Fourer, R., Gay, D. M., Hill, M., Kernighan, B. W., & Laboratories, T. B. (1990). AMPL : A Mathematical Programming Language. *Management Science*, *36*, 519–554.

Fourer, R., Gay, D. M., & Kernighan, B. W. (2003). AMPL - A Modeling Language for Mathematical Programming: Second Edition, 519–554.

Fredenslund, A., Gmehling, J., & Rasmussen, P. (1977). *Vapor-Liquid Equilibria Using Unifac: A Group-Contribution Method*. Elsevier Science.

García-Llobodanin, L., Roca, J., López, J. R., Pérez-Correa, J. R., & López, F. (2011). The lack of reproducibility of different distillation techniques and its impact on pear spirit composition. *International Journal of Food Science & Technology*, *46*(9), 1956–1963.

Gole, H., Barve, P., Kesarkar, A. A., & Selvaganesan, N. (2014). Investigation of fractional control performance for magnetic levitation experimental set-up. *IEEE Proceedings of the INternational Conference On Emerging Trends in Science Engineering and Technology: Recent Advancements on Science and Engineering Innovation, INCOSET 2012*, 500–504.

Goutelle, S., Maurin, M., Rougier, F., Barbaut, X., Bourguignon, L., Ducher, M., & Maire, P. (2008). The Hill equation: A review of its capabilities in pharmacological modelling. *Fundamental and Clinical Pharmacology*, *22*(6), 633–648.

Hamamci, S. E. (2007). An algorithm for stabilization of fractional-order time delay systems using fractional-order PID controllers. *IEEE Transactions on Automatic Control*, *52*(10), 1964–1969.

Han Kim, Y. (1999). Optimal design and operation of a multi-product batch distillation column using dynamic model. *Chemical Engineering and Processing: Process Intensification*, *38*, 61–72.

Hedengren, J. D., Shishavan, R. A., Powell, K. M., & Edgar, T. F. (2014). Nonlinear modeling, estimation and predictive control in APMonitor. *Computers & Chemical Engineering*, *70*, 133–148.

Hernández-Gómez, L. F., Úbeda, J., & Briones, A. (2003). Melon fruit distillates: Comparison of different distillation methods. *Food Chemistry*, *82*, 539–543.

Jain, S., Kim, J. K., & Smith, R. (2012). Operational optimization of batch distillation systems. *Industrial and Engineering Chemistry Research*, *51*, 5749–5761.

Jauregui, C., Duarte Mermoud, M., Orostica, R., Travieso Torres, J. C., & Beytia, O. (2016a). Conical Tank Level Control with Fractional PID. *IEEE Latin America Transactions*, *14*(6), 2598–2604.

Jauregui, C., Duarte Mermoud, M., Orostica, R., Travieso Torres, J. C., & Beytia, O. (2016b). Experimental evaluation of conical tank level control using fractional PID. In *2016 12th IEEE International Conference on Control and Automation (ICCA)* (pp. 299–304).

Jolliffe, I. T. (2002). *Principal Component Analysis, Second Edition*. *Encyclopedia of Statistics in Behavioral Science* (Vol. 30).

Kameswaran, S., & Biegler, L. T. (2006). Simultaneous dynamic optimization strategies: Recent advances and challenges. *Computers & Chemical Engineering*, *30*, 1560–1575.

Lambrechts, M. G., & Pretorius, I. S. (2000). Yeast and its Importance to Wine Aroma - A Review. *South African Journal of Enology and Viticulture*, *21*(Special Issue), 97–129.

Léauté, R. (1990). Distillation in Alambic. *American Journal of Enology and Viticulture*, *41*(1), 90–103.

Li, P., Garcia, H. A., Wozny, G., & Reuter, E. (1998). Optimization of a Semibatch Destillation Process with Model Validation on the Industrial Site. *Ind. Eng. Chem. Res.*, *37*(97), 1341–1350.

Li, Y., Ang, K. H., & Chong, G. C. Y. (2006). Patents, Software, and Hardware for PID Control: An Overview and Analysis of the Current Art. *IEEE Control Systems*, *26*(1), 42–54.

Logsdon, J. S., Diwekar, U. M., & Biegler, L. T. (1990). On the simultaneous optimal design and operation of batch distillation columns. *Chemical Engineering Research and Design*, *68*, 434–444.

López, F., Rodríguez-Bencomo, J. J., Orriols, I., & Pérez-Correa, J. R. (2017). Chapter 10 - Fruit Brandies. In M. R. Kosseva, V. K. Joshi, & P. S. Panesar (Eds.), *Science and Technology of Fruit Wine Production* (pp. 531–556). San Diego: Academic Press.

Luna, R., Duarte-Mermoud, M. A., & Pérez-correa, J. R. (2018). *Fractional Order Control in Charentais Alembic Distillation*. Manuscript submitted for publication.

Luna, R., López, F., & Pérez-Correa, J. R. (2018). Minimizing methanol content in experimental charentais alembic distillations. *Journal of Industrial and Engineering Chemistry*, *57*, 160–170.

Luna, R., Matias-Guiu, P., Lopéz, F., & Pérez-correa, J. R. (2019). *Modeling and Multi-Objective Dynamic Optimization of Muscat Wine Batch Distillations*. Manuscript submitted for publication

Madhuranthakam, C. R., Elkamel, A., & Budman, H. (2008). Optimal tuning of PID controllers for FOPTD, SOPTD and SOPTD with lead processes. *Chemical Engineering and Processing: Process Intensification*, *47*(2), 251–264.

Matias-Guiu, P., Rodríguez-Bencomo, J. J., Orriols, I., Pérez-Correa, J. R., & López, F. (2016). Floral aroma improvement of Muscat spirits by packed column distillation with variable internal reflux. *Food Chemistry*, *213*, 40–48.

Matias-Guiu, P., Rodríguez-Bencomo, J. J., Pérez-Correa, J. R., & López, F. (2018). Aroma profile design of wine spirits: Multi-objective optimization using response surface methodology. *Food Chemistry*, *245*, 1087–1097.

Meenakshipriya, B., Prakash, M., & Maheswari, C. (2015). Experimental investigations on fractional order PIλcontroller in pH neutralization system. *International Journal of Control Theory and Applications*, *8*(3), 867–875.

Miettinen, K., & Hakanen, J. (2009). Why Use Interactive Multi-Objective Optimization in Chemical Process Design. *Multi-Objective Optimization: Techniques and Applications in Chemical Engineering*, (Mcdm), 153–188.

Mujtaba, I. M. (2004). *Batch Distillation: Design and Operation*. Imperial College Press.

Mujtaba, I. M., & Macchietto, S. (1993). Optimal operation of multicomponent batch distillation—multiperiod formulation and solution. *Computers & Chemical Engineering*, *17*(12), 1191–1207.

Mujtaba, I. M., & Macchietto, S. (1996). {S}imultaneous optimization of design and operation of multicomponent batch distillation column - single and multiple separation duties. *Journal of Process Control*, *6*(1), 27–36.

Mujtaba, I. M., & Macchietto, S. (1997). Efficient Optimization of Batch Distillation with Chemical Reaction Using Polynomial Curve Fitting Techniques. *Industrial & Engineering Chemistry Research*, *36*, 2287–2295.

Narasimhan, S., & Jordache, C. (2000). *Data reconciliation and gross error detection: An intelligent use of process data*. Gulf Professional Publishing.

Neuburg, H. J., & Perez-Correa, j. R. (1994). Dynamic and steady state modelling of a pilot binary tray distillation column. *Latin American Applied Research*, *24*(1), 1–15.

Noeres, C., Dadhe, K., Gesthuisen, R., Engell, S., & Górak, a. (2004). Model-based design, control and optimisation of catalytic distillation processes. *Chemical Engineering and Processing: Process Intensification*, *43*, 421–434.

Odepa. (2017). *Evolución de la producción y mercado del Pisco : noviembre de 2017*. Retrieved from www.odepa.gob.cl

Ohta, T., Morimitsu, Y., Sameshima, Y., Samuta, T., & Ohba, T. (1991). Transformation from geraniol, nerol and their glucosides into linalool and α-terpineol during shochu distillation. *Journal of Fermentation and Bioengineering*, *72*(5), 347–351.

Ortiz-Quisbert, M. E., Duarte-Mermoud, M. A., Milla, F., Castro-Linares, R., & Lefranc, G. (2018). Optimal fractional order adaptive controllers for AVR applications. *Electrical Engineering*, *100*(1), 267–283.

Osorio, D., Pérez-Correa, J. R., Biegler, L. T., & Agosin, E. (2005). Wine distillates: practical operating recipe formulation for stills. *Journal of Agricultural and Food Chemistry*, *53*(16), 6326–6331.

Osorio, D., Pérez-Correa, R., Belancic, A., & Agosin, E. (2004). Rigorous dynamic modeling and simulation of wine distillations. *Food Control*, *15*(7), 515–521.

Oustaloup, A. (1991). *La commande CRONE: commande robuste d'ordre non entier*. Hermès.

Padula, F., & Visioli, A. (2011). Tuning rules for optimal PID and fractional-order PID controllers. *Journal of Process Control*, *21*(1), 69–81.

Padula, F., & Visioli, A. (2015). *Advances in robust fractional control*. *Advances in Robust Fractional Control*.

Pérez-Correa, J. R., Lefranc, G., & Fernández-Fernández, M. (2015). A new application of the hill repressor function: Automatic control of a conic tank level and local stability analysis. *Mathematical Problems in Engineering*, *2015*.

Pérez-Correa, J. R., Luna-Hérnandez, R., Jopia, D., Díaz, S., Huerta, F., & López, F. (2013). Impacto de las condiciones de operación de un alambique Charentais en las curvas de recuperación de destilado (p. 8). Madrid: XII Congreso de los Grupos de Investigación Enológica (Gienol).

Pozo, C., Ruíz-Femenia, R., Caballero, J., Guillén-Gosálbez, G., & Jiménez, L. (2012). On the use of Principal Component Analysis for reducing the number of environmental objectives in multi-objective optimization: Application to the design of chemical supply chains. *Chemical Engineering Science*, *69*(1), 146–158.

Prausnitz, J. M., Lichtenthaler, R. N., & de Azevedo, E. G. (1998). *Molecular Thermodynamics of Fluid-Phase Equilibria*. Pearson Education.

Reche, R. V., Neto, A. F. L., Da Silva, A. A., Galinaro, C. A., De Osti, R. Z., & Franco, D. W. (2007). Influence of type of distillation apparatus on chemical profiles of Brazilian cachaças. *Journal of Agricultural and Food Chemistry*, *55*, 6603–6608.

Ribéreau-Gayon, P., Dubourdieu, D., Glories, Y., & Maujean, A. (2006). *The Chemistry of Wine*. *Handbook of Enology, volume 2: The Chemistry of Wine and Stabilization and Treatments* (Vol. 2).

Rodríguez-Bencomo, J. J., Pérez-Correa, J. R., Orriols, I., & López, F. (2016). Spirit Distillation Strategies for Aroma Improvement Using Variable Internal Column Reflux. *Food and Bioprocess Technology*, *9*, 1885–1892.

Sacher, J., García-Llobodanin, L., López, F., Segura, H., & Pérez-Correa, J. R. (2013). Dynamic modeling and simulation of an alembic pear wine distillation. *Food and Bioproducts Processing*, *91*(4), 447–456.

Sacher, J., García-Llobodanin, L., López, F., Segura, H., & Pérez-Correa, J. R. (2017). The Spirit World: Can chemical engineering help spirits distillers close the loop between historic roots and modern modelling methods? *The Chemical Engineer*, (910), 32–35.

Safdarnejad, S. M., Gallacher, J. R., & Hedengren, J. D. (2016). Dynamic parameter estimation and optimization for batch distillation. *Computers and Chemical Engineering*, *86*, 18–32.

Safdarnejad, S. M., Hedengren, J. D., Lewis, N. R., & Haseltine, E. L. (2015). Initialization strategies for optimization of dynamic systems. *Computers and Chemical Engineering*, *78*, 39–50.

Scanavini, H. F. a, Ceriani, R., Cassini, C. E. B., Souza, E. L. R., Maugeri Filho, F., & Meirelles, A. J. a. (2010). Cachaça production in a lab-scale alembic: Modeling and computational simulation. *Journal of Food Process Engineering*, *33*(2010), 226–252.

Scanavini, H. F. a, Ceriani, R., & Meirelles, a. J. a. (2012). Cachaça distillation investigated on the basis of model systems. *Brazilian Journal of Chemical Engineering*, *29*(02), 429–440.

Shah, P., & Agashe, S. (2016). Review of fractional PID controller. *Mechatronics*, *38*, 29–41.

Shampine, L. F., & Reichelt, M. W. (1997). The MATLAB ODE Suite. *SIAM Journal on Scientific Computing*, *18*(1), 1–22.

Sharma, S., & Rangaiah, G. P. (2013). Multi-Objective Optimization Applications in Chemical Engineering. In *Multi-Objective Optimization in Chemical Engineering* (pp. 35–102). Wiley-Blackwell.

Small, R. W., Couturier, M., & Godfrey, M. (2011). *Beverage Basics: Understanding and Appreciating Wine, Beer, and Spirits*. Wiley.

Smith, C. A., & Corripio, A. B. (1985). *Principles and practice of automatic process control*. Wiley.

Spaho, N. (2017). Distillation Techniques in the Fruit Spirits Production. In M. F. Mendes (Ed.), *Distillation - Innovative Applications and Modeling*. Rijeka: InTech.

Spaho, N., Dürr, P., Grba, S., Velagić-Habul, E., & Blesić, M. (2013). Effects of distillation cut on the distribution of higher alcohols and esters in brandy produced from three plum varieties. *Journal of the Institute of Brewing*, *119*(1–2), 48–56.

Srinivasan, B., Bonvin, D., Visser, E., & Palanki, S. (2003). Dynamic optimization of batch processes. *Computers & Chemical Engineering*, *27*, 27–44.

Swain, S. K., Sain, D., Mishra, S. K., & Ghosh, S. (2017). Real time implementation of fractional order PID controllers for a magnetic levitation plant. *AEU - International Journal of Electronics and Communications*, *78*, 141–156.

Swiegers, J. H., Bartowsky, E. J., Henschke, P. A., & Pretorius, I. S. (2005). Yeast and bacterial modulation of wine aroma and flavour. *Australian Journal of Grape and Wine Research*, *11*(2), 139–173.

Swift, R., & Davidson, D. (1998). Alcohol hangover, mechanisms and mediatirs. *Alcohol Health and Research World*, *22(1)*, 54–60.

Valderrama, J. O., Faúndez, C. a., & Toselli, L. a. (2012). Advances on modeling and simulation of alcoholic distillation. Part 1: Thermodynamic modeling. *Food and Bioproducts Processing*, *90*(4), 819–831.

Valderrama, J. O., Pizarro, C., & Rojas, R. (2001). Vapor-liquid equilibrium in complex mixtures for the simulation of distillation processes of musts and wines. *Alimentaria*, *39*, 151–156.

Valderrama, J. O., Rojas, R., & Pizarro, C. (2000). Comparative study of thermodynamic models to describe complex mixtures present in wine disstillation. *Información Tecnológica*, *11(6)*, 189–192.

Valenzuela, L. (2002). *Política de destilación y calidad del destilado (pisco). Tesis (Magister en Ciencias de la Ingeniería).* Pontificia Universidad Católica.

Valerio, D., & Da Costa, J. S. (2004). Ninteger: A non-integer control toolbox for Matlab. In *Proceedings of the 1st IFAC Workshop on Fractional Differentiation and its Applications*. Bodeaux, France.

Vali, M., Rezaei Estakhrouiyeh, M., & Gharaveisi, A. (2016). Application of fractional order iterative learning controller for a type of batch bioreactor. *IET Control Theory & Applications*, *10*(12), 1374–1383.

Vassiliadis, V. S., Sargent, R. W. H., & Pantelides, C. C. (1994a). Solution of a Class of Multistage Dynamic Optimization Problems. 1. Problems without Path Constraints. *Industrial & Engineering Chemistry Research*, *33*, 2111–2122.

Vassiliadis, V. S., Sargent, R. W. H., & Pantelides, C. C. (1994b). Solution of a Class of Multistage Dynamic Optimization Problems. 2. Problems with Path Constraints. *Industrial & Engineering Chemistry Research*, *33*, 2123–2133.

Vinopraba, T., Sivakumaran, N., Narayanan, S., & Radhakrishnan, T. K. (2013). *Design of fractional order controller for Biochemical reactor*. *IFAC Proceedings Volumes (IFAC-PapersOnline)* (Vol. 12). IFAC.

Weise, T. (2008). *Global Optimization Algorithms - Theory and Applications*.

Willner, B., Granvogl, M., & Schieberle, P. (2013). Characterization of the key aroma compounds in bartlett pear brandies by means of the sensomics concept. *Journal of Agricultural and Food Chemistry*, *61*(40), 9583–9593.

Wine, I. O. of V. and. (2009). Method OIV-MA-AS312-03B. *Compendium of International Methods of Analisys-OIV: Methanol*, 3.

Zavala, J. C., & Coronado, C. (2008). Optimal control problem in batch distillation using thermodynamic efficiency. *Industrial and Engineering Chemistry Research*, *47*(2), 2788–2793.